

ADDIS ABABA UNIVERSITY
ADDIS ABABA INSTITUTE OF TECHNOLOGY
SCHOOL OF CIVIL AND ENVIRONMENTAL ENGINEERING



**Effect of Aggregate Size and Type on Shear Capacity
of Normal Strength Reinforced Concrete Beams**

A Thesis in Structural Engineering

By Sadik Muzeyin

March, 2016

Addis Ababa

Submitted in Partial Fulfillment of the Requirements for the Degree of Master of Science

ADDIS ABABA UNIVERSITY
ADDIS ABABA INSTITUTE OF TECHNOLOGY
SCHOOL OF CIVIL AND ENVIRONMENTAL ENGINEERING

“Effect of Aggregate Size and Type on Shear Capacity of Normal Strength Reinforced Concrete
Beams”

By

Sadik Muzeyin

Approved by the Board of Examiners:

Dr. Esayas G/Youhannes

Advisor

Signature

Date

Dr. Ing. Adil Zekaria

Internal Examiner

Signature

Date

Dr. Ing. Girma Zerayouhannes

External Examiner

Signature

Date

ACKNOWLEDGMENTS

First and at most, greatest thanks from the depth of my heart are to ALLAH for endowing me with the courage, strength as well as health throughout my life.

Next, it is my deepest gratitude and respect to my advisor Dr. Esayas G/Youhannes, for his valuable advice, sincerity, very humble way of approach for the successful completion of this research which is never been forgotten.

I would like to take this opportunity to express my heartfelt appreciation to my esteemed colleagues Mekdes Tadesse, Sadik Nuredin, Samson Walelign and Shemsedin Mohammed for giving me all the support I needed throughout the Experimental program. I am grateful to Fikru B., Demis and Wubet A. in the construction materials testing laboratory for assisting me in many different ways.

I would like to thank my Spouse Leyla Temam for all the support she offered and for helping me get through the difficult times.

TABLE OF CONTENTS

CONTENTS

ACKNOWLEDGMENTS	3
TABLE OF CONTENTS	1
LIST OF FIGURES	4
LIST OF TABLES	6
ABSTRACT	7
CHAPTER 1 INTRODUCTION	8
1.1 General Background.....	8
1.2 Significance.....	9
1.3 Objectives.....	10
1.4 Scope	10
1.5 Methodology	11
CHAPTER 2 LITERATURE REVIEW	12
2.1 Theoretical Background	12
2.1.1 Shear Failures and Shear Distress in Structural Members	12
2.1.2 Basic Mechanisms of Shear Transfer in Reinforced Concrete	13
2.2 Shear in Beams	15
2.2.1 Stress in an un Cracked Elastic Beam	15
2.2.2 Behavior and Strength of beams failing in shear	17
2.3 Historical Development of Shear Design Provision.....	27
2.4 Shear Design Models for Members without Transverse Reinforcement	32
2.4.1 Fracture Mechanics Approaches	32
2.4.2 Simple Strut-and-Tie Models.....	32
2.4.3 Tooth Model for Slender Members.....	33
2.4.4 Truss Models with Concrete Ties	35
2.4.5 Modified Compression Field Theory.....	37
2.4.6 Toward a Consistent Method	40

2.5	Building Codes and Shear Design Provisions	41
2.5.1	Overview of current ACI Design Procedures (ACI 318-14).....	42
2.5.2	Overview of Recent European Codes (EN 1992:2004).....	43
CHAPTER 3 SHEAR STRENGTH OF REINFORCED CONCRETE SLENDER BEAMS WITHOUT WEB REINFORCEMENT.....		45
3.1	Introduction	45
3.2	Evaluation of Design Equations	46
3.3	Effect of Influencing Factors	49
3.4	Proposed Empirical Equation.....	51
CHAPTER 4 EXPERIMENTAL PROGRAM		52
4.1	Specimens.....	52
4.2	Materials.....	55
4.2.1	Concrete	55
4.2.2	Steel.....	57
4.3	Specimen Fabrication	58
4.4	Test Setup.....	60
4.5	Instrumentation	60
CHAPTER 5 FINITE-ELEMENT ANALYSIS USING DUCOM-COM3		63
5.1	About the software.....	63
5.2	Specimens.....	63
5.3	Materials.....	65
5.4	Modeling	65
5.5	Support condition and loading.....	66
CHAPTER 6 RESULT AND DISCUSSION		67
6.1	Result from experiment	67
6.1.1	Result	67
6.1.2	Effect of Aggregate Size.....	72
6.1.3	Effect of aggregate type.....	74
6.2	Result from finite element analysis using DuCOM-COM3.....	75
6.2.1	Result	75
6.2.2	Effect of aggregate size and type	77

6.3	Comparison between result from analytical simulation and experiment	77
6.4	Comparison of Code equations with experimental results.....	80
CHAPTER 7	CONCLUSION AND RECOMMENDATION.....	82
7.1	Conclusion.....	82
7.2	Recommendation	83
REFERENCES.....		84
APPENDIX		86

List of Figures

Figure 1:1: Failure surface at critical shear crack in beams without stirrups: (a) rough crack surface in beam with gravel aggregate; and (b) smooth crack surface due to aggregate fracture in beam with limestone aggregate.(Sagaseta and Vollum)	10
Figure 2:1: Shear in homogeneous rectangular beams (Arthur H. Nilson et al., 2010)	15
Figure 2:2: Stress trajectories in homogeneous rectangular beam.....	16
Figure 2:3: Types of Inclined Cracks	18
Figure 2:4: Failures of Slender Beams	19
Figure 2:5: Typical Shear Failure in Short Beams.....	20
Figure 2:6: Modes of Failure of Deep Beams (ASCE-ACI Task Committee 426, June 1973).....	20
Figure 2:7: Effect of a/d ratio on shear capacity of beams (McGregor et al., 2012).....	21
Figure 2:8: Internal forces in a cracked beam without web reinforcements	23
Figure 2:9: Internal forces in a cracked beam with web reinforcements.....	26
Figure 2:10: Distribution of Internal shears in a beam with web reinforcement	27
Figure 2:11: Crack Pattern at Shear Failure of Beam with Unsafe Strut-and-Tie Model(Kupfer and Gerstle 1973).....	33
Figure 2:12: Kani's Tooth Model (Kani 1964).....	34
Figure 2:13: Dimensioning Diagram for Ultimate Shear Force Derived from Mechanical Model by Reineck (1991c).	35
Figure 2:14: Refined Strut-and-Tie Models Proposed by Al-Nah-lawi and Wight (1992)	36
Figure 2:15: Refined Strut-and-Tie Models Proposed by Muttoni (1990).....	36
Figure 2:16: Refined Strut-and-Tie Model for Crack Friction and Dowel Action (Reineck 1991c): (a) Constant Friction Stresses; (b) Simple and Refined Strut-and-Tie Model for Dowel Action Combined with Friction	37
Figure 3:1: Comparison of prediction of Code equations with experimental results.	47
Figure 4:1: Experiment specimens.....	54
Figure 4-2 Compressive and tensile strength testing machine.....	55
Figure 4:3: Tensile Strength testing machine.....	57
Figure 4:4: Reinforcement cage and formwork of the specimens	58
Figure 4:5: Reinforcement cage of specimens inside the formwork	59
Figure 4:6: Curing process of the specimens	60
Figure 4:7: Load applying hydraulic jack	60

Figure 4:8: Displacement measuring tool.....	61
Figure 4:9: Load Cell.....	61
Figure 4:10: Data Logger	61
Figure 4:11: Test Setup.....	62
Figure 6:1: Diagonal tension failure in Specimen NWNo.9	67
Figure 6:2: Diagonal tension failure in Specimen NWNo.7	67
Figure 6:3: Diagonal tension failure in Specimen NWNo.5	68
Figure 6:4: Diagonal tension failure in Specimen NWNo.4	68
Figure 6:5: Diagonal tension failure in Specimen LWNo.5.....	68
Figure 6:6 : Load – Deflection diagram for specimen NWNo. 4	69
Figure 6:7: Load – Deflection diagram for specimen NWNo. 5	69
Figure 6:8: Load – Deflection diagram for specimen NWNo. 7	70
Figure 6:9: Load – Deflection diagram for specimen NWNo. 9	70
Figure 6:10: Load – Deflection diagram for specimen LWNo. 5	71
Figure 6:11: Comparison between Load – Deflection diagrams of the specimens	71
Figure 6:12: Load-Deflection diagram for different aggregate sizes with the similar concrete compressive strength.....	72
Figure 6:13 : Roughness of the cracked surface of specimens	73
Figure 6:14: Load-Deflection diagram for specimen NWNo.5 and LWNo.5	74
Figure 6:15: Summary of Load-deflection diagram from the finite element analysis	76
Figure 6:16: Load – Deflection diagram	77
Figure 6:17: Load – Deflection Diagram	78
Figure 6:18: Load-Deflection diagram.....	78
Figure 6:19: Load-Deflection diagram.....	79
Figure 6:20: Comparison of prediction of Code equations with experimental results.	80

List of Tables

Table 2-1: Values of β and θ for members with less than minimum shear reinforcement (AASHTO LRFD, 1994)	39
Table 3-1: Summary of results for the Average Margin of Safety (V_{exp}/V_{pre}) _{avg} of empirical equations used in different Codes for predicting the shear capacity of normal strength and high strength reinforced concrete slender beams.	48
Table 3-2: Summary of results showing the Average Margin of Safety with coefficient of correlation for NSC and HSC reinforced slender beams.	49
Table 3-3: Summary of results showing the Average Margin of Safety with coefficient of correlation for NSC and HSC reinforced slender beams including the size effect	50
Table 4-1: Grading requirements for coarse aggregates	53
Table 4-2: Details of investigated specimens	54
Table 4-3: Mix proportions of concrete	55
Table 4-4: 14th day strength of cylinder samples	56
Table 4-5: Test day strength of cylinder samples	56
Table 4-6 Mechanical properties of reinforcement	57
Table 5-1: Specimens description	63
Table 5-2: Mechanical property of concrete	65
Table 5-3: Mechanical property of reinforcement bar	65
Table 6-1: Load-deflection and failure mode of finite element analysis	75
Table 6-2: Margin of Safety (V_{exp}/V_{pre}) of empirical equations used in different Codes for predicting the shear capacity of normal strength reinforced concrete slender beams.	81

ABSTRACT

Shear behavior of reinforced concrete beams is a major area of research for more than 100 years. However, a single globally accepted theory like the flexure theory is not yet developed due to involvement of number of parameters. Aggregate size and type has not been given emphasis as one of the factors affecting the shear behavior of beams.

This paper presents the results of finite element analysis and experimental tests conducted on five reinforced concrete beams. The analysis and tests were performed principally to investigate the effect of aggregate size and type on shear capacity of normal strength reinforced concrete beams. Test specimens consisted of five simply supported slender beams with steel flexural reinforcement of which four are with normal aggregate and different aggregate sizes (37.5mm, 25mm, 12.5mm & 4.75) and one with light weight Aggregate (scoria).

Through the experimental and analytical investigation it was observed that the shear capacity increases with increasing of aggregate size and shear capacity of light weight aggregate concrete is approximately similar to the capacity of mortar.

CHAPTER 1 INTRODUCTION

1.1 General Background

In the design of concrete structures an adequate margin of safety must be provided against any mode of failure that might occur under the forces that act upon the structure during its life time. One general type of failure that must be prevented is the so-called “shear failure” [8]. It has long been a goal of the engineering profession to improve the quality of reinforced concrete design procedures for shear. Shear design methods for reinforced concrete structures should be simple, rational, and general. Above all, however, they should be safe and accurate. Unlike flexural failures, reinforced concrete shear failures are brittle and can occur without warning [6]. Furthermore, they tend to be less predictable than flexural failures due to more complex failure mechanisms whereas flexural design provisions are based on the simple assumption that plane sections remain plane¹. Shear behavior of reinforced concrete beams is a major area of research for more than 100 years. However, a single globally accepted theory like the flexure theory is not yet developed.

Traditionally, shear dimensioning and checking of structural concrete elements is performed differently on members with or without shear reinforcement. Several well-established theories based on equilibrium considerations (strut-and-tie models and stress fields) can be applied when shear reinforcement is provided, leading to safe design solutions. Theories also considering Compatibility conditions the tensile strength of concrete (compression field-based theories and fixed-angle softened-truss model) have also been developed allowing accurate predictions of the shear response of transversely reinforced members. Some general theories, such as the modified compression field theory (MCTF), have been successfully applied to members without shear reinforcement [9].

Shear is transmitted from one plane to another in various ways in reinforced concrete members. The behavior, including the failure modes, depends on the modes of shear transmission. Some of the principal shear mechanism is relatively recent and therefore the definite evaluation of the contribution of these shear carrying components is yet only tentative. The main type of shear transfer is the following: (a) Shear stress in the un cracked concrete; (b) interface shear transfer; (c) dowel action; (d) arch action; and (e) shear reinforcement [8].

The primary mechanism of shear transfer in beams and slabs constructed without shear reinforcement is aggregate interlock, and failure is initiated by breakdown of aggregate interlock

capacity at a crack [1]. There is no evidence to assume that the entire shear force is transferred in the compression zone. Clearly, then, shear design provisions that are intended to match experimental observations should recognize the critical importance of aggregate interlock. Beams without web reinforcement will fail when inclined cracking occurs or shortly afterwards. For this reason, the shear capacity of such members is taken equal to the inclined cracking shear. The inclined cracking load of a beam is affected by; Tensile strength of concrete (the inclined cracking load is a function of the tensile strength of the concrete, f_{ct}) [10].

Concrete is one of the versatile and widely used building material in the world construction industry. Fine and coarse aggregates make about 70% by volume of concrete production. It goes without saying that the quality of concrete is thus strongly influenced by aggregate's physical and mechanical properties as well as chemical composition of the parent aggregate making material [11].

The compressive strength, elastic modulus, splitting tensile strength, specific creep, and other properties of lightweight concrete are significantly affected by the structural properties of the lightweight aggregate used [2].

In different codes the effect of aggregate type is considered. Eg. EC 1992 and ACI-318. But the effect of aggregate size is not incorporated in different building codes including EBCS-1995. In this thesis the effect of Aggregate size and type on shear capacity of normal strength reinforced concrete beam will be addressed.

1.2 Significance

The research done by Zdenek P. Bazant and Hsu-Huei Sun, "size effect in diagonal shear failure", the results confirm that the size effect (aggregate size and beam size) on the concrete shear strength still exists in the presence of stirrups, but it is milder than without stirrups.

In high-strength (HSC) and lightweight aggregate concrete (LWAC), the bond between the aggregate particles and the cement paste can be strong enough for the aggregate to fracture at cracks, as shown in Figure 1.1 Aggregate fracture results in smoother crack surfaces and can reduce shear transfer through aggregate interlock.⁷

The Ethiopian Building Code Standard 2 (Structural Use of Concrete) provisions on shear design of reinforced concrete members doesn't consider effect of aggregate size and type. Thus, this research might answer the question of whether or not size and type of aggregate has an effect on the shear

behavior of beams. Furthermore if the effect of aggregate size and type is found to enhance the capacity, results of this research might suggest an improved way of choosing aggregate size and type while designing reinforced concrete members.

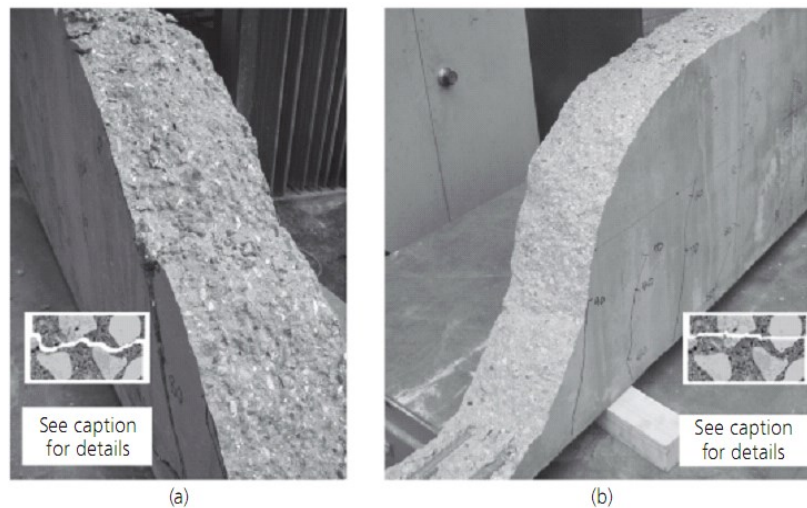


Figure 1:1: Failure surface at critical shear crack in beams without stirrups: (a) rough crack surface in beam with gravel aggregate; and (b) smooth crack surface due to aggregate fracture in beam with limestone aggregate.(Sagasetta and Vollum)

1.3 Objectives

The main objective of this research is to study whether or not size and type of aggregate affect the shear behavior of beams and to observe the extent of this effect.

On the other hand, if size and type of aggregate is found to be a factor affecting the shear capacity of beams, a better way of choosing aggregate size and type will be recommended while designing reinforced concrete members.

1.4 Scope

This research will include only normal beams with internal force of flexure and shear. Deep beams, beam-columns, Pre-stressed beams and beams made of high-strength concrete will not be covered in this document.

1.5 Methodology

The overall process of this research includes literature review, examination of building codes, experimental program and analytical simulation using non-linear finite element modeling.

First the basic shear design theories such as the truss model and modified compression field approaches will be studied and checked if size and type of aggregate is a factor affecting the shear behavior of beams in this models. Then, the most widely used building codes provisions and their shear design provisions will be reviewed.

After the desk analysis is finished, finite element analysis for different size and type of aggregate using a nonlinear finite element analysis tool called DuCOM-COM3 will be done. Then again, the exactness of the result of this tool will be verified by conducting an experiment for selected specimens.

CHAPTER 2 LITERATURE REVIEW

2.1 Theoretical Background

2.1.1 Shear Failures and Shear Distress in Structural Members [8]

In the design of concrete structures an adequate margin of safety must be provided against any mode of failure that might occur under the forces that act upon the structure during its lifetime. One general type of failure that must be prevented is the so-called “shear failure,” which in reality is a failure under combined shearing force and bending moment, plus, occasionally, axial load, or torsion, or both. Such failures reduce the strength of structural elements below the flexural capacity and considerably reduce the ductility of the elements. Especially for the latter reason, Shear failures are generally considered undesirable.

Shear distress and failures have been reported in beams in beams, columns, walls, slabs, brackets, and other members. In general each member exhibits different modes of cracking and failure, although the mechanisms by which shear is transferred within the member may be similar. For a beam subjected to a concentrated load, the major variable affecting the mode of failure is probably the ratio of the distance, a , from load to the support to the depth of the member, d .

(a) Beams

Reinforce concrete and pre-stressed concrete beams of moderate slenderness (a/d or $M/Vd=2-6$) develop inclined cracks due to the combination of shear and flexural stresses. Beams may exhibit a number of different modes of shear failure, the most common of which is the crushing or shearing of the compression flange over the inclined crack which is often accompanied or initiated by splitting along the tension reinforcement.

(b) Deep Beams

Shearing failures of deep beams, brackets, and similar members differ considerably from those in normal beams. This is largely due to the much steeper inclined cracks in deep members. This, in turn, changes the relative importance of the various shear transfer mechanisms as compared to normal beams.

(c) Shear Walls

Depending on their height to width ratio, shear walls represent a special case of beams or deep members.

(d) Columns

Columns may fail in shear in earthquakes. These failures appear to be of two types: either similar to that in an axially loaded beam involving inclined cracking or complete destruction of the column core apparently prior to inclined cracking.

(e) Beam-Column Joints

Inclined cracks may develop within the joints in reinforced concrete structures subjected to unbalanced gravity loads or seismic loads.

(f) Construction Joints and Joints in Precast Construction

Frequently shearing forces must be transferred across an interface such as a construction joint in a shear wall, the interface between a beam and a composite slab, or at the supports of precast elements. This action will be referred to as interface shear transfer.

(g) Slabs and Footing

So-called punching shear failures occur in slabs and footings. The shear capacity decreases as the moment transferred from the column to the slab, or vice versa, increases. Therefore, failures are more likely for exterior column connections or connections where moment transfer occurs because of either the loading conditions or the location of perforations adjacent to the column.

2.1.2 Basic Mechanisms of Shear Transfer in Reinforced Concrete [8]

Shear is transmitted from one plane to another in various ways in reinforced concrete members, depends on the method of shear transmission. The main types of shear transfer are the following:

(a) Shear Transfer by Concrete Shear Stress

The simplest method of shear transfer is by shearing stresses. This occurs in uncracked members or in the uncracked portions of structural members. The interaction of shear stresses with tensile and compressive stresses produces principal stresses which may cause inclined cracking or a crushing failure of the concrete.

(b) Interface Shear Transfer

There are several instances in which shear must be transferred across a definite plane or surface where slip may occur. Researchers have called this mechanism aggregate interlock, surface roughness shears transfer, shear friction, tangential shear transfer. If the plane under consideration is an existing crack or interface, failure usually involves slippage or relative movement along the crack or plane. If plan is located in monolithic concrete, a number of diagonal cracks occur across the interface and failure involves a truss action along the plane.

(c) Dowel Shear

If reinforcing bars cross a crack, shearing displacements along the crack will be resisted by, in part, by a dowelling force in the bar. The dowelling force gives rise to tensions in the surrounding concrete and these in combination with the wedging action of the bar deformations produce splitting cracks along the reinforcement. This in turn decreases the stiffness of concrete around the bar and therefore the dowel force. Relative to other shear transfer mechanisms, the dowel shear force is generally not dominant in beams. In beams, splitting cracks develop along the tension reinforcement at inclined cracks as a result of the dowel effects. This allows the inclined cracks to open, which in turn reduces the interface shear transfer along the diagonal crack and thus leads to failure.

(d) Arch Action

In deep beams and slab part of the load is transmitted to the supports by arch action. Arch action does permit the transfer of a vertical concentrated force to a reaction in a deep member and thereby reduces the contribution of the other types of shear transfer.

(e) Shear Reinforcement

In addition to any shear carried by the stirrup itself, when an inclined crack crosses shear reinforcement, the steel may contribute significantly to the capacity of the member by increasing or maintaining the shear transferred by interface shear transfer, dowel action, and arch action. Thus, shear reinforcement restricts the widening of inclined cracks in beams and thus slows the decrease of interface shear transfer quite effectively.

2.2 Shear in Beams

2.2.1 Stress in an un Cracked Elastic Beam [10]

The stresses acting in homogenous beams can be derived from mechanics of elastic materials. Shear stresses

$$\nu = \frac{VQ}{Ib} \quad (1)$$

act at any section in addition to the bending stresses

$$\sigma = \frac{My}{I} \quad (2)$$

Except for those locations at which the shear force V happens to be zero.

The role of shear stresses is easily visualized by the performance under load of the laminated beam of Figure 2-1; it consists of two rectangular pieces bonded together along the contact surface. If the adhesive is strong enough, the member will deform as one single beam, as shown in Figure 2-1a . On the other hand, if the adhesive is weak, the two pieces will separate and slide relative to each other, as shown in Figure 2-1b .

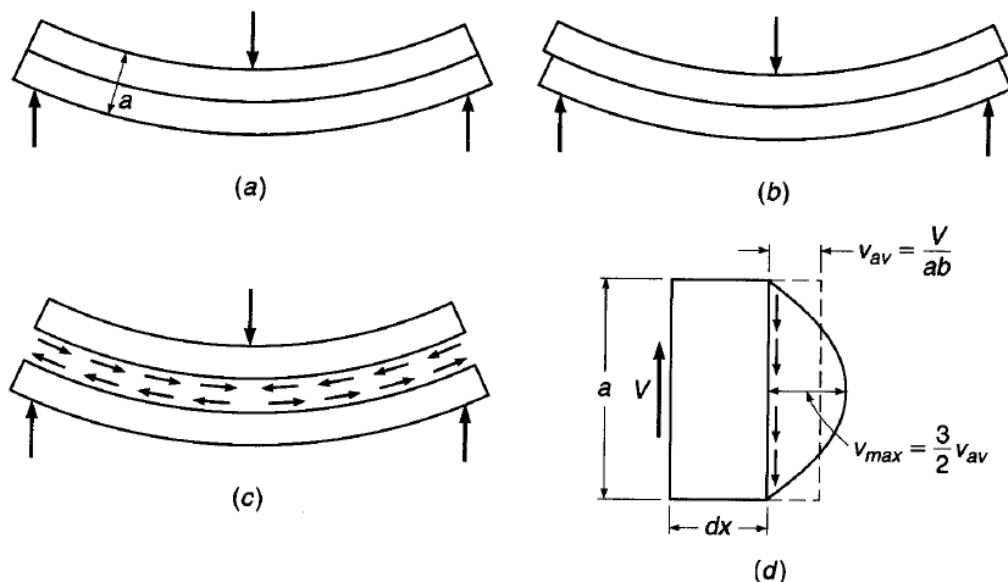


Figure 2-1: Shear in homogeneous rectangular beams (Arthur H. Nilson et al., 2010)

Evidently, then, when the adhesive is effective, there are forces or stresses acting in it that prevent this sliding or shearing. These horizontal shear stresses are shown in Figure 2-1c as they act, separately, on the top and bottom pieces. The same stresses occur in horizontal planes in single-piece beams; they are different in intensity at different distances from the neutral axis.

Figure 2-1d shows a differential length of a single-piece rectangular beam acted upon by a shear force of magnitude V . Upward translation is prevented; i.e., vertical equilibrium is provided by the vertical shear stresses ν . Their average value is equal to the shear force divided by the cross-sectional area $\nu_{av} = V / ab$, but their intensity varies over the depth of the section. The shear stress is zero at the outer fibers and has a maximum of $1.5\nu_{av}$ at the neutral axis, the variation being parabolic. If a small square element located at the neutral axis of such a beam is isolated as shown in Figure 2-2b, the vertical shear stresses on it, equal and opposite on the two faces for reasons of equilibrium, act as shown. However, if these were the only stresses present, the element would not be in equilibrium; it would spin. Therefore, on the two horizontal faces there exist equilibrating horizontal shear stresses of the same magnitude. That is, at any point within the beam, the horizontal shear stresses of Figure 2-2b are equal in magnitude to the vertical shear stresses of Figure 2-2d.

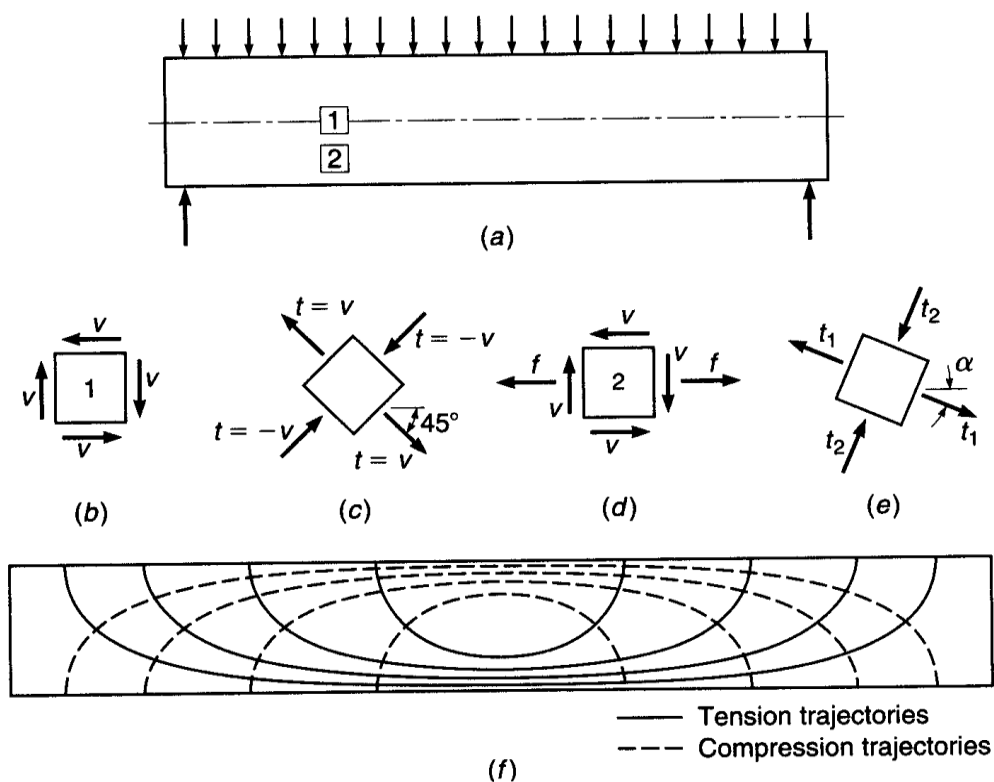


Figure 2:2: Stress trajectories in homogeneous rectangular beam

(Arthur H. Nilson et al., 2010)

It is proved in any strength-of-materials text that on an element cut at 45° these shear stresses combine in such a manner that their effect is as shown in Figure 2-2c. That is, the action of the two pairs of shear stresses on the vertical and horizontal faces is the same as that of two pairs of normal stresses, one tensile and one compressive, acting on the 45° faces and of numerical value equal to that of the shear stresses. If an element of the beam is considered that is located neither at the neutral axis nor at the outer edges, its vertical faces are subject not only to the shear stresses but also to the familiar bending stresses. The six stresses that now act on the element can again be combined into a pair of inclined compressive stresses and a pair of inclined tensile stresses that act at right angles to each other. They are known as principal stresses (Figure 2-2e).

Since the magnitudes of the shear stresses ν and the bending stresses f change both along the beam and vertically with distance from the neutral axis, the inclinations as well as the magnitudes of the resulting principal stresses also vary from one place to another. Figure 2-2f shows the inclinations of these principal stresses for a uniformly loaded rectangular beam. That is, these stress trajectories are lines which, at any point, are drawn in that direction in which the particular principal stress, tension or compression, acts at that point. It is seen that at the neutral axis the principal stresses in a beam are always inclined at 45° to the axis. In the vicinity of the outer fibers they are horizontal near mid span.

An important point follows from this discussion. Tensile stresses, which are of particular concern in view of the low tensile strength of the concrete, are not confined to the horizontal bending stresses f that are caused by bending alone. Tensile stresses of various inclinations and magnitudes, resulting from shear alone (at the neutral axis) or from the combined action of shear and bending, exist in all parts of a beam and can impair its integrity if not adequately provided for. It is for this reason that the inclined tensile stresses, known as diagonal tension, must be carefully considered in reinforced concrete design.

2.2.2 Behavior and Strength of beams failing in shear [8]

2.2.2.1 Modes of Inclined Cracking and Shear Failure

Shear failures of beams are characterized by the occurrence of inclined cracks. In some cases inclined cracking is immediately followed by member failure and in other cases, the inclined cracks stabilize and substantially more shear force may be applied before the member fails.

Inclined cracks in the web of a beam may develop either before a flexural crack occurs in their vicinity or as an extension of a previously developed flexural crack. The first type of inclined crack is often referred to as a “web-shear crack”, see Figure 2-3 a. The second type is often identified as a

“flexural-shear crack;” and the flexural crack causing the inclined crack is referred to as the “initiating flexural crack”, see Figure 2-3 b. in addition to the primary cracks (flexural and the two types of inclined cracks), secondary cracks often result from splitting forces developed by the deformed bars when slip between concrete and steel reinforcement occurs, or from dowel action forces in the longitudinal bars transferring shear across the crack.

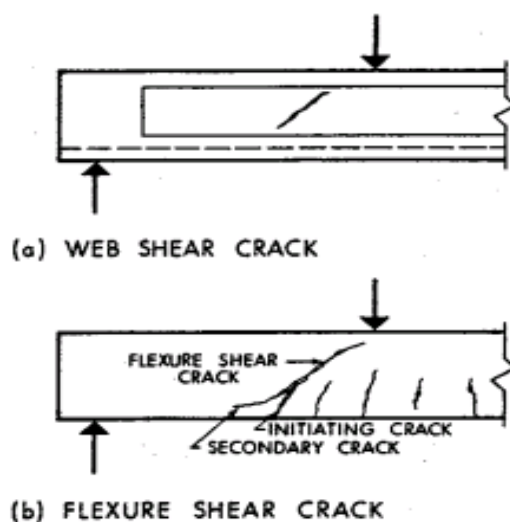


Figure 2:3: Types of Inclined Cracks
(ASCE-ACI Task Committee 426, June 1973)

In addition to the primary cracks (flexural and the two types of inclined cracks), secondary cracks often result from splitting forces developed by the deformed bars when slip between concrete and steel reinforcement occurs, or from dowel action forces in the longitudinal bars transferring shear across the crack. The manner in which inclined cracks develop and grow and the type of failure that subsequently develops is strongly affected by the relative magnitudes of the shearing stress, v , and flexural stress, f .

The variation in the inclined cracking load and shear capacity of rectangular beams may be conveniently considered as a function of varying a/d , i.e., the ratio of shear-span, a to depth, d . When all other things are kept constant, the influence of the a/d ratio on the cracking of rectangular simply supported reinforced concrete beam can be illustrated by considering beams of varying slenderness with two symmetrically placed concentrated loads placed a distance, a , from the supports.

(a) Normal and Long Beams of Rectangular Cross Section ($a/d > 2.5$)

Very shallow beams will usually fail in flexure (Figure 2-4(a)). The first crack will form due to flexural tension at the cross section of maximum moment. As the beam load increases prior to failure, the tensile cracking may spread to regions of lesser moment, but failure occurs in flexure near the section of maximum moment. For a beam with somewhat smaller value of a/d , the fatal crack may well be a flexure-shear crack, as shown in figure 2-3 (b). Such a crack may cause the beam to fail before its full flexural capacity is developed. In moderately slender beams one of the cracks may continue to propagate through the beam with further load until at some stage it becomes unstable and extends through the beam as shown in Figure 2.4 (b). This type of failure is called a “diagonal tension failure.”

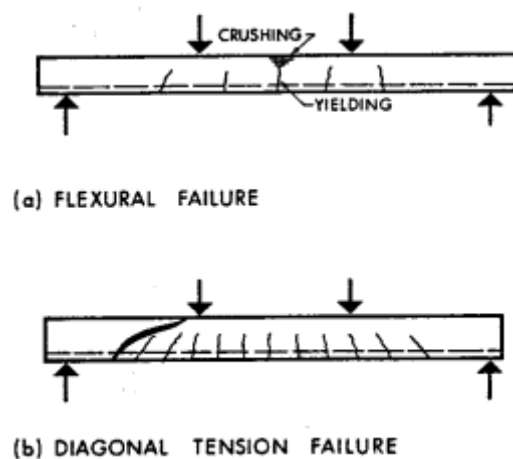


Figure 2:4: Failures of Slender Beams
(ASCE-ACI Task Committee 426, June 1973)

(b) Short Beams: $1 < a/d < 2.5$

A curved tensile crack in a region of combined moment and shear may also trigger one of two additional modes of failure. A secondary crack may propagate backward along the longitudinal reinforcement from the inclined crack, perhaps because of dowel action in the longitudinal reinforcement (Figure 2-5(a)). This crack will cause a loss of bond. As the main reinforcement begins to slip, the wedging action of the bar deformations contributes to the crack, resulting in an anchorage failure of the longitudinal reinforcement, called a “shear-tension” failure. Alternatively, the concrete above the upper end of the inclined crack may fail by crushing (Figure 2-5(b)) resulting in a “shear-compression” failure.

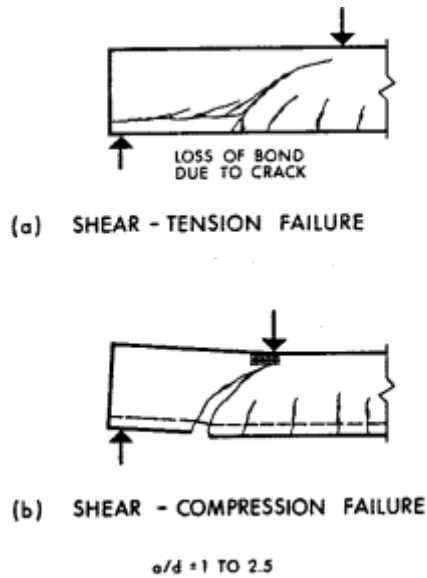


Figure 2:5: Typical Shear Failure in Short Beams
(ASCE-ACI Task Committee 426, June 1973)

(c) Deep Beams: $0 < a/d < 1$

In the design of deep beams, shearing stresses and vertical normal stresses require more consideration than flexural stresses. Significant principal compression and tensions, respectively, exist along and across the line joining the load and the reactions, and inclined cracks occur immediately inside the reaction plates (Figure 2-6). The numbering in Figure 2-6 correspond to the following modes of failure: (1) Anchorage failure of the tension reinforcement, usually combined with a dowel splitting effect; (2) Crushing failure at the reactions; (3) flexural failure-either of the steel reinforcement due to yielding or fracture, or of the “crown of the arch” when the concrete crushes; or (4) tension failure of the “arch-rib” by cracking over the support; followed by (5) crushing along the crack.

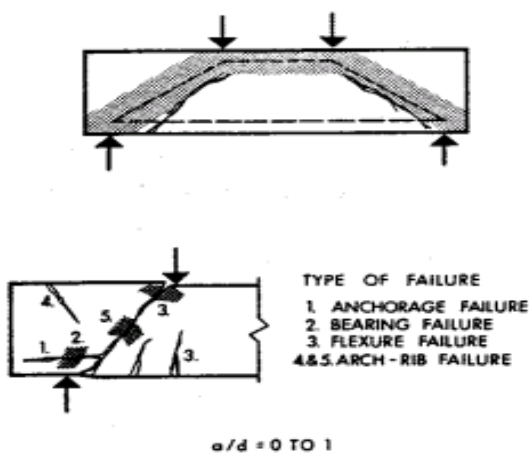


Figure 2:6: Modes of Failure of Deep Beams
(ASCE-ACI Task Committee 426, June 1973)

2.2.2.2 Behavior of beams without web reinforcement

The behavior of beams failing in shear varies widely, depending on the relative contributions of beam action and arch action and the amount of web reinforcement.

The moments and shear at inclined cracking and failure of rectangular beams without web reinforcement are plotted in the Figure 2-7 as a function of the ratio of the shear span a to the depth d .

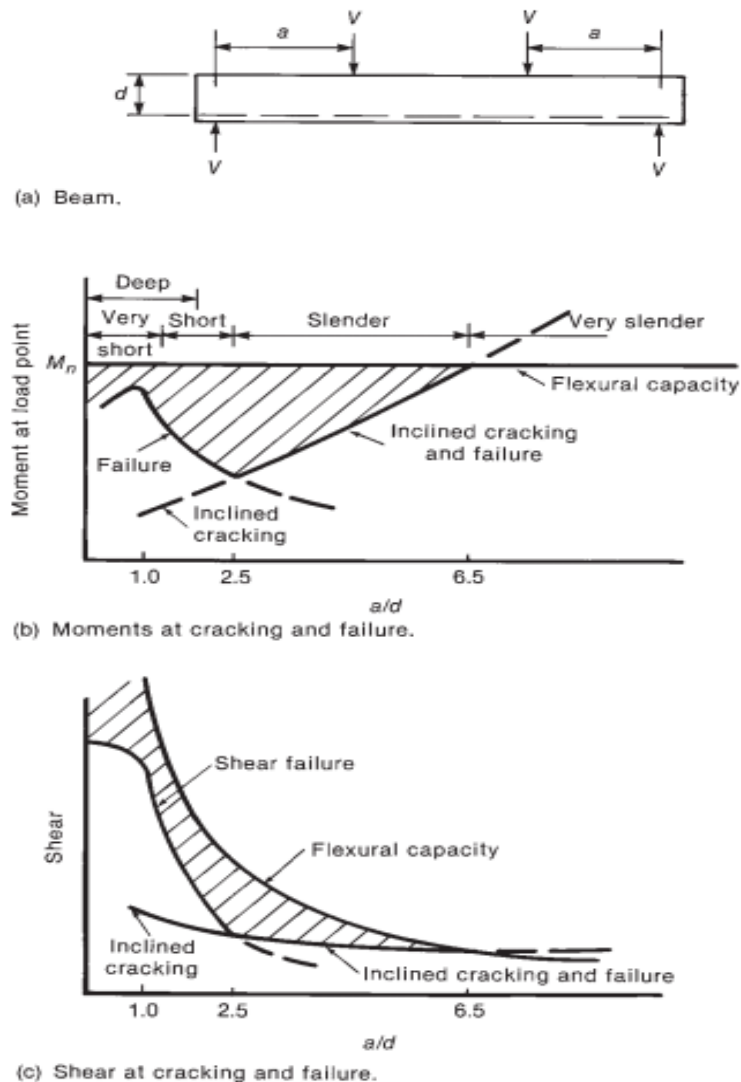


Figure 2-7: Effect of a/d ratio on shear capacity of beams (McGregor et al., 2012)

The beam cross section remains constant as the span is varied. The maximum moment capacity, M_n , of the cross section plotted as a horizontal line in Figure 2-7(b). The shaded areas in this figure show the reduction in strength due to shear. Web reinforcement is normally provided to ensure that the beam reaches the full flexural capacity, M_n .

The figure suggests that the shear spans can be divided into three types: short, slender, and very slender shear spans. The term deep beam is also used to describe beams with short shear spans. Very short shear spans, with a/d from 0 to 1, develop inclined cracks joining the load and the support. These cracks, in effect, destroy the horizontal shear flow from the longitudinal steel to the compression zone, and the behavior changes from beam action to arch action. Here, the reinforcement serves as the tension ties of a tied arch and has a uniform tensile force from support to support. The most common mode of failure in such beams is an anchorage failure at the ends of the tension tie.

Short shear spans with a/d from 1 to 2.5 develop inclined cracks and, after a redistribution of internal forces, are able to carry additional load, in part by arch action. The final failure of such beams will be caused by bond failure, a splitting failure, or a dowel failure along the tension reinforcement or by crushing of the compression zone over the top of the crack. The latter is referred to as a shear compression failure. Because the inclined crack generally extends higher into the beam than does a flexural crack, failure occurs at less than the flexural moment capacity.

In slender shear spans, those having a/d from about 2.5 to about 6, the inclined cracks disrupt equilibrium to such an extent that the beam fails at the inclined cracking load. Very slender beams, with a/d greater than about 6, will fail in flexure prior to the formation of inclined cracks.

It is important to note that, for short and very short beams, a major portion of the load capacity after inclined cracking is due to load transfer by the compression struts. If the beam is not loaded on the top and supported on the bottom, these compression struts will not form and failure occurs at, or close to the inclined cracking load.

Because the moment at the point where the load is applied is $M = Va$ for a beam loaded with concentrated loads. Figure 2-7(b) can be reported in terms of shear capacity. The shear corresponding to a flexural failure is the upper curved line. If web reinforcements are not provided, the beam will fail at the shear given by the “shear failure” line. This is roughly constant for a/d greater than about 2. Again, the shaded area indicates the loss in capacity due to shear. Note that the inclined cracking loads of the short shear spans and slender shear spans are roughly constant. This is recognized in design by ignoring a/d in the equations for the shear at inclined cracking. In case of slender beams, inclined cracking causes an immediate shear failure if no web reinforcement is provided.

The forces transferring shear across an inclined crack in a beam without web reinforcements are illustrated in Figure 2-8.

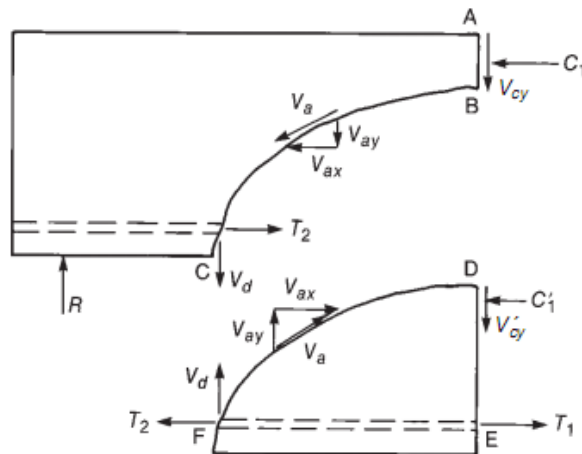


**Figure 2:8: Internal forces in a cracked beam without web reinforcements
(McGregor et al., 2012)**

Shear is transferred across line A-B-C by V_{cy} , the shear in the compression zone, by V_{ay} , the vertical component of the shear transferred across the crack by interlock of the aggregate particles on the two faces of the crack, and by V_d , the dowel action of the longitudinal reinforcement. Immediately after inclined cracking, as much as 40 to 60 percent of the total shear is carried by V_d and V_{ay} together.

Considering D-E-F portion of the beam below the crack and summing moments about the reinforcement at point E shows that V_d and V_a cause a moment about E that must be equilibrated by a compression force C_1' . Horizontal force equilibrium on section A-B-D-E shows that $T_1 = C_1 + C_1'$, and finally, T_1 and $C_1 + C_1'$ must equilibrate the external moment at this section.

As the crack widens, V_a decreases, increasing the fraction of the shear resisted by V_{cy} and V_d . The dowel shear, V_d , leads to a splitting crack in the concrete along the reinforcement. When this crack occurs, V_d drops, approaching zero. When V_a and V_d disappear, so do V_{cy}' and C_1' , with the result that all the shear and compression are transmitted in the depth AB above the crack. At this point in the life of the beam, the section A-B is too shallow to resist the compression forces needed for equilibrium. As a result, this region crushes or buckles upward.

Note also that if $C_1' = 0$, then $T_2 = T_1$, and as a result, $T_2 = C_1$. In other words, the inclined crack has made the tensile force at point C a function for the moment at section A-B-D-E. This shift in the tensile force must be considered in detailing the bar cut off points and in anchoring the bars.

2.2.2.3 Factors affecting the shear strength of beams without web reinforcement [10]

Beams without web reinforcement will fail when inclined cracking occurs or shortly afterwards. For this reason, the shear capacity of such members is taken equal to the inclined cracking shear. The inclined cracking load of a beam is affected by five principal variables, some included in design equations and others not.

- Tensile strength of concrete

The inclined cracking load is a function of the tensile strength of the concrete, f_{ct} . The stress state in the web of the beam involves biaxial principal tension and compression stresses. A similar biaxial state of stress exists in a split-cylinder tension test, and the inclined cracking load is frequently related to the strength from such a test. As discussed earlier, the flexural cracking that precedes the inclined cracking disrupts the elastic-stress field to such an extent that inclined cracking occurs at a principal tensile stress roughly half of f_{ct} for the uncracked section.

- Longitudinal reinforcement ratio, ρ_w

When the steel ratio, ρ_w , is small, flexural cracks extend higher into the beam and open wider than would be the case for large values of ρ_w . And increase in crack width causes a decrease in the maximum values of the components of shear, V_d and V_{ay} , that are transferred across the inclined cracks by dowel action or by shear stresses on the crack surfaces. Eventually, the resistance along the crack drops below that required to resist the loads, and the beam fails suddenly in shear.

- Shear span to depth ratio, a/d

The shear span to depth ratio, a/d or MV/d , affects the inclined cracking shears and ultimate shears of portions of members with a/d less than 2.

- Lightweight aggregate concrete

Lightweight aggregate concrete has a lower tensile strength than normal weight concrete for a given concrete compressive strength. Because the shear strength of a concrete member without shear

reinforcement is directly related to the tensile strength of a concrete, equations for shear capacity must be modified for members constructed with light weight concrete.

- Size of beam

An increase in the overall depth of a beam with very little (or no) web reinforcement results in a decrease in the shear at failure for a given f_c' , ρ_w , and a/d. The width of an inclined crack depends on the product of the strain in the reinforcement crossing the crack and the spacing of the cracks. With increasing beam depth, the crack spacing and the crack widths tend to increase. This leads to a reduction in the maximum shear stress that can be transferred across the crack by aggregate interlock. An unstable situation develops when the shear stresses transferred across the crack exceeds the shear strength. When this occurs, the faces of the crack slip, one relative to the other.

- Axial forces

Axial tensile forces tend to decrease the inclined cracking load, while axial compressive forces tend to increase it. As the axial compressive force is increased, the onset of flexural cracking is delayed, and the flexural cracks do not penetrate as far into the beam. Axial tension forces directly increase the tension stress, and hence the strain, in the longitudinal reinforcement. This causes an increase in the inclined crack width, which, in turn, results in a decrease in the maximum shear tension stress that can be transmitted across the crack. This reduces the shear failure load.

A similar increase is observed in pre-stressed concrete beams. The compression due to pre-stressing reduces the longitudinal strain, leading to a higher failure load.

- Coarse aggregate size

As the size (diameter) of the coarse aggregate increases, the roughness of the crack surfaces increases, allowing higher shear stresses to be transferred across the cracks. In high strength concrete beams and some light weight concrete beams, the cracks penetrate pieces of the aggregate rather than going around them, resulting in a smoother crack surface. This decrease in the shear transferred by aggregate interlock along the cracks reduces V_c .

2.2.2.4 Behavior of beams with web reinforcement

Inclined cracking causes the shear strength of beams to drop below the flexural capacity. The purpose of web reinforcement is to ensure that the full flexural capacity can be developed.

Prior to inclined cracking, the strain in the web reinforcement is equal to the corresponding strain of the concrete. Because concrete cracks at a very small strain, the stress in the web reinforcements prior to inclined cracking will not exceed 3 to 6 ksi. Thus, web reinforcements do not prevent inclined cracks from forming; they come into play after the cracks have formed.

The forces in a beam with web reinforcements and an inclined crack are shown in Figure 2-9.

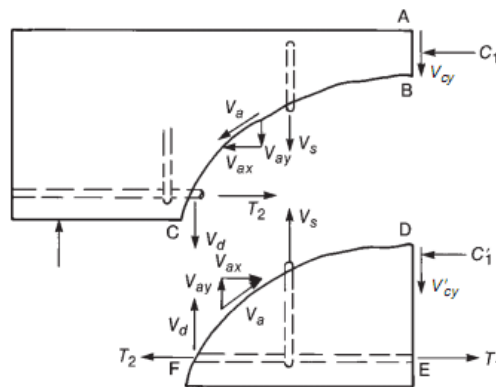


**Figure 2:9: Internal forces in a cracked beam with web reinforcements
(McGregor et al., 2012)**

The shear transferred by tension in the web reinforcements, V_s , does not disappear when the crack opens wider, so there will always be a compression force C_1' and a shear force V_{cy}' acting on the part of the beam below the crack. As a result, T_2 will be less than T_1 , the difference depending on the amount of web reinforcement. The force T_2 will however, be larger than the flexural tension $T = M / jd$ based on the moment at C. The loading history of such a beam is shown qualitatively in Figure 2-9.

The components of the internal shear resistance must equal the applied shear, indicated by the upper 45° line. Prior to flexural cracking, the entire shear is carried by the uncracked concrete. Between flexural and inclined cracking, the external shear is resisted by V_{cy} , V_{ay} , and V_d . Eventually, the web reinforcements crossing the crack yield, and stay constant for higher applied shears. Once the web reinforcements yield, the inclined crack opens more rapidly. As the inclined crack widens, V_{ay} and V_{ax} decrease further, forcing V_{cy} and V_d to increase at an accelerated rate, until either a splitting (dowel) failure occurs, the compression zone crushes due to combined shear and compression, or the web crushes.

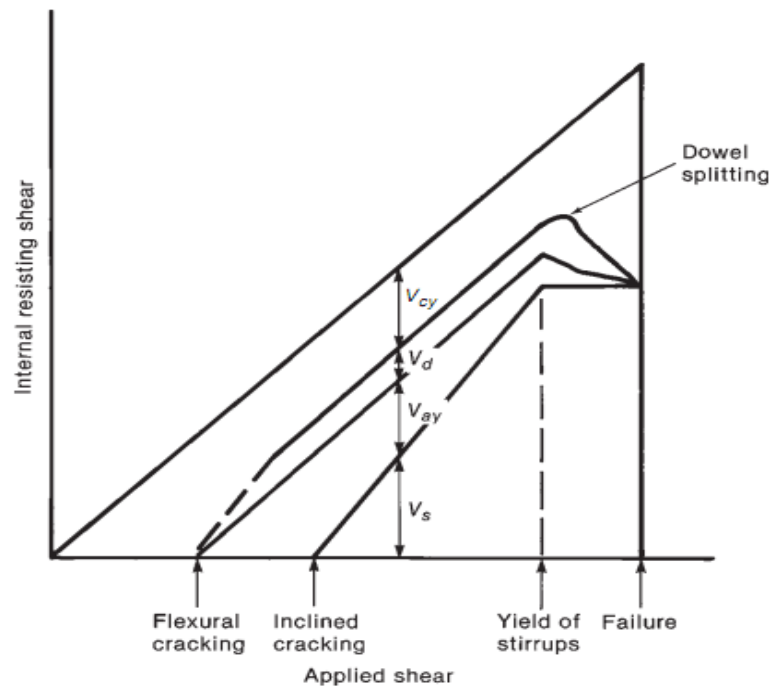


**Figure 2:10: Distribution of Internal shears in a beam with web reinforcement
(McGregor et al., 2012)**

Each of the components of this process except V_s has a brittle load-deflection response. As a result, it is difficult to quantify the contributions of V_{cy} , V_d , and V_{ay} . In design, these are lumped together as V_c , referred to somewhat incorrectly as “the shear carried by the concrete.” Thus, the nominal shear strength, V_n , is assumed to be

$$V_n = V_c + V_s \quad (3)$$

2.3 Historical Development of Shear Design Provision [12]

Most codes of practice use sectional methods for design of conventional beams under bending and shear. ACI building Code 318-95M assumes that flexure and shear can be handled separately for the worst combination of flexure and shear at a given section.

In the early 1900s, truss models were used as conceptual tools in the analysis and design of reinforced concrete beams. Ritter (1989) postulated that after a reinforced concrete beam cracks due to diagonal tension stresses, it can be idealized as a parallel chord truss with compression diagonals inclined at 45° with respect to the longitudinal axis of the beam. Morsch (1920, 1922) later

introduced the use of truss models for torsion. These truss models neglected the contribution of the concrete in tension. Withey (1907, 1908) introduced Ritter's truss model into the American literature and pointed out that this approach gave conservative results when compared with test evidence. Talbot (1909) confirmed this finding.

Historically, shear design in the United States has included a concrete contribution, V_c , to supplement the 45° sectional truss model to reflect test results in beams and slabs with little or no shear reinforcement and to ensure economy in the practical design of such members. ACI Standard Specification No. 23 (1920) permitted an allowable shear stress of $0.025f'_c$, but not more than 0.41 MPa, for beams without web reinforcement, and with longitudinal reinforcement that did not have 'mechanical anchorage.' If the longitudinal reinforcement was anchored with 180° hooks or with plates 'rigidly connected' to the bars, the allowable shear stress was increased to $0.03f'_c$ or a maximum of 0.62 MPa. Web reinforcement was designed by the equation

$$A_v f_v = V' s \sin \alpha / jd \quad (4)$$

Where

A_v	area of shear reinforcement within distance s
f_v	allowable tensile stress in the shear reinforcement
Jd	flexural lever arm
V'	total shear minus $0.02f'_c bjd$ (or $0.03f'_c bjd$ with special anchorage)
B	width of the web
S	spacing of shear steel measured perpendicular to its direction
α	angle of inclination of the web reinforcement with respect to the horizontal axis of the beam.

The limiting value for the allowable shear stresses at service load was $0.06f'_c$ or a maximum of 1.24 MPa, or with anchorage of longitudinal steel $0.12f'_c$ or a maximum of 2.48 MPa. This shear stress was intended to prevent diagonal crushing failures of the web concrete prior to yielding of the web reinforcements. These specifications of the code calculated the nominal shear stress as $v = V / bjd$.

This procedure, which formed the basis for future ACI codes, lasted from 1921 to 1951, with each edition providing somewhat less conservative design procedures. In 1951 the distinction between members with and without 'mechanical anchorage' was omitted and replaced by the requirement that all plain bars must be hooked, and deformed bars must meet ASTM A 305. Therefore, the maximum allowable shear stress on the concrete for beams without web reinforcement (ACI 318-51) was $0.03f'_c$, and the maximum allowable shear stress for beams with web reinforcement was $0.12f'_c$.

ACI 318-51, based on allowable stresses, specified that web reinforcement must be provided for the excess shear if the shear stress at service loads exceeded $0.03f'_c$. Calculation of the area of shear reinforcement continued to be based on a 45° truss analogy in which the web reinforcement must be designed to carry the difference between the total shear and the shear assumed to be carried by the concrete.

The August 1955 shear failure of beams in the warehouse of Wilkins Air Force Depot in Shelby, Ohio, brought into question the traditional ACI shear design procedures. These shear failures, in conjunction with intensified research, clearly indicated that shear and diagonal tension was a complex problem involving many variables and resulted in a return to forgotten fundamentals.

Talbot (1909) pointed out the fallacies of such procedures as early as 1908 in talking about the failure of beams without web reinforcement. Based on 106 beam tests, he concluded that

“It will be found that the value of shear stress at failure will vary with the amount of reinforcement, with the relative length of the beam, and with other factors which affect the stiffness of the beam... In beams without web reinforcement, web resistance depends upon the quality and strength of the concrete... The stiffer the beam the larger the vertical stresses which may be developed. Short, deep beams give higher results than long slender ones, and beams with high percentage of reinforcement [give higher results] than beams with a small amount of metal.”

Unfortunately, Talbot's findings about the influence of the percentage of longitudinal reinforcement and the length-to-depth ratio were not reflected in the design equations until much later. The research triggered by the 1956 Wilkins warehouse failures brought these important concepts back to the forefront.

More recently, several design procedures were developed to economize on the design of the web reinforcement one approach has been to add a concrete contribution term to the shear reinforcement capacity obtained, assuming a 45° truss (for example, ACI Building Code 318-95). Another procedure has been the use of a truss with a variable angle of inclination of the diagonals. The inclination of the truss diagonals is allowed to differ from 45° within certain limits suggested on the basis of the theory of plasticity. This approach is often referred to as the ‘standard truss model with no concrete contribution,’ and is explained by the existence of aggregate interlock and dowel forces in the cracks, which allow a lower inclination of the compression diagonals and the further

mobilization of the web reinforcement. A combination of the variable-angle truss and a concrete contribution has also been proposed. This procedure has been referred to as the modified truss model approach (CEB 1978; Ramirez and Breen 1991). In this approach, in addition to a variable angle of inclination of the diagonals, the concrete contribution for non pre-stressed concrete members, the concrete contribution is not considered to vary with the level of shear stress. For pre-stressed concrete members, the concrete contribution is not considered to vary with the level of stress and is taken as a function of the level of pre-stress and the stress in the extreme tension fiber.

As mentioned previously, the truss model does not directly account for the components of the shear failure mechanism, such as aggregate interlock and friction, dowel action of the longitudinal steel, and shear carried across un cracked concrete. For pre-stressed beams, the larger the amount of pre-stressing is the lower the angle of inclination at first diagonal cracking. Therefore, depending on the level of compressive stress due to pre-stress, pre-stressed concrete beams typically have much lower angles of inclined cracks at failure than non pre-stressed beams and hence require smaller amounts of web reinforcements.

Traditionally in North American practice, the additional area of longitudinal tension steel for shear has been provided by extending the bars a distance equal to d beyond the flexural cutoff point. Although adequate for a truss model with 45° diagonals, this detailing rule is not adequate for trusses with diagonals inclined at lower angles. The additional longitudinal tension force due to shear can be determined from equilibrium conditions of the truss model as $V \cot \theta$, with θ as the angle of inclination of the truss diagonals. Because the shear stresses are assumed uniformly distributed over the depth of the web and the tension acts at the section mid-depth.

The upper limit of shear strength is established by limiting the stress in the compression diagonals, f_d , to a fraction of the concrete cylinder strength. The concrete in the cracked web of a beam is subjected to diagonal compressive stresses that are parallel or nearly parallel to the inclined cracks. The compressive strength of this concrete must be established so as to prevent web crushing failures. The strength of this concrete is a function of (1) the presence or absence of cracks and the orientation of these cracks; (2) the tensile strain in the transverse direction; and (3) the longitudinal strain in the web.

The pioneering work from Ritter and Morsch received new impetus in the period from the 1960s to the 1980s, and therefore in more recent design codes modified truss models are used. Attention was focused on the truss model with diagonals having a variable angle of inclination as a viable model

for shear and torsion in reinforced and pre-stressed concrete beams (Kupfer 1964; Caflisch et al. 1971; Lampert and Thurlimann 1971; Thurlimann et al. 1983). Further development of plasticity theories extended the applicability of the model to non-yielding domains (Nielsen Braestrup 1975; Muller 1978; Marti 1980). Schlaich et al. (1987) extended the truss model for beams with uniformly inclined diagonals, all parts of the structure in the form of strut-and-tie models (STM). This approach is particularly relevant in regions where the distribution of strains is significantly nonlinear along the depth. Schlaich et al. introduced the concept of D and B regions, where, where D stands for discontinuity or disturbed, and B stands for beam or Bernouli. In D regions the distribution of strains is nonlinear, whereas the distribution is linear in B regions. A structural concrete member can consist entirely of a D region; however, more often D and B regions will exist within the same member or structure. In this case, D regions extend a distance equal to the member depth away from any discontinuity, such as a change in cross section or the presence of concentrated loads. For typical slender members, the portions of the structure or member between D regions are B regions.

By analyzing a truss model consisting of linearly elastic members and neglecting the concrete tensile strength, Kupfer (1964) provided a solution for the inclination of the diagonal cracks. Collins and Mitchell (1980) abandoned the assumption of linear elasticity and developed the compression field theory (CFT) for members subjected to torsion and shear. Based on extensive experimental investigation, Vecchio and Collins (1982, 1986) presented the modified compression field theory (MCFT), which included a rationale for determining the tensile stresses in the diagonally cracked concrete. Although the CFT works well with medium to high percentages of transverse reinforcement, the MCFT provides a more realistic assessment for members having a wide range of amount of transverse reinforcement including the case of no web reinforcement. Parallel to these developments of the truss model with variable strut inclinations and the CFT, the last decade also saw the further development of shear friction theory. In addition, a general theory was developed for beams in shear using constitutive laws for friction and by determining the strains and deformations in the web. Because this approach considers the discrete formation of cracks, the crack spacing and crack width must be determined and equilibrium checked along the crack to evaluate the crack-slip mechanism of failure.

2.4 Shear Design Models for Members without Transverse Reinforcement [12]

2.4.1 Fracture Mechanics Approaches

Fracture mechanics approaches account for the fact that there is a peak tensile stress near the tip of a crack and a reduced tensile stress (softening) in the cracked zone. For the case of a beam that fails in shear due to the propagation of a single critical diagonal crack, fracture mechanics can be considered a more rational approach than empirical methods. This approach offers a possible explanation for the size effect in shear.

A number of different fracture mechanics models have been proposed over recent years. Among them, two well known ones are the fictitious crack model, by Hillerborg et al. (1976), and the crack band model, by Bazant and Oh (1983). A survey of fracture mechanics applications was recently given by Reinhardt (1986). Further information on fracture mechanics can be found in the 1989 ACI Committee 446 state-of-the-art report.

Fracture mechanics approaches are usually numerically demanding because of the complexity of the tensile stress-crack displacement relationships. As a result, empirical formulas are sometimes developed in terms of fracture mechanics parameters, like that by Bazant and Kim (1984) or Rimmel (1994). These equations give little explanation of structural behavior, so the end result is often very similar to empirical formulas, as was pointed out by Walraven (1987).

2.4.2 Simple Strut-and-Tie Models

The application of strut-and-tie models, which has its theoretical basis from the lower-bound theorem of plasticity (Drucker 1961; Nielsen et al. 1978; Marti 1985), requires a minimum amount of distributed reinforcement in all directions (including transverse reinforcement) to ensure sufficient ductility for redistribution of internal stresses after cracking. In the elastic stress distribution of deep members, significant shear is transmitted directly to the support by diagonal compression. This means that less redistribution is required after cracking, and it would seem reasonable to apply strut-and-tie models (cautiously) to deep members without transverse reinforcement. When members are very deep, all of the shear will be transferred directly to the support by compression stresses; however, premature failure of a compression strut without minimum distributed reinforcement may result from transverse splitting due to spreading of compression stress (Schlaich et al. 1987). Walraven and Lehwalter (1994) carried out tests to investigate the capacity increase beyond that due to spreading of the compression stress; in a bottle-like shape, they proposed a failure criterion for the compression strut that included a size effect.

The simple strut-and-tie approach has also been suggested for more slender members without transverse reinforcement; however, this may result in an unsafe solution, as shown in Figure 2-10. Solutions have been suggested using a reduced compressive strength of the strut. One method (Collins and Mitchell 1986) for accomplishing this involves considering strain compatibility between the concrete strut and tension tie. As the strut becomes flatter, the transverse tensile strain in the strut increases, which reduces the diagonal "crushing" strength of concrete (Vecchio and Collins 1986). An alternate approach is that of Braestrup (1990), where the maximum diagonal compressive stress is not related to the strut inclination, but the shear capacity reduces with increasing shear span because of the geometry of the nodal zone, which depends on the support dimension, the cover-to-Longitudinal reinforcement, and an assumed hydrostatic stress in the nodal zones.

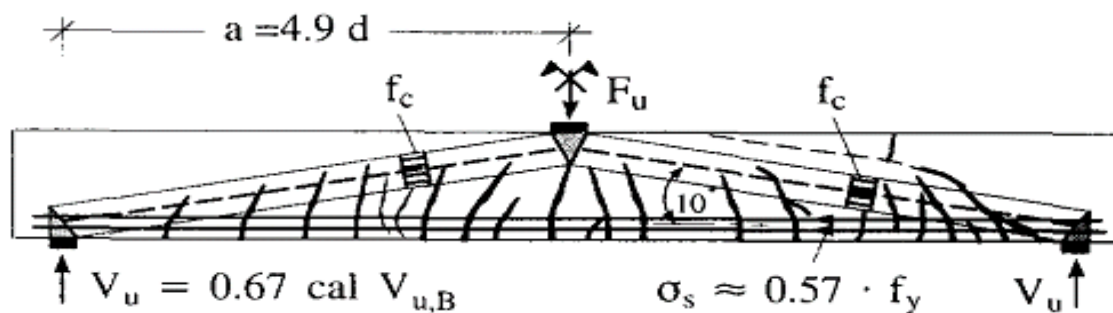


Figure 2:11: Crack Pattern at Shear Failure of Beam with Unsafe Strut-and-Tie Model(Kupfer and Gerstle 1973)

2.4.3 Tooth Model for Slender Members

An early attempt to develop a rational model to explain flexure-shear cracking was Kani's tooth model (1964), in which the secondary diagonal cracks were believed to result from bending of concrete "teeth." The concrete between two adjacent flexural cracks was considered to be analogous to a tooth in a comb (Figure 2-11). The concrete teeth were assumed to be free cantilevers fixed in the compression zone of the beams and loaded by the horizontal shear from bonded reinforcement.

Kani's model was evaluated by Fenwick and Paulay (1968) as well as Taylor (1974), who pointed out that the teeth are restricted from bending freely by the friction of the crack faces and the dowel action of the longitudinal reinforcement. Tooth models have been developed further to include these mechanisms (MacGregor and Walters 1967; Hamadi and Regan 1980; Reineck 1991c). With his tests, Chana (1987) confirmed the basic mechanisms of the tooth model by extensive measurements of the deformations prior to failure.

The main features of the tooth model are that discrete cracks are assumed and assumptions have to be made for the inclination and spacing of the cracks. Hamadi and Regan (1980) assume that the cracks are vertical and that their spacing is equal to half the effective depth ($s = d/2$) for a particular beam, whereas Reineck (1991c) assumes the cracks are inclined at 60° with a spacing of 70% of the crack height determined from a flexural analysis; i.e., $s = 0.7(d - c)$, where c = depth of compression. For a given crack spacing, the shear displacement and crack width can be calculated if the strains are known. This requires kinematic considerations, but as a result, gives the actual contributions of the different shear transfer mechanisms in the highly indeterminate system.

Based on extensive experimental work in interface shear, Hamadi and Regan (1980) developed a tooth model with simplified assumptions for the interface shear and the geometry of the tooth. Reineck (1991c) further developed the tooth model, considering all the shear transfer mechanisms, and carried out a full nonlinear calculation including compatibility. The distribution of the shear force on the different shear mechanisms was similar to those found earlier by Taylor (1974); interface shear was the dominant shear mechanism, and dowel action was important for heavily reinforced members

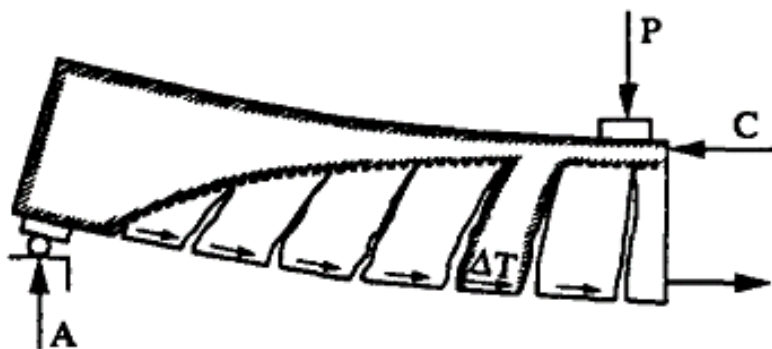


Figure 2:12: Kani's Tooth Model (Kani 1964)

Based on his mechanical model, Reineck (1991c) derived an explicit formula for the ultimate shear force, which for members without axial force or pre-stress is

$$V_u = \frac{0.4b_wdf_{ct} + V_{du}}{(1 + 0.054\lambda)} \quad (5)$$

Where

f_{ct} = axial tensile strength = $0.246f_c'^{2/3}$ (Mpa); and V_{du} = dowel force $[V_{du}/b_wdf_c' = 1.33\rho^{8/9}/(f_c')^{2/3}$, with f_c' in Mpa units and d in m]. The parameter λ is a dimension-free value for the crack width, which determines the friction capacity, and is defined by

$$\lambda = f_c' d / E_s \rho w_u \quad (6)$$

Where $w_u = 0.09$ mm = a limiting crack width; d = effective depth (mm); $E_s = 2,000,000$ (Mpa); and $\rho = A_s/b_wd$.

This parameter comprises the reinforcing ratio ρ and the depth d of the member; therefore, the formula can be presented in a simple diagram for the dimensionless shear force $v_u/f_c' = V_u/b_wdf_c'$ (Figure 2-12), in which the concrete tensile strength is the only parameter. Similar diagrams could be developed using the more common parameters ρ and d (Reineck 1991c). Comparisons showed that this theoretically derived formula matches the tests as well as many empirical formulas.

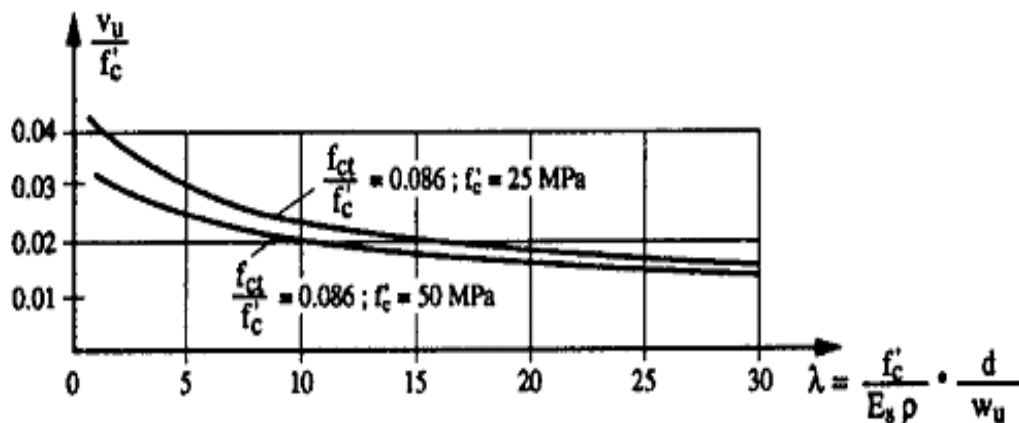


Figure 2:13: Dimensioning Diagram for Ultimate Shear Force Derived from Mechanical Model by Reineck (1991c).

2.4.4 Truss Models with Concrete Ties

Although it may be possible to extend the simple strut-and-tie model approach to more slender members, clearly a different approach is needed to capture the shear failure of very slender members without transverse reinforcement where the concrete tensile stresses have the major role. Marti (1980) extended the plasticity approach by using a Coulomb-Mohr yield criterion for concrete that includes tensile stresses. Schlaich et.al. (1987) suggested a refined strut-and-tie approach that includes concrete tension ties. Al-Nahlawi and Wight (1992) proposed a truss model with concrete compression struts inclined at either 45° or 35° and concrete tension ties perpendicular to the struts

(Figure 2-13). An empirical rule was used for limiting the tension tie force based on the geometry of the truss. Muttoni (1990) proposed a truss model for less slender members (Figure 2-14) in which, rather than going directly from the load point to the support, the inclined compression is bent around the initial flexural compression zone.

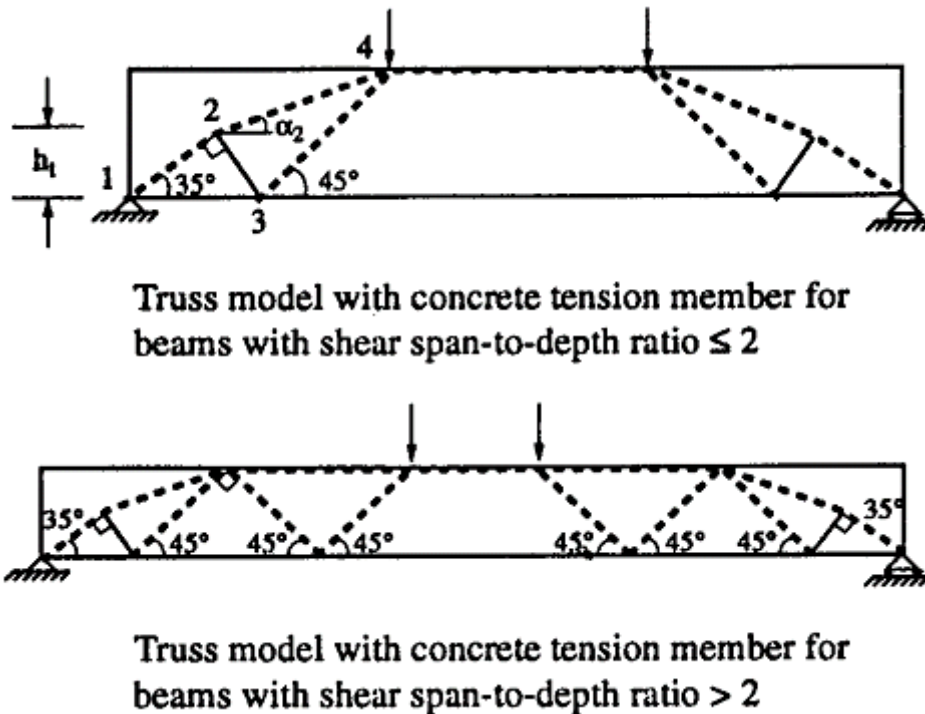


Figure 2:14: Refined Strut-and-Tie Models Proposed by Al-Nah-lawi and Wight (1992)

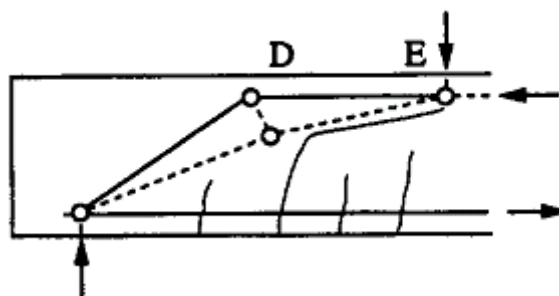


Figure 2:15: Refined Strut-and-Tie Models Proposed by Muttoni (1990)

Reineck (1991c, 1982) has shown that such truss models with concrete ties fully comply with the tooth model discussed above. In the tooth model, the state of the stress in the B region is defined by the stresses at the crack, but from these stresses, the principal stresses in the tooth between the cracks may also be determined. The dominant action due to the friction along the crack surfaces then results in a biaxial tension-compression field, shown in Figure 2-15(a) for constant friction stresses (Reineck 1982). The inclination of the principal compressive stress is equal to half the inclination of the

cracks, which Reineck assumes to be at 60° . The dowel action induces a concentrated tension force in the lower part of the tooth and results in bending of the tooth, which is resisted by friction stresses. Therefore, the strut-and-tie model of Figure 2-15(b) for the resulting state of stress shows, in the upper part of the tooth, an inclined stress field similar to Figure 2-15(a).

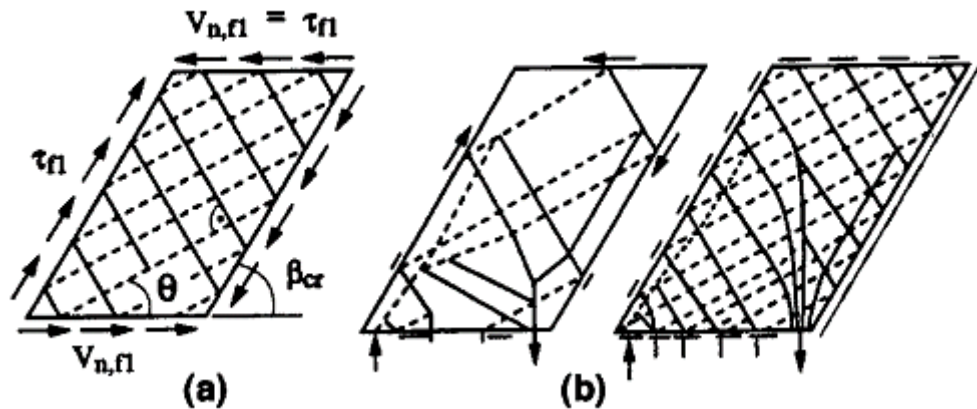


Figure 2:16: Refined Strut-and-Tie Model for Crack Friction and Dowel Action (Reineck 1991c): (a) Constant Friction Stresses; (b) Simple and Refined Strut-and-Tie Model for Dowel Action Combined with Friction

2.4.5 Modified Compression Field Theory

The modified compression field theory (Vecchio and Collins1986) can be implemented in different ways with varying levels of complexity, from a full, nonlinear finite-element analysis, to a multilayer sectional analysis that accounts for the variation of crack width over the section (Vecchio and Collins1988), to the simplest case where only the crack width at the level of the flexural tension reinforcement is considered (Collins and Mitchell 1991). The latter case, which is most suitable for design, is analogous to a variable-angle truss model with diagonal concrete tension ties.

The modified compression field theory is usually formulated in terms of average stresses; however, the method includes a check to ensure that the loads resisted by the average stresses can be transmitted across cracks. For members without transverse reinforcement, the stresses locally at a crack always control the capacity of the member, and the average stress calculation is used only in estimating the inclination of the critical diagonal crack. In calculating the stresses locally at a crack, it is assumed that the crack plane can resist only shear stress (no normal stress). As the horizontal plane must also be free of normal stress, the principal directions of the stresses locally at a crack must bisect the angles between the crack plane and the horizontal plane. In other words, the inclination of the principal compression stress (which is perpendicular to the direction of the

principal tension stress) is half the inclination of the diagonal cracks. One important consequence is that the shear stress on the crack plane is equal to the shear stress on the vertical and horizontal planes. Thus, the shear strength of a member is equal to the shear stress that can be resisted by the critical crack. Based on Walraven's experimental results (1981) for the maximum shear stress that can be resisted by a crack without the beneficial effects of compression, the shear resistance of a diagonally cracked member is given by

$$v_c \leq \frac{0.18\sqrt{f_c'}}{0.3 + \frac{24w}{(a_g + 16)}} \quad (7)$$

Where w = crack width; a_g = maximum aggregate size in mm; and f_c' is in MPa (Vecchio and Collins 1986).

As in the tooth models, the width of a crack depends on the assumed crack spacing; however, unlike in the tooth models, the crack spacing and the inclination of the diagonal cracks are not assumed a priori in the modified compression field theory. The crack spacing depends on the crack inclination. Cracks that are inclined at 90° to the member axis are assumed to have a spacing $S_x = d_v$ (for members with one layer of reinforcement), whereas cracks at other inclinations, β , are assumed to have a spacing $S_\theta = S_x/\sin\beta$. This simple expression reflects the fact that longitudinal reinforcement has less ability to control cracks as they become flatter (smaller β).

In the modified compression field theory, the inclination of diagonal cracks is calculated using a strain compatibility procedure involving average stresses and average strains. The diagonal cracks are assumed to be perpendicular to the principal tensile average stress direction. In that way, the influence of the loading (for example, the axial load and bending moment) on the inclination of the diagonal cracks (initial diagonal crack as well as the more important secondary diagonal cracks) are properly accounted for. For members without transverse reinforcement, the inclination of the diagonal cracks is given by

$$\theta = \tan^{-1} \left[\frac{\left(\frac{0.33\sqrt{f_c'}}{1 + \sqrt{500\varepsilon_s}} \right)}{v_c} \right] \quad (8)$$

Where the numerators within the bracket are an empirical expressions (Collins and Mitchell 1991) for the principal tensile average stress as a function of the principal tensile average strain ε_s .

When sections do not contain at least the minimum amount of shear reinforcement, the value of β can be calculated as

$$\beta = \frac{4.8}{(1+750\varepsilon_s)} \frac{51}{(39 + s_{xe})} \quad (9)$$

Table 2-1: Values of β and θ for members with less than minimum shear reinforcement (AASHTO LRFD, 1994)

s_{xe}^* (in)		Longitudinal Strain, $\varepsilon_x \times 1000$										
		≤ -0.20	≤ -0.10	≤ -0.05	≤ 0	≤ 0.125	≤ 0.25	≤ 0.50	≤ 0.75	≤ 1.00	≤ 1.50	≤ 2.00
≤ 5	θ	25.4°	25.5°	25.9°	26.4°	27.7°	28.9°	30.9°	32.4°	33.7°	35.6°	37.2°
	β	6.36	6.06	5.56	5.15	4.41	3.90	3.26	2.86	2.58	2.21	1.96
≤ 10	θ	27.6°	27.6°	28.3°	29.3°	31.6°	33.5°	36.3°	38.4°	40.1°	42.7°	44.7°
	β	5.78	5.78	5.38	4.89	4.05	3.52	2.88	2.50	2.23	1.88	1.65
≤ 15	θ	29.5°	29.5°	29.7°	31.1°	34.1°	36.5°	39.9°	42.4°	44.4°	47.4°	49.7°
	β	5.34	5.34	5.27	4.73	3.82	3.27	2.64	2.27	2.01	1.68	1.46
≤ 20	θ	31.2°	31.2°	31.2°	32.3°	36.0°	38.8°	42.7°	45.5°	47.6°	50.9°	53.4°
	β	4.99	4.99	4.99	4.61	3.65	3.09	2.46	2.09	1.85	1.52	1.31
≤ 30	θ	34.1°	34.1°	34.1°	34.2°	38.9°	42.3°	46.9°	50.1°	52.6°	56.2°	59.0°
	β	4.46	4.46	4.46	4.43	3.39	2.82	2.19	1.84	1.61	1.30	1.10
≤ 40	θ	36.6°	36.6°	36.6°	36.6°	41.1°	45.0°	50.2°	53.7°	56.3°	60.2°	63.0°
	β	4.06	4.06	4.06	4.06	3.20	2.62	2.00	1.66	1.43	1.14	0.95
≤ 60	θ	40.8°	40.8°	40.8°	40.8°	44.5°	49.2°	55.1°	58.9°	61.8°	65.8°	68.6°
	β	3.50	3.50	3.50	3.50	2.92	2.32	1.72	1.40	1.18	0.92	0.75
≤ 80	θ	44.3°	44.3°	44.3°	44.3°	47.1°	52.3°	58.7°	62.8°	65.7°	69.7°	72.4°
	β	3.10	3.10	3.10	3.10	2.71	2.11	1.52	1.21	1.01	0.76	0.62

ε_s is the net longitudinal tensile strain in the section at the centroid of the tension reinforcement. In lieu of more involved procedures, ε_s may be determined by

$$\varepsilon_s = \frac{\left(\frac{|M_u|}{d_v} + 0.5N_u + |V_u - V_p| - A_{ps}f_{po} \right)}{E_s A_s + E_p A_{ps}} \quad (10)$$

The crack spacing parameter, s_{xe} , shall be determined as:

$$s_{xe} = s_x \frac{1.38}{a_g + 0.63} \quad (1)$$

Where:

A_c	Area of concrete on the flexural tension side of the member (in. ²)
A_{ps}	Area of pre-stressing steel on the flexural tension side of the member (in. ²)
A_s	Area of non pre-stressed steel on the flexural tension side of the member at the section under consideration (in. ²)
a_g	Maximum aggregate size (in.)
f_{po}	A parameter taken as modulus of elasticity of pre-stressing tendons multiplied by the locked in difference in strain between the pre-stressing tendons and the surrounding concrete
N_u	Factored axial force, taken as positive if tensile and negative if compressive (kip)
$ M_u $	Absolute value of the factored moment, not to be taken less than $ V_u - V_p d_v$ (kip-in.)
s_x	The lesser of either d_v or the maximum distance between layers of longitudinal crack control reinforcement, where the area of the reinforcement in each layer is not less than $0.003b_v s_x$ (in.)
V_u	Factored shear force (kip)

2.4.6 Toward a Consistent Method

Although the refined tooth models and the modified compression field theory approach the problem from different directions, the end result of these two methods is very similar for members without transverse reinforcement. Although the two methods use different approaches to estimate the crack inclination and crack width, both methods consider that the ability of diagonal cracks to transfer interface shear stress is most important in determining the shear strength of members without transverse reinforcement.

The biaxial tension-compression field in the concrete (teeth) between the cracks for a constant shear stress along the cracks may be visualized by a truss model. This representation of the concrete stresses due to interface shear stresses was first developed by Reineck (1982) based on his tooth model (Reineck 1991c). As discussed earlier, the principal stresses locally at a crack (that is, the compression struts and tension ties of the truss model) bisect the angles between the diagonal crack and the horizontal plane. Reineck assumes that the inclination of the critical diagonal cracks will be 60°; therefore, the inclinations of his compression struts are at 30° (Figure 2-16). In the modified

compression field theory approach, the inclination of the critical diagonal cracks depends on the loading and the ability of the longitudinal reinforcement to control the secondary diagonal cracks. A generalization of Reineck's model involves a truss with compression struts inclined at half the inclination of the diagonal cracks, which may have any inclination (Adebar and Collins 1996).

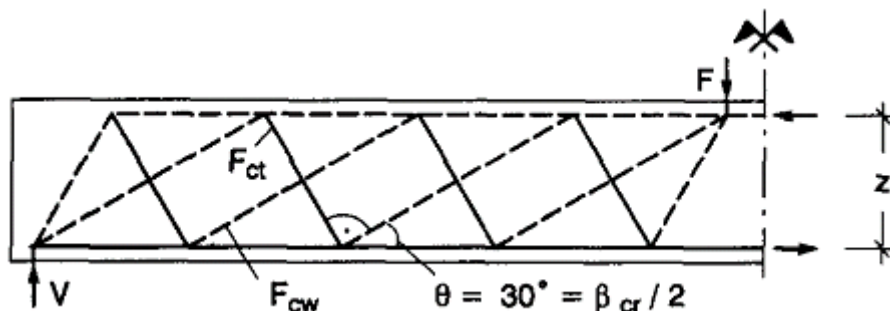


Figure 2-17: Refined Strut-and-Tie Model for Diagonally Cracked Member without Stirrups (Reineck 1991)

2.5 Building Codes and Shear Design Provisions

Developing a comparable theory for the shear strength of reinforced concrete members has been the objective of a major worldwide research effort for more than 40 years. For members with significant amounts of shear reinforcement, a variable angle truss model based on the lower bound theory of plasticity has been developed and is incorporated into Euro code 2. However for the potentially more dangerous cases of members without shear reinforcement, Euro code 2 uses totally empirical procedures not “supported by an adequate theory”. [14]

While flexural design is concerned with ensuring that the two sides of a member can resist the appropriate magnitudes of tensile or compressive longitudinal forces, shear design is intended to ensure that the two sides of the member continue to act as a unit. This involves identifying where shear reinforcement is required to link together the two sides of the member and determining how much of this reinforcement is needed to prevent a premature shear failure. For regions not containing shear reinforcement, a shear failure can occur without warning and typically involves the opening of a major diagonal crack. Traditional American shear design procedures assumed that such failures of members without shear reinforcement would not occur if the calculated shear stress, $V/(b_w d)$, at service loads was less than about $0.03f'_c$. If the shear stress was higher than this allowable stress, than shear reinforcement (e.g, links) would be added to carry the excess. The capacity added by the links was given by the 45° truss model of Ritter and Morsch as $\rho_w f_s$ where f_s was the allowable tensile

stress in the links. Such shear reinforcement controls the opening of diagonal cracks and permits much higher shear stresses to be resisted. Irrespective of the amount of links, however, an upper limit of $0.12f_c'$ was placed on the shear stress at service load. In traditional German shear design, by contrast, once the shear stress at service load exceeded about 0.4 MPa, shear reinforcement was provided to carry the entire shear using the 45° truss model. Because of these differences in shear design requirements, American reinforced concrete beams typically contained much less shear reinforcement than comparable German beams.[14]

2.5.1 Overview of current ACI Design Procedures (ACI 318-14)

The current ACI design procedure for shear defines the nominal shear strength as the sum of the shear strength provided by shear reinforcement, V_s , and the shear strength provided by concrete, V_c , which is assumed to be the same for beams with and without shear reinforcement and is taken as the shear causing significant inclined cracking.

The value of V_c is defined for members subject to shear and flexure only and for members subject to axial compression separately. Two alternatives are presented for calculation of V_c . The first alternative has a simple formula. Unlike its European counterpart, the ACI provision for calculation of the concrete contribution doesn't contain the longitudinal reinforcement ratio as a factor. It only depends on the compressive strength of the concrete and the size of the member.

The second alternative contains a more detailed calculation. In this case, many factors including ρ_w and $V_u d / M_u$ are shown to affect the concrete contribution.

To account for the use of lightweight concrete, unless specifically noted otherwise, a modification factor λ appears as a multiplier of $\sqrt{f_c'}$ in all applicable equations of this ACI Code, where $\lambda = 0.85$ for sand-lightweight concrete and 0.75 for all-light-weight concrete. Linear interpolation between 0.75 and 0.85 shall be permitted, on the basis of volumetric fractions, when a portion of the lightweight fine aggregate is replaced with normal weight fine aggregate. Linear interpolation between 0.85 and 1.0 shall be permitted, on the basis of volumetric fractions, for concrete containing normal weight fine aggregate and a blend of lightweight and normal weight coarse aggregates. For normal weight concrete, $\lambda = 1.0$. If average splitting tensile strength of lightweight concrete, f_{ct} , is specified, $\lambda = f_{ct}/(6.7 \sqrt{f_c'}) \leq 1.0$. Factor λ reflects the lower tensile strength of light-weight concrete, which can reduce shear strength, friction properties, splitting resistance, bond between concrete and

reinforcement, and increase development length, compared with normal weight concrete of the same compressive strength.

The contribution of the shear reinforcement is based on the modified truss analogy. As it is presented in the commentary, the truss analogy assumes that the total shear is carried by shear reinforcement. However, considerable research has indicated that shear reinforcement needs to be designed to carry only the shear exceeding that which causes inclined cracking provided the diagonal members in the truss are assumed to be inclined at 45 degrees. Thus, the ACI approach of calculating the shear reinforcement contribution can be generalized as modified 45 degree truss analogy.

Shear reinforcement restrains the growth of inclined cracking. Ductility is increased and a warning of failure is provided. In an unreinforced web, the sudden formation of inclined cracking might lead directly to failure without warning. Such reinforcement is of great value if a member is subjected to an unexpected tensile force or an overload. Accordingly, due to the reason stated above, a provision for providing minimum shear reinforcement for all members except for solid slabs, footings and joists is stipulated in ACI318.

2.5.2 Overview of Recent European Codes (EN 1992:2004)

In the current European Code, the shear resistance of a member with shear reinforcement is defined to be the shear resistance offered by the web reinforcements. Shear reinforcement is not necessary if the resulted shear force is less than the member design shear resistance without shear reinforcement. However minimum shear reinforcement is required except in slabs and members of minor importance.

An empirical formula is given for calculation of the contribution from the concrete in resisting shear. The empirical formula for concrete contribution takes into account the longitudinal reinforcement ratio, the compressive stress capacity of the concrete and the presence of axial force.

The calculation of shear force resistance contribution of the transverse reinforcement is based on the variable angle Truss analogy. Unlike the ACI, this code doesn't have a specific value for the crack inclination angle θ . But it gives a recommended limit of $1 < \cot \theta < 2.5$. On the other hand, following the Truss analogy, it gives a maximum limit for the shear force to insure that the diagonal compression force will not exceed the diagonal crushing force of the concrete, νf_{cd} where ν is 0.6 for concrete grades greater than 60 MPa and $0.9 - f_{ck} / 200 > 0.5$ for concrete grades greater than 60 MPa.

As per the variable angle truss analogy (section 2.3.1.1), there is an additional tensile stress that will be resulted on the longitudinal reinforcement and European code has a provision to take care of this additional tensile stress as per the analogy.

CHAPTER 3 SHEAR STRENGTH OF REINFORCED CONCRETE SLENDER BEAMS WITHOUT WEB REINFORCEMENT [13]

3.1 Introduction

Extensive research over the years on the combined effects of flexure and shear on the resistance capacity of the structure has not yielded a generalized theory of combined flexure shear for computing the resistance capacity of reinforced concrete members. As a result, the design for shear is uncoupled with respect to the flexural design.

Most of the code of practices uses empirical equations to estimate the shear capacity of reinforced concrete beams. In addition to the equations in the Codes, there are number of empirical equations proposed in the literature by different researchers. Empirical equations developed from experimental results for calculating V_c involves different influencing parameters based on the variable considered in the experimental program by the researcher. Each researcher has selected different influencing parameters as there is no general consensus or accepted theory for evaluating the ultimate shear capacity of reinforced concrete beams without web reinforcement [13].

In this chapter, Design equations used in six Design Codes of practice were evaluated using the experimental data contained in ACCESS shear database. Predictive accuracy of 17 empirical equations proposed in the literature for predicting the shear capacity of reinforced concrete slender beams $a/d > 2.5$, were studied using the experimental data contained in ACCESS shear database. On the basis of results, for slender reinforced concrete beams, empirical equations used in some Codes are identified to be superior to others. Among the proposed empirical equations in the literature, equations that use the $(f'c)^{1/3}$ function and include depth factor are found to be superior to others¹³.

On the basis of experimental results of reinforced concrete beams having shear span to depth ratio $a/d \geq 2.5$, empirical equations are proposed which include basic parameters i.e. concrete compressive strength $f'c$, shear span to depth ratio a/d and ratio of longitudinal reinforcement ρ . The coefficient of correlation (COR) for proposed empirical equation for predicting the shear capacity of reinforced concrete beams having depth $d < 300\text{mm}$ and $d \geq 300\text{mm}$ without web reinforcement comes out to be 0.869 and 0.953 respectively [13].

3.2 Evaluation of Design Equations [13]

Equations 12 to 17 shows empirical equations in different Codes of practice along with their limits of applicability used to predict the shear capacity of reinforced concrete slender beams. For the study of predictive accuracy of the Code equations, experimental data for slender beams from the shear database was used.

It can be seen that to reflect the effect of concrete compressive strength f'_c on the shear capacity of reinforced concrete beams, ACI Code Eq. 12, Canadian Code Eq.13 and New Zealand Code Eq. 14 use function $(f'_c)^{1/2}$, whereas the Euro code EC2 Eq.15, Spanish Code EHE-99 Eq. 16 and CEB-FIP Model Code Eq.17 use function $(f'_c)^{1/3}$. The influence of size effect on the shear capacity is not included in the equations of ACI Code Eq. 12, and New Zealand Code Eq. 14, whereas the equations of the other Codes have terms that accommodate the influence of size effect.

$$v_c = 0.16\sqrt{f'_c} + 17.2\rho\frac{V_d}{M} \quad \text{For } a/d \geq 2.5 \quad (12)$$

$$v_c = 0.2\sqrt{f'_c} \quad \text{For } d \leq 300\text{mm} \quad (13)$$

$$v_c = \left(\frac{260}{1000+d} \right) \sqrt{f'_c} \geq 0.1\sqrt{f'_c} \quad \text{For } d > 300\text{mm}$$

$$v_c = (0.07 + 10\rho)\sqrt{f'_c} \quad \text{For } a/d > 2 \quad (14)$$

$$v_c = \frac{0.18}{\gamma_c} K (100\rho f_{ck})^{1/3} + 0.15\sigma_{cp} \quad (15)$$

$$v_c \text{ min} = 0.035k^{3/2}f_{ck}^{1/2}$$

Where

$$f_{ck} \leq 1000\text{MPa}$$

$$k = 1 + \sqrt{\frac{200}{d}} \leq 2,$$

Where d is in mm

$$\rho_l = \frac{As}{b_w d} \leq 0.02$$

$$v_c = 0.12 \xi (\rho_s f_{ck})^{1/3} - 0.15 \sigma_{cd} \quad (16)$$

Where

$$\xi = 1 + \sqrt{\frac{200}{d}}$$

$$v_c = 0.12 \left(1 + \sqrt{\frac{200}{d}} \right) \left(\frac{3d}{a_s} \right)^{1/3} (\rho_s f_{ck})^{1/3} - 0.15 \sigma_{cd} \quad (17)$$

Where

N_d = Factored Axial Force

A_c = Area of concrete

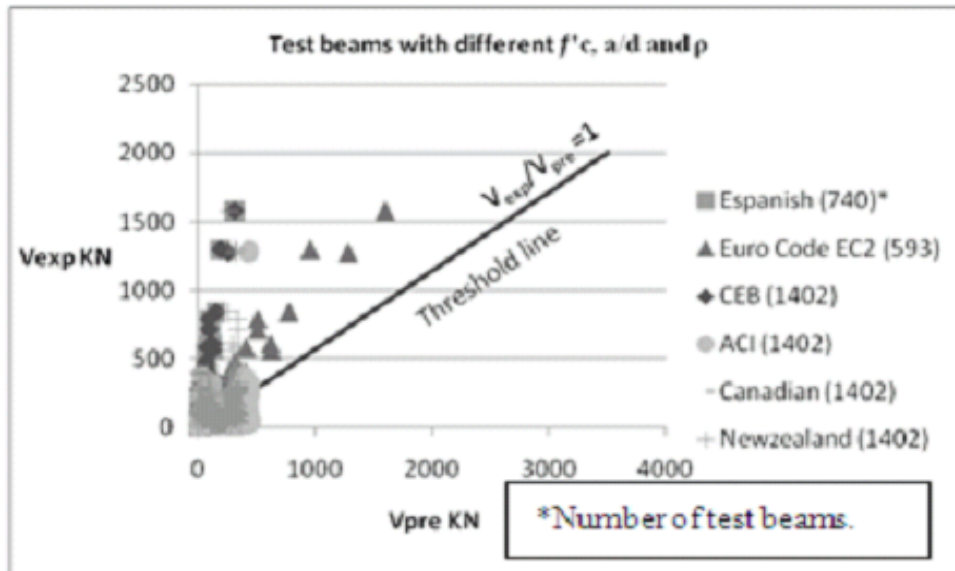


Figure 3.1: Comparison of prediction of Code equations with experimental results [13].

Figure 3.1 shows the plot of the experimental (measured) ultimate shear force (V_{exp}) and predicted ultimate shear force (V_{pre}), for all the 6 code equations, along with the threshold line ($V_{exp}/V_{pre} = 1$). It can be seen from Figure 3.1, the (V_{exp}/V_{pre}) of CEB-FIP Model Code Eq. 17 and Spanish EHE-99 Code Eq. 16 are much greater than 1, which shows that these two codes significantly

underestimate the shear capacity of reinforced concrete slender beams, as compared to ACI Code Eq. 12, Euro Code EC2 Eq. 15, New Zealand Code Eq. 14 and Canadian Code Eq. 13.

Table 3-1: Summary of results for the Average Margin of Safety $(V_{exp}/V_{pre})_{avg}$ of empirical equations used in different Codes for predicting the shear capacity of normal strength and high strength reinforced concrete slender beams [13].

Code	No. of Beams used for Evaluation	*Average Margin of Safety $(V_{exp}/V_{pre})_{avg}$
CEB-FIP Model	1402	7.214
Espanish EHE-99	740	6.539
ACI	1402	1.314
Eurocode EC2	593	1.273
NewZealand Code	1402	1.207
Canadian Code	1402	1.209

Table 3.1 shows the summary of results in terms of the comparison of the average Margin of Safety $(V_{exp}/V_{pre})_{avg}$ of design equations used in different Codes of practice for predicting the shear capacity of reinforced concrete slender beams. The number of beams, whose data was used, varies for each case, because of the relative constraints or the limits in the respective empirical equations of the Codes. From Table 3.1 it can be seen that the average Margin of Safety $(V_{exp}/V_{pre})_{avg}$ for CEB-FIP Model Code [Eq. 17 and Espanish EHE-99 Code Eq. 16 is 7.214 and 6.539 respectively which is much higher than $(V_{exp}/V_{pre})_{avg}$ values, when using the ACI Code Eq. 12, Euro Code EC2 Eq. 15, New Zealand Code Eq. 14 and Canadian Code Eq. 13. Which are 1.325, 1.273, 1.207 and 1.209 respectively. Thus the CEB-FIP Model Code Eq. 17 and Espanish EHE-99 Code Eq. 16 estimations are significantly more conservative (order of 6 or higher) as compared to other codes and are not considered in the further evaluation¹³.

3.3 Effect of Influencing Factors [13]

Two major factors are studied, the concrete compressive strength and the size effect. Table 3.2 shows the summary of results showing the Average Margin of Safety (V_{exp}/V_{pre})_{avg} with coefficient of correlation (COR) for Normal Strength Concrete (NSC) having $f'_c < 40\text{MPa}$ and High Strength Concrete (HSC) having $f'_c \geq 40\text{MPa}$ reinforced slender beams. It can be seen from Table 3.2 that in case of NSC beams, COR for Euro code EC2 Code Eq. 15 is 0.974, which is higher as compared to New Zealand Code Eq. 14, Canadian Code Eq. 13 and ACI Code Eq. 12, which are 0.855, 0.932 and 0.899 respectively.

In case of HSC beams, COR for Euro code EC2 Eq. 15 is 0.974 which is higher as compared to New Zealand Code Eq. 14, Canadian Code Eq. 13 and ACI Code Eq. 12 which are 0.882, 0.932 and 0.90 respectively. It should be noted that Euro code EC2 Eq. 15 equation uses cubic root function $(f'_c)^{1/3}$ rather than the square root function $(f'_c)^{1/2}$ used by ACI Code Eq. 12, Canadian Code Eq. 13 and Newzealand Code Eq. 14 to reflect the effect of the concrete compressive strength f'_c on the shear capacity of reinforced concrete beams. This implies that $(f'_c)^{1/2}$ function used in the ACI Code Eq. 12, Canadian Code Eq. 13 and Newzealand Code may not be adequate to reflect the effect of the f'_c on the shear capacity of high strength reinforced concrete beams.

Table 3-2: Summary of results showing the Average Margin of Safety with coefficient of correlation for NSC and HSC reinforced slender beams [13].

Code	Strength of Concrete			
	No. of Beams used for evaluation	NSC	Average Margin of Safety	COR
		HSC		
Eurocode EC2	593	370	1.60	0.974
		223	1.14	0.974
New Zealand Code	1402	951	1.25	0.855
		451	1.12	0.882
Canadian Code	1402	951	1.28	0.932
		451	1.04	0.932
ACI Code	1402	951	1.38	0.899
		451	1.16	0.907

Table 3.3 shows the summary of results showing the Average Margin of Safety $(V_{exp}/V_{pre})_{avg}$ with COR for NSC and HSC reinforced slender beams including the size effect. It can be also seen from Table 3.3 that in case of beams with effective depth $d < 300\text{mm}$ the COR for Euro code EC2 (2002) Code Eq. 5 is 0.985, which is higher as compared to Canadian Code Eq. 13 (1994), ACI Code Eq. 12 (2008) and New Zealand Code Eq. 14 (1995) which are 0.932, 0.90 and 0.674 respectively. In case of beams with effective depth $d \geq 300\text{mm}$ the COR or Euro code EC2 Eq. 15 is 0.975, which is higher as compared to Canadian Code Eq. 13, ACI Code Eq. 12 and New Zealand Code Eq. 14 which are 0.938, 0.90 and 0.899 respectively. It should be noted that the Euro code EC2 Eq. 15 and Canadian code Eq. 13 equations that are identified to have higher values of coefficient of correlation COR use depth factor in their respective expressions, whereas ACI Code Eq. 12 and New Zealand Code Eq. 14 equations do not use depth factor in their relative expressions. Although the COR of Euro code EC2 Code Eq. 15 is higher, however the applicability over the number of beams is limited, due to constraints or the limits in the empirical equation as compared New Zealand Code Eq. 3, Canadian Code Eq. 13 and ACI Code Eq. 12 for which a larger number of test beams were used to assess the predictive accuracy.

Table 3-3: Summary of results showing the Average Margin of Safety with coefficient of correlation for NSC and HSC reinforced slender beams including the size effect [13]

Code	No. of Beams used for evaluation	Size Effect		
		$d < 300\text{mm}$	Average Margin of Safety	COR
		$d \geq 300\text{mm}$		
Eurocode EC2	593	292	1.35	0.985
		301	1.20	0.975
New Zealand Code	1402	1046	1.19	0.674
		356	1.23	0.899
Canadian Code	1402	1046	1.31	0.932
		356	0.90	0.938
ACI Code	1402	1046	1.44	0.884
		356	0.92	0.916

3.4 Proposed Empirical Equation [13]

On the basis of shear data base of the experimental test results, an empirical equation is developed for predicting the shear capacity of reinforced concrete beams having shear span to depth ratio $a/d \geq 2.5$.

For $d < 300\text{mm}$ and $a/d \geq 2.5$

$$v_c = 0.35 \left(\frac{a}{d} f'_c \right)^{0.33} \rho^{0.1} \quad (18)$$

For $d \geq 300\text{mm}$ and $a/d \geq 2.5$

$$v_c = \xi 0.35 \left(\frac{a}{d} f'_c \right)^{0.33} \rho^{0.1} \quad (19)$$

Where

$$\xi = \frac{17.32}{\sqrt{d}} \quad (20)$$

The proposed empirical equations (Eq. 18 and Eq. 19), contains basic parameters i.e. concrete compressive strength f'_c , shear span to depth ratio a/d and ratio of longitudinal reinforcement ρ . In addition to these basic parameters, proposed equation also uses depth factor ξ to account the effect of size effect on the shear capacity of reinforced concrete beams without web reinforcement. In order to assess the predictive accuracy of proposed empirical equations (Eq. 18 and Eq. 19), test results of 1085 reinforced concrete beams without web reinforcement from ACCESS shear database (Rafeeqi et al 2011) were used. The COR for Eq.18 comes out to be 0.869. For the predictive accuracy of Eq. 19 test results of 393 reinforced concrete beams without web reinforcement from ACCESS shear database were used. The COR for Eq. 19 comes out to be 0.953 [13].

CHAPTER 4 EXPERIMENTAL PROGRAM

This chapter describes the experimental program completed at the Construction Materials Laboratory, Addis Ababa Institute of Technology to study the effect of aggregate size and type on the shear behavior of reinforced concrete beams.

The main variable used in the current study is aggregate size and type. A 1.7m (Based on a/d ratio) long beam was selected for the experimental program and shear failure was ensured by choosing slender beam ($a/d > 2.5$), avoiding web reinforcement and by providing sufficient longitudinal reinforcement bar. Prior to the experiment, shear failure was further confirmed by comparing the flexural and shear capacity using hand calculation.

Five specimens were selected. All the five specimens had similar cross section, longitudinal reinforcement, and no web reinforcement.

4.1 Specimens

The experimental program consists of 5 simply supported RC beam specimens with rectangular cross section and constant width (b) and depth (D) of 200mm and 250 mm respectively. Figure 4-1 shows details and reinforcement arrangement of the specimens.

The Specimens are selected based on maximum coarse aggregate size and aggregate type. The coarse aggregate in Specimens NWNo.4 (37.5mm), NWNo.5 (25mm), and NWNo.7 (12.5mm) & NWNo.9 (4.75mm) is normal weight aggregate. The coarse aggregate in Specimen LWNo.5 (25mm) is light weight aggregate (scoria).

a) For Aggregate size

Four different nominal maximum coarse aggregate sizes are chosen for the experiment from ASTM C33 gradation requirement of coarse aggregates as shown in table 4.1.

- ✓ 1) No. 4 (37.5 to 19 mm)
- ✓ 2) No. 5 (25 to 12.5 mm)
- ✓ 3) No. 7 (12.5 to 4.75 mm)
- ✓ 4) No. 9 (4.75 to 1.18 mm)

Size Number	Nominal Size (Sieves with Square Openings)	Amounts Finer than Each Laboratory Sieve (Square-Openings), Mass Percent													
		100 mm (4 in.)	90 mm (3½ in.)	75 mm (3 in.)	63 mm (2½ in.)	50 mm (2 in.)	37.5 mm (1½ in.)	25.0 mm (1 in.)	19.0 mm (¾ in.)	12.5 mm (½ in.)	9.5 mm (⅜ in.)	4.75 mm (No. 4)	2.36 mm (No. 8)	1.18 mm (No. 16)	300 µm (No. 50)
1	90 to 37.5 mm (3½ to 1½ in.)	100	90 to 100	...	25 to 60	...	0 to 15	...	0 to 5
2	63 to 37.5 mm (2½ to 1½ in.)	100	90 to 100	...	0 to 15	...	0 to 5
3	50 to 25.0 mm (2 to 1 in.)	100	90 to 100	35 to 70	0 to 5
357	50 to 4.75 mm (2 in. to No. 4)	100	95 to 100	...	35 to 70	...	10 to 30	0 to 5
4	37.5 to 19.0 mm (1½ to ¾ in.)	100	90 to 100	20 to 55	0 to 15	...	0 to 5
467	37.5 to 4.75 mm (1½ in. to No. 4)	100	95 to 100	...	35 to 70	...	10 to 30	0 to 5
5	25.0 to 12.5 mm (1 to ½ in.)	90 to 100	20 to 55	0 to 10	0 to 5
56	25.0 to 9.5 mm (1 to ⅜ in.)	90 to 100	40 to 85	10 to 40	0 to 15	0 to 15	0 to 5
57	25.0 to 4.75 mm (1 in. to No. 4)	95 to 100	...	25 to 60	0 to 10	0 to 5
6	19.0 to 9.5 mm (¾ to ⅜ in.)	100	90 to 100	20 to 55	0 to 15	0 to 15	0 to 5
67	19.0 to 4.75 mm (¾ in. to No. 4)	100	90 to 100	...	20 to 55	20 to 55	0 to 10	0 to 5
7	12.5 to 4.75 mm (½ in. to No. 4)	100	90 to 100	40 to 70	40 to 70	0 to 15	0 to 5
8	9.5 to 2.36 mm (⅜ in. to No. 8)	100	85 to 100	85 to 100	10 to 30	0 to 10	0 to 5
89	9.5 to 1.18 mm (⅜ in. to No. 16)	100	90 to 100	90 to 100	20 to 55	5 to 30	0 to 10	0 to 5	...
9 ^A	4.75 to 1.18 mm (No. 4 to No. 16)	100	85 to 100	10 to 40	0 to 5	0 to 10	0 to 5	...

Table 4-1: Grading requirements for coarse aggregates

b) For Aggregate type

Light weight aggregate (scoria) with aggregate gradation type No.5 is used for specimen LWNo.5 in this paper.

Table 4-2: Details of investigated specimens

Specimen	Overall height, h, (mm)	Effective depth, d, (mm)	Shear span, a, (m)	a/d	concrete cover to web reinforcement, (mm)	Area of Longitudinal Rebar (mm ²)	Aggregate Type	Maximum aggregate size (mm)
NWNo. 4	250	211	0.65	3.08	25	603	Normal Weight	37.5
NWNo. 5	250	211	0.65	3.08	25	603	Normal Weight	25
NWNo. 7	250	211	0.65	3.08	25	603	Normal Weight	12.5
NWNo. 9	250	211	0.65	3.08	25	603	Normal Weight	4.75
LWNo.5	250	211	0.65	3.08	25	603	Light Weight	25

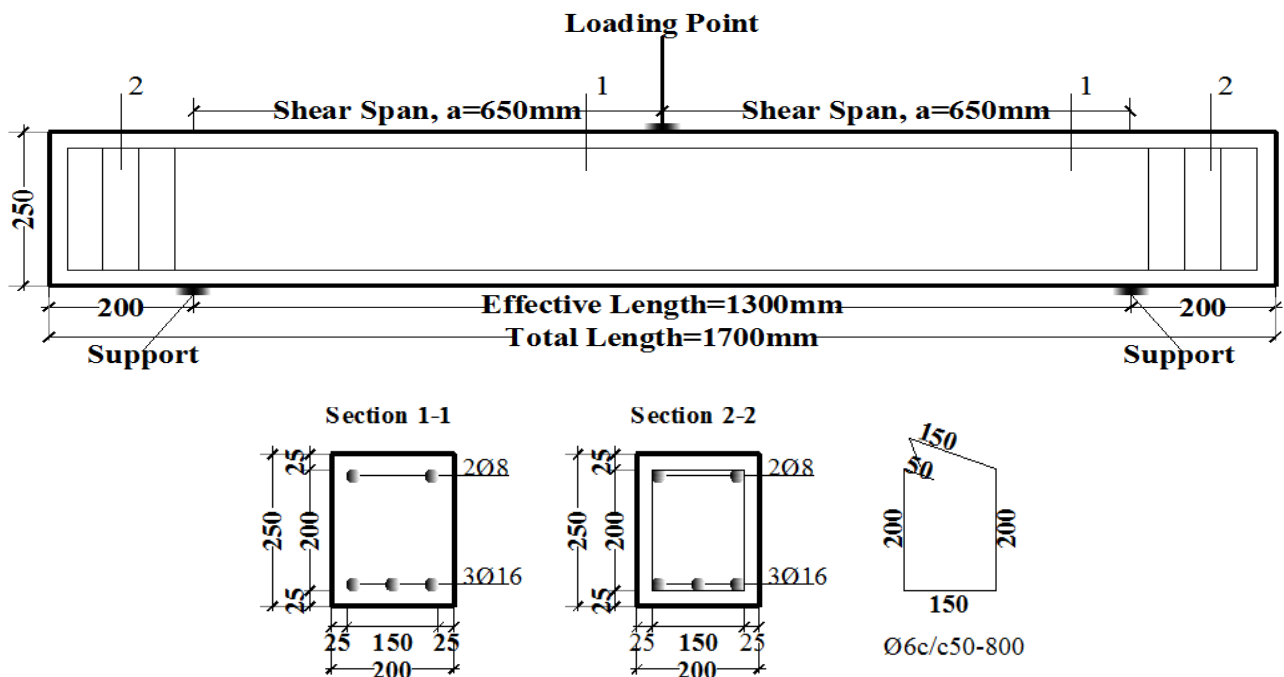


Figure 4:1: Experiment specimens

4.2 Materials

4.2.1 Concrete

The specimens were cast in wooden molds using cast in situ concrete. During the casting process of concrete, samples of concrete cylinders were prepared in 4 cylinder of diameter 100mm and height 200 mm for Compressive Strength and 4 cylinders of diameter 150mm and height 300 mm for tensile strength were taken from each beam specimen and 2 of them were tested 14 days after the casting day and the rest 2 samples were tested the day of testing (See Table 4-4 and Table 4-5). In the mix proportions of concrete (detailed mixed design is attached in the annex part), the target strength was C-25, ordinary Portland cement was used and water-cement ratio was kept at 0.61 (See Table 4-3)

Table 4-3: Mix proportions of concrete

Material	NWNo.4	NWNo.5	NWNo.7	NWNo.7	LWNo.5
Max. aggregate size	37.5 mm	25 mm	12.5 mm	4.75	25 mm
Free-water (kg/m ³)	167.73	179.98	203.173	222.44	179.98
Cement content (kg/m ³)	296.721	316.393	354.098	388.115	316.393
Coarse aggregate (kg/m ³)	1143.496	1077.21	878.337	387.794	0.65 m ³ **
Fine aggregate (kg/m ³)	788.831	793.4	861.564	1219.841	793.4
Water-cement ratio	0.61	0.61	0.61	0.61	0.61

**For Specimen LWNo. 5 equivalent volume of normal weight aggregate in specimen NWNo.4 is replaced by lightweight aggregate (Scoria).

Cylinders were tested using a compression testing machine (shown in Figure 4-2).



Figure 4-2 Compressive and tensile strength testing machine

Table 4-4: 14th day strength of cylinder samples

Specimen	Compressive strength (MPa)			Tensile strength (MPa)		
	Cylinder 1	Cylinder 2	Average	Cylinder 1	Cylinder 2	Average
NWNO.4	14	11	12.5	1.74	1.37	1.56
NWNO.5	12.13	10.91	11.52	1.36	1.78	1.57
NWNO.7	16.6	17.67	17.135	1.72	1.79	1.76
NWNO.9	12.58	13.44	13.01	1.99	1.53	1.76
LWNO.5	16.08	19.32	17.7	1.47	1.68	1.58

Table 4-5: Test day strength of cylinder samples

Specimen	Compressive strength (MPa)			Tensile strength (MPa)		
	Cylinder 1	Cylinder 2	Average	Cylinder 1	Cylinder 2	Average
NWNO.4	16.01	13.57	14.79	2.15	2.33	2.24
NWNO.5	15.68	16.95	16.315	2.19	1.92	2.05
NWNO.7	17.57	19.91	18.74	2.74	1.79	2.26
NWNO.9	17.34	15.46	16.4	1.94	1.79	1.87
LWNO.5	18.15	14.47	16.31	1.78	2.49	2.13

4.2.2 Steel

In all test specimens, plain reinforcement bar with a diameter of 6 mm was welded for the tie reinforcement out of the effective length and deformed bars were used for the top and the bottom reinforcement. Tension tests were conducted on the longitudinal reinforcement steel to determine the mechanical property of the reinforcements. The mechanical properties of reinforcements used are given in Table 4-6.



Figure 4:3: Tensile Strength testing machine

Table 4-6 Mechanical properties of reinforcement

Specimen No	Diameter(mm)		Yield Load (KN)	Failure Load (KN)	Elongation(mm)	Length (mm)	Strain (ϵ)
	D1	D2					
1	6.52	8.27	28.7	33.1	18	200	0.09
2	6.4	8.07	27.6	32.2	17	200	0.085
3	6.65	8.01	24.6	29.2	20	200	0.1
4	14.8	17.62	108.4	128.7	26	200	0.13
5	15.04	17.73	115.2	135.1	20	200	0.1
6	14.76	17.41	106.1	131.5	27	200	0.135

4.3 Specimen Fabrication

This section describes in brief the details of the specimen construction process. The test specimens were constructed at the Construction Materials Laboratory. First, the reinforcement cages were assembled outside the forms. During the fabrication of the cages, the web reinforcement to outside the effective length was welded in the mechanical laboratory. Figure 4-4 shows the steel cage after assembly.



Figure 4:4: Reinforcement cage and formwork of the specimens

The formworks were made from sawn zigba and stiffened at the mid span to avoid bulging of concrete during casting. After the formwork was erected, form releasing agent was applied on the inner surface of the forms for easy stripping of formwork. Once the formwork was ready, the steel cages were placed inside, maintaining a concrete clear cover of 25 mm on all sides as shown in Figure 4-5.



Figure 4:5: Reinforcement cage of specimens inside the formwork

Concrete was casted in the laboratory and vibrator was used to consolidate the concrete. The concrete surface exposed to air was moist cured by covering the beams with wet cotton and by casing it with a plastic sheet to avoid evaporation. Curing Process is shown in the Figure 4-6.



Figure 4:6: Curing process of the specimens

4.4 Test Setup

The beam was setup on steel plates with a roller in between the plates. The steel roller supports were installed on concrete members anchored to the strong floor. A concentrated load was applied using a hydraulic jack (shown in Figure 4-7) of maximum capacity 300 kN. Figure 4-11 shows the test setup.



Figure 4:7: Load applying hydraulic jack

4.5 Instrumentation

All beams were fully instrumented to measure the applied loads on the beams and the deflections. In brief, the instrumentation consisted of a load cell which measures the applied load (shown in Figure 4-9), deflection measurement tool (shown in Figure 4-8) for the mid span deflection. All of the instrumentations were connected to a data logger and the experimental data was directly obtained in a USB (shown in Figure 4-10).



Figure 4:8: Displacement measuring tool



Figure 4:9: Load Cell



Figure 4:10: Data Logger

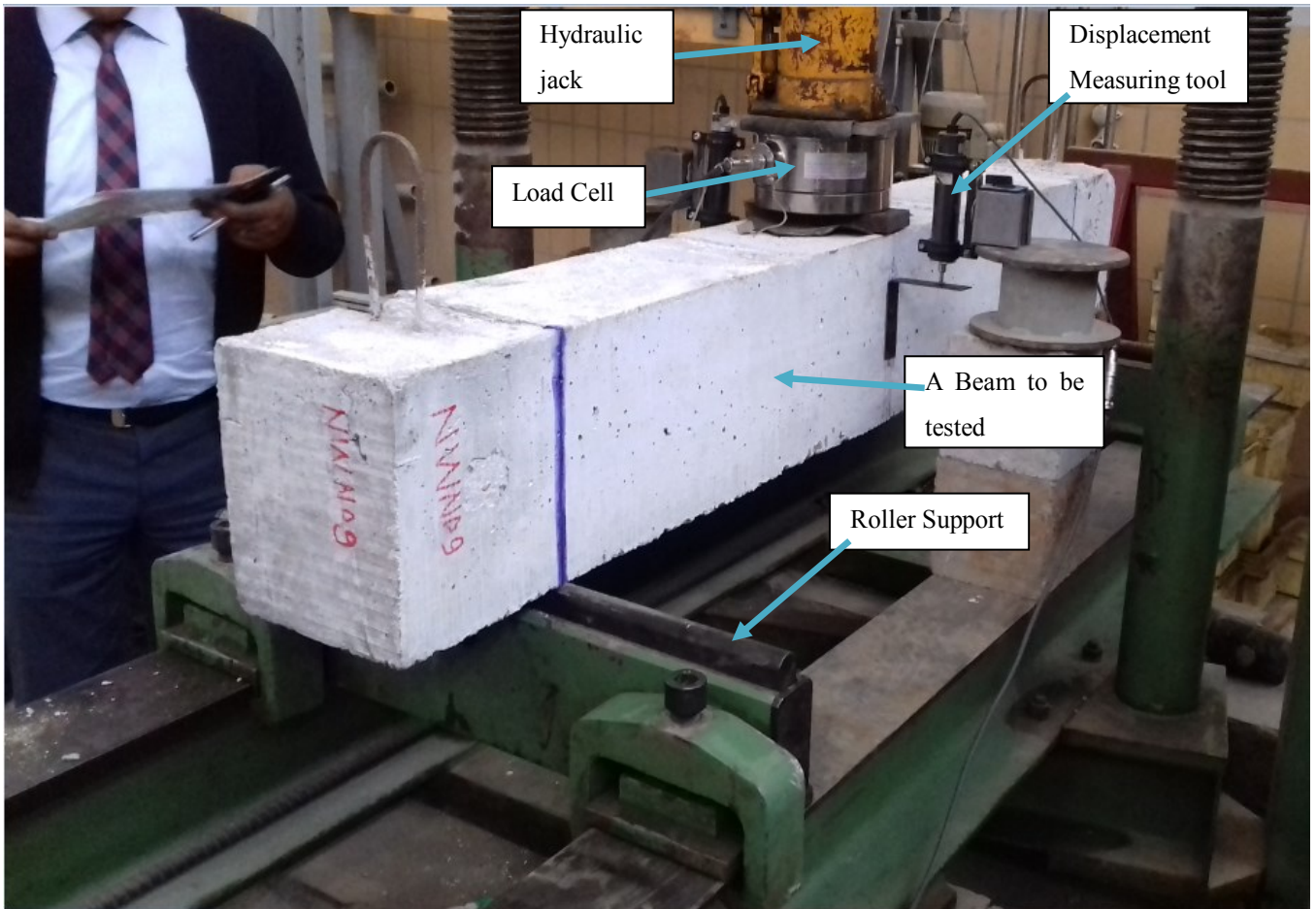


Figure 4:11: Test Setup

CHAPTER 5 FINITE-ELEMENT ANALYSIS USING DUCOM-COM3

5.1 About the software

For the analytical simulation of this study, the DuCOM-COM3 system which is developed in the University of Tokyo is used. This is a multi-scale analysis code that links the thermo-chemo-physics platforms DuCOM and COM3. DuCOM is an integrated thermo-hydro analysis code that includes cement hydration in concrete mixture, micro-pore structure formation and mass transport models for concrete ranging from 10^{-3} to 10^{-9} meter scales of micro-voids, while COM3 is a 3D finite-element analysis platform for structural concrete with and without cracks. As a result, DuCOM-COM3 is capable of predicting the change in concrete material properties from casting to dismantling of entire structures and taking this material development into account for predicting the response of structural concrete. With this integration, the long-term structural response under actual ambient conditions can be predicted in a realistic manner.

5.2 Specimens

Three - dimensional nonlinear finite element analyses were carried out for 5 specimens. The specimens modeled in Ducom-Com3 are similar to the one used in experiment. Table 5-1 shows the description of the 5 specimens.

Table 5-1: Specimens description

Specimen	Coarse Aggregate type	Max. Aggregate size (mm)	Concrete Grade (MPa)
NWNo.4	Normal Weight	37.5	25
NWNo.5	Normal Weight	25	25
NWNo.7	Normal Weight	12.5	25
NWNo.9	Normal Weight	4.75	25
LWNo.5	Light Weight	25	25

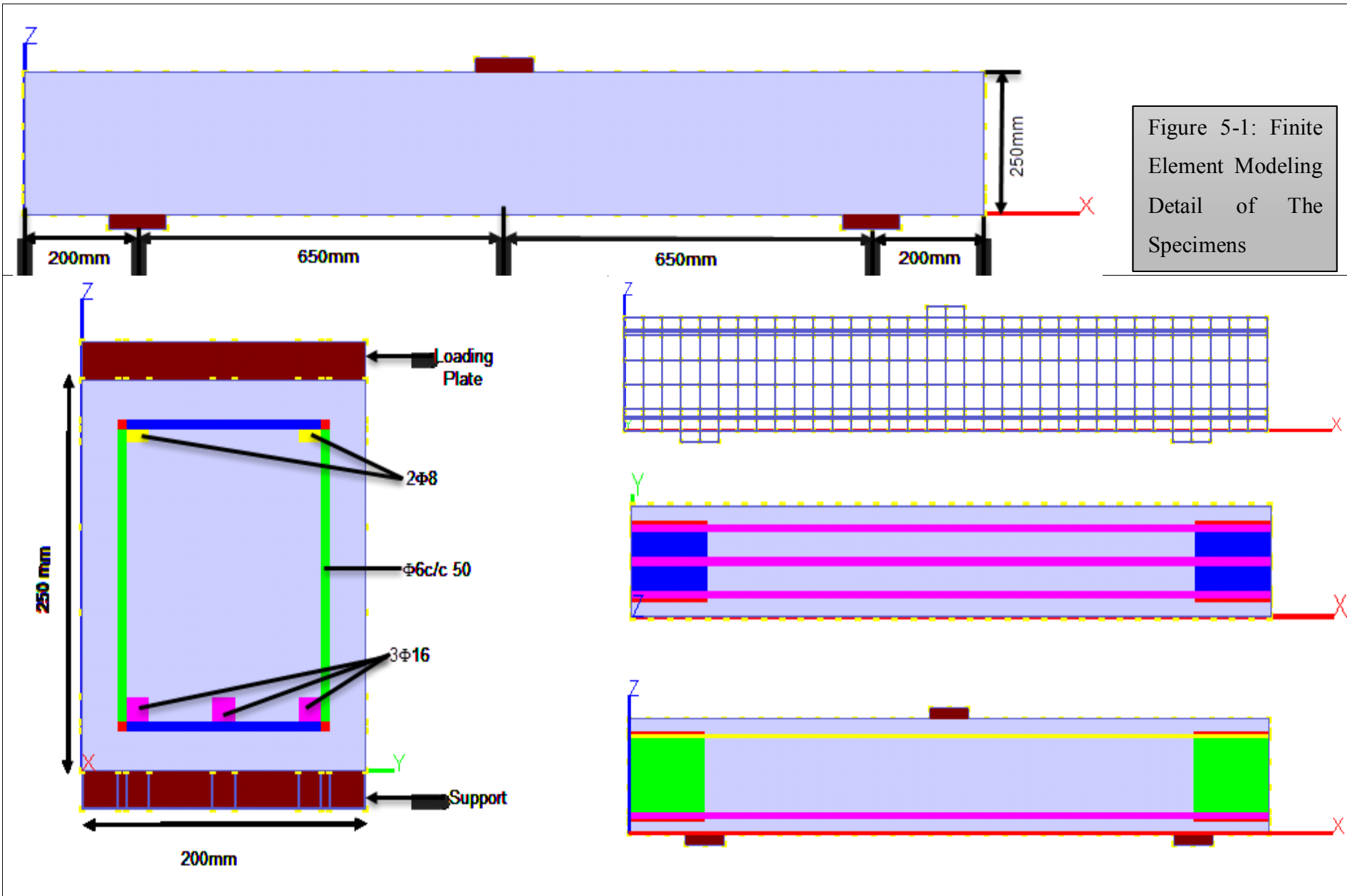


Figure 5-1: Finite Element Modeling Detail of The Specimens

5.3 Materials

Concrete grade of the specimens was determined from the experiment. Modulus of elasticity of the concrete was calculated by a formula recommended in [14].

$$E_c = 3320\sqrt{f_c} + 6900 \quad (21)$$

Mechanical properties of concrete in the specimens are presented in Table 5-2.

Table 5-2: Mechanical property of concrete

Mechanical property	Specimen				
	NWNo.4	NWNo.5	NWNo.7	NWNo.9	LWNo.5
Initial Stiffness (Gpa)	19.66798	20.31009	21.27219	20.34498	20.30803
Compressive strength (Mpa)	14.79	16.315	18.74	16.4	16.31
Tensile strength (Mpa)	2.24	2.05	2.26	1.87	2.13
Poisson's ratio	0.2	0.2	0.2	0.2	0.2
Unit weight (KN/m ³)	25	25	25	25	23

Tensile Strength test was done for the reinforcements used in the specimens. Detail property of the reinforcing steel bars is described in Table 5-3.

Table 5-3: Mechanical property of reinforcement bar

	Longitudinal bar	Top reinforcement
Initial Stiffness (Gpa)	200	200
Yield strength (Mpa)	682.521	720.742
Tension rupture strength (Mpa)	806.6523	851.688
Tension rupture strain	0.12	0.12
Poisson ratio	0.2	0.2
Unit weight (KN/m ³)	78	78

5.4 Modeling

The analysis was performed using the multi - directional fixed crack FE framework. All steel bars were modeled as embedded smeared reinforcement inside the elements. Concrete elements without steel bars were modeled as plain concrete element. Concrete with steel reinforcement was modeled as RC elements characterized by tension stiffening. Loading plates and support bearings were modeled as elastic elements characterized by unyielding behavior.

5.5 Support condition and loading

The beams were simply supported with 1.3 m clear distance between the supports. Elastic bearings were used at the support and at the point of load application. To capture the post peak behavior of the beams, a displacement controlled analysis was performed by applying a downward displacement of 0.02 cm per minute for 40 load steps at the mid span.

CHAPTER 6 RESULT AND DISCUSSION

6.1 Result from experiment

6.1.1 Result

In all the five specimens, a typical shear failure was observed. The beams failed with a diagonal tension failure. Figure 6-1 to Figure 6-5 shows the diagonal tension failure in the beams.



Figure 6:1: Diagonal tension failure in Specimen NWNo.9



Figure 6:2: Diagonal tension failure in Specimen NWNo.7



Figure 6:3: Diagonal tension failure in Specimen NWNo.5



Figure 6:4: Diagonal tension failure in Specimen NWNo.4



Figure 6:5: Diagonal tension failure in Specimen LWNo.5

As it was shown in Figure 4-11, Load was applied using a medium sized hydraulic jack. The jack was set on the load cell and it gets the reaction from the rigid steel frame above it. Deflection measuring tools were attached to the beam at the mid span. Load and deflection data were recorded by the Data logger and taken by USB (flash disc).

The load deflection diagram for the specimens is shown in the following figures.

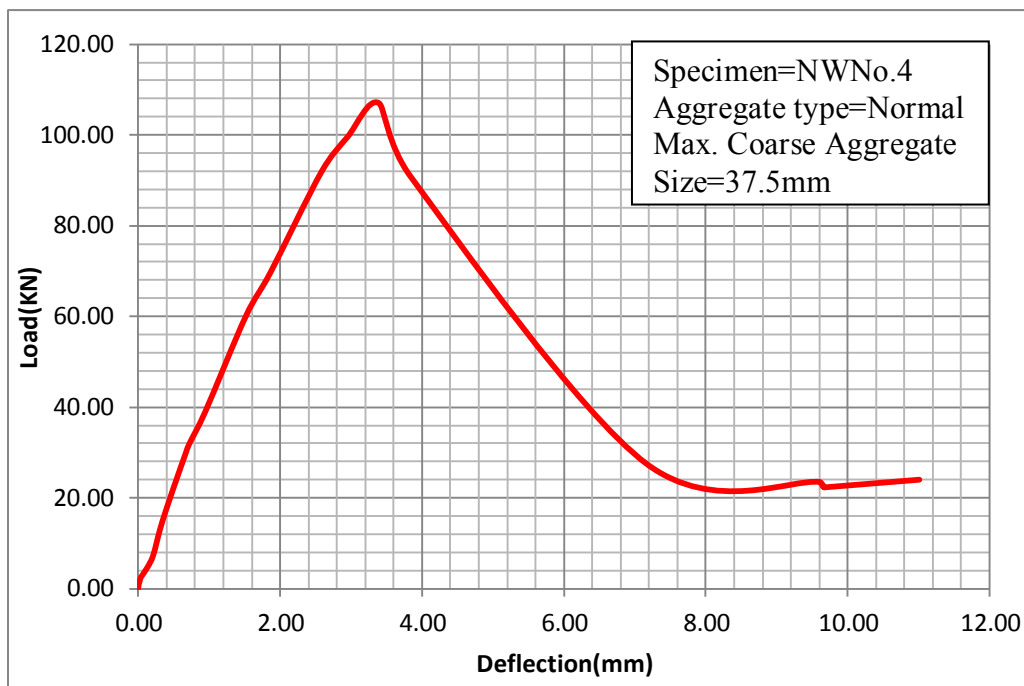


Figure 6:6 : Load – Deflection diagram for specimen NWNo. 4

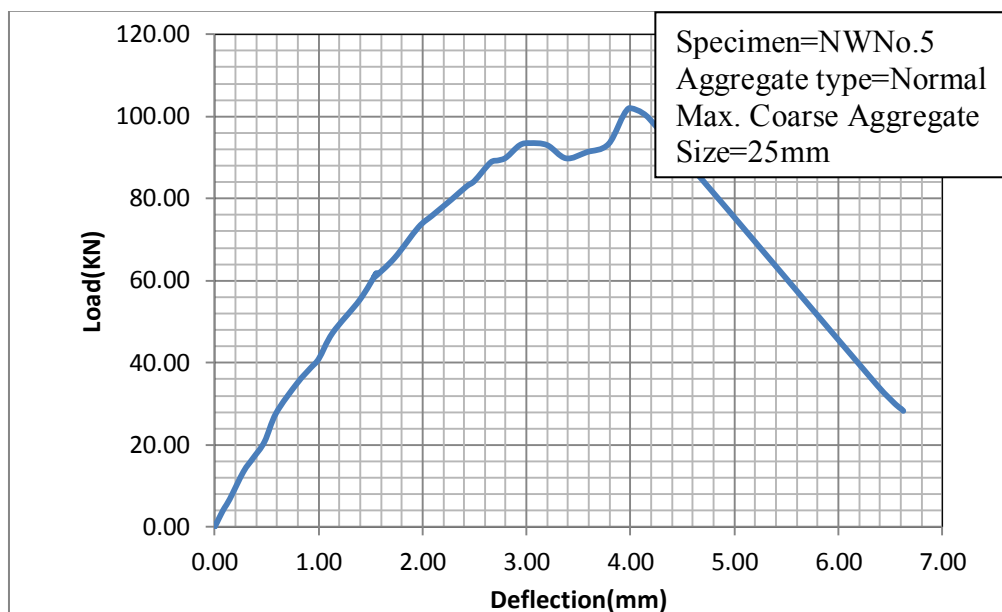


Figure 6:7: Load – Deflection diagram for specimen NWNo. 5

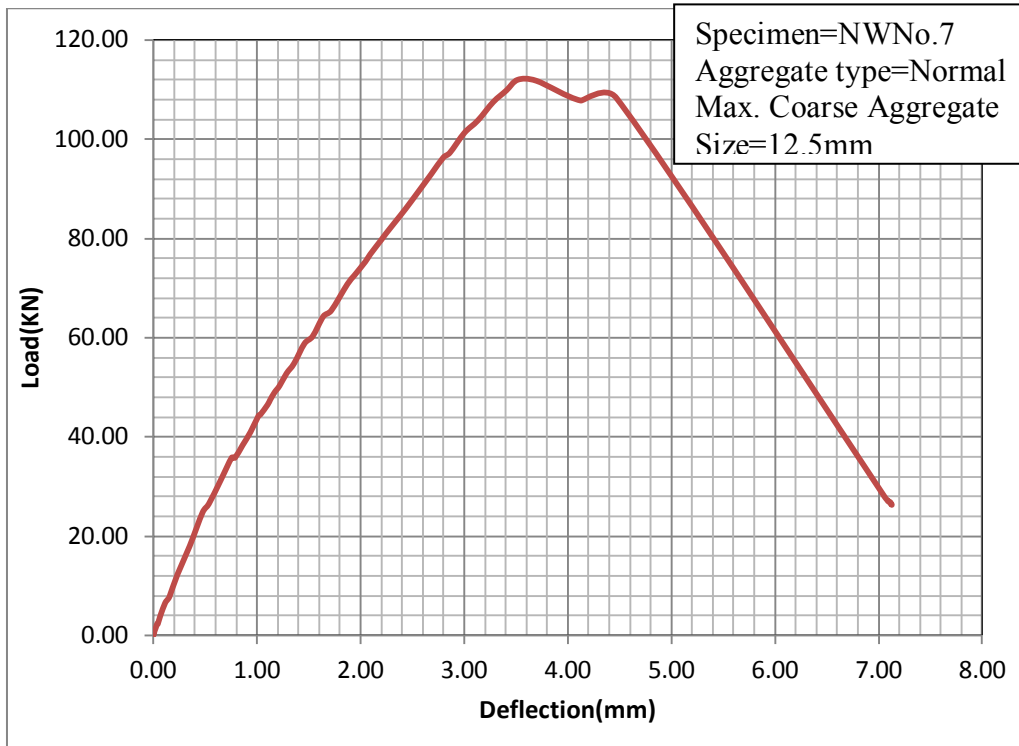


Figure 6:8: Load – Deflection diagram for specimen NWNo. 7

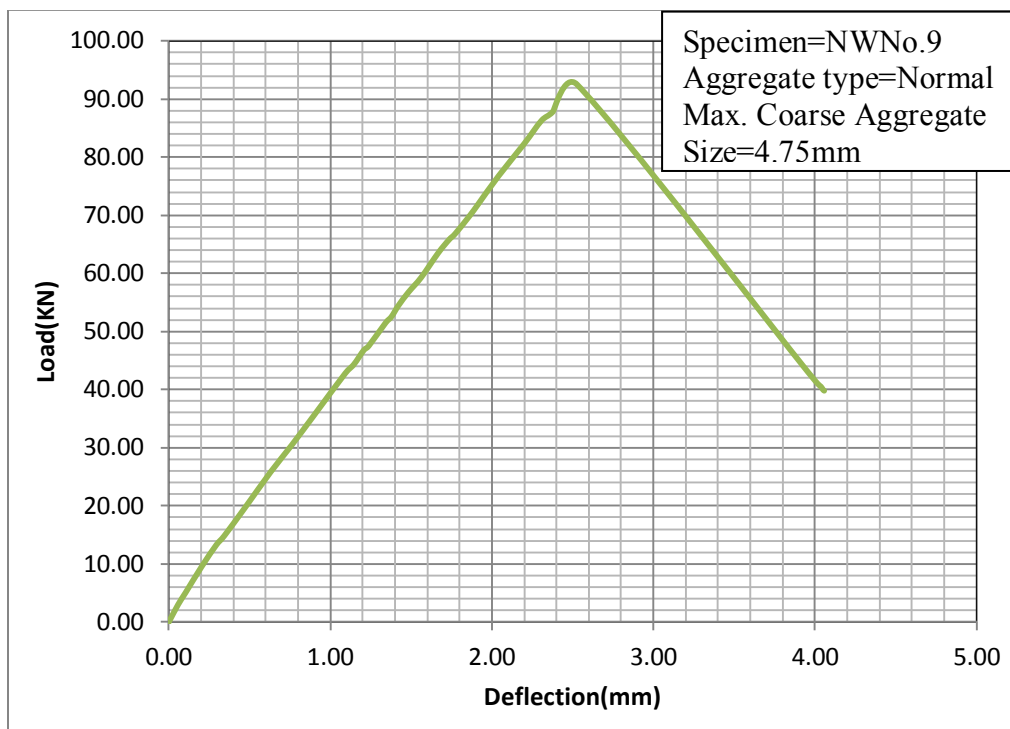


Figure 6:9: Load – Deflection diagram for specimen NWNo. 9

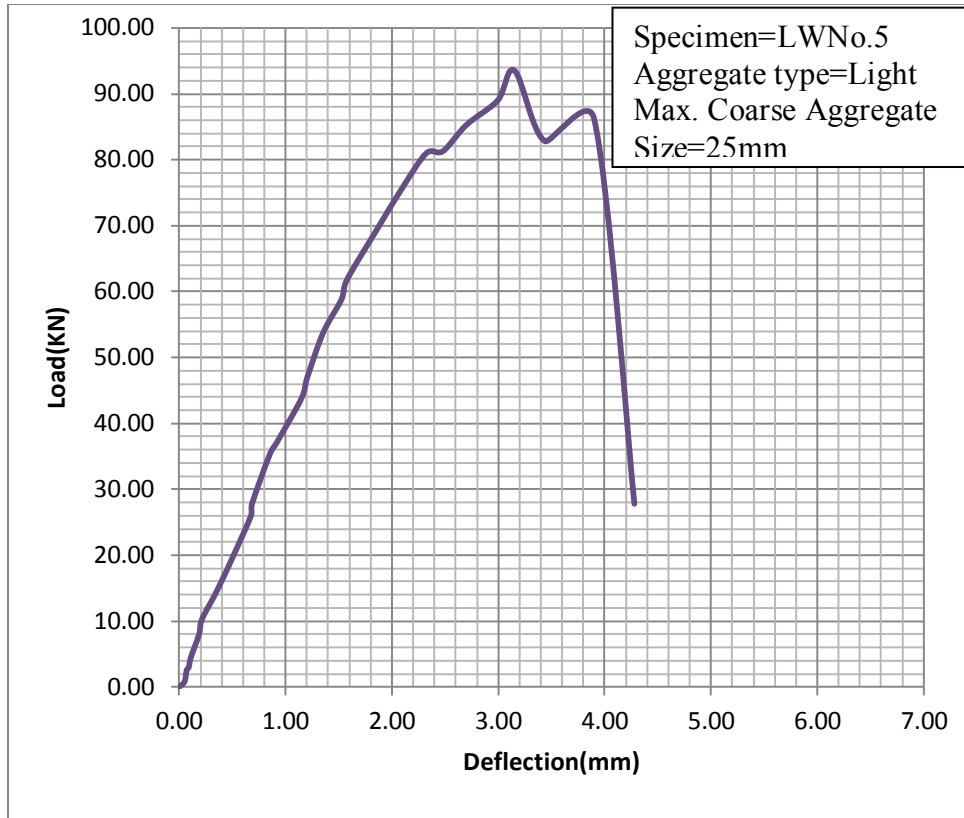


Figure 6:10: Load – Deflection diagram for specimen LWNo. 5

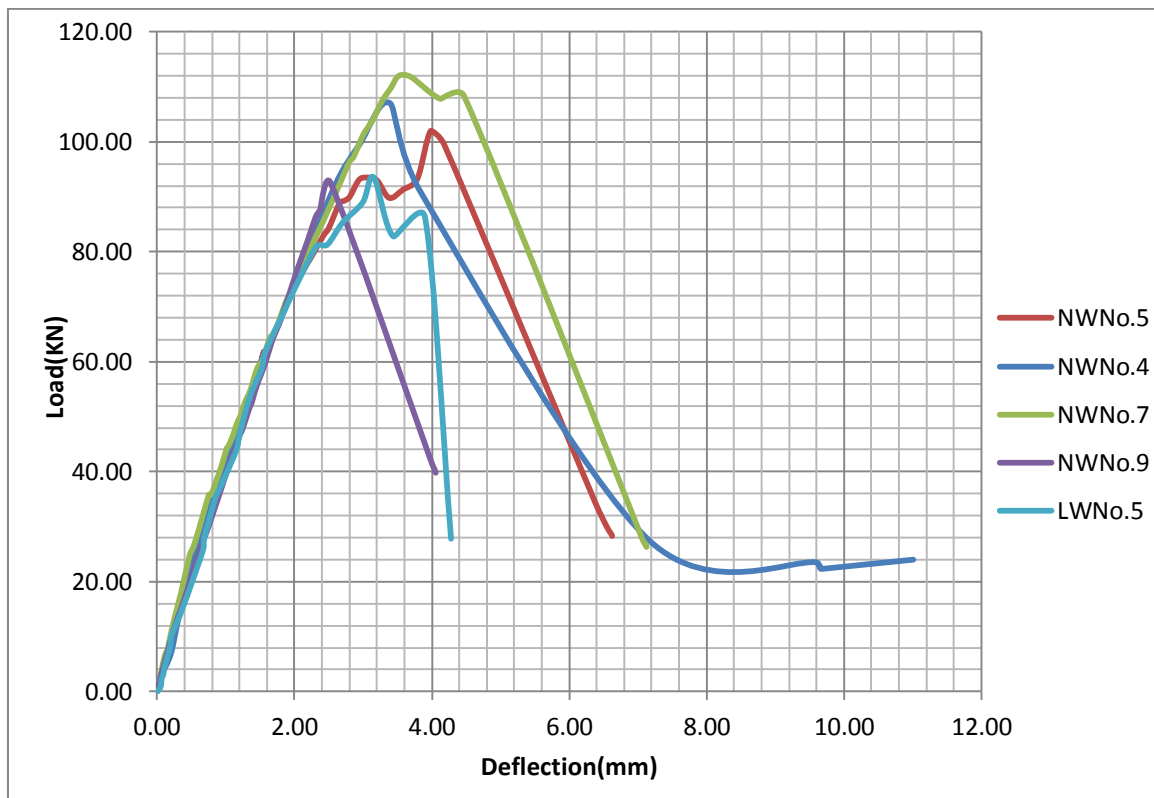


Figure 6:11: Comparison between Load – Deflection diagrams of the specimens

6.1.2 Effect of Aggregate Size

As it was discussed in section 2.2.2.3, one of the factors affecting shear strength of beams without web reinforcement is compressive strength. Experimental results show that the specimens have different compressive strength (shown in table 4-5). Since the objective of this research is to identify the effect of aggregate size and type, the contribution of compressive strength is normalized by $f_{ck}^{1/2}$. Because different codes and empirical equations account the contribution of compressive strength in the form of, $f_{ck}^{1/2}$.

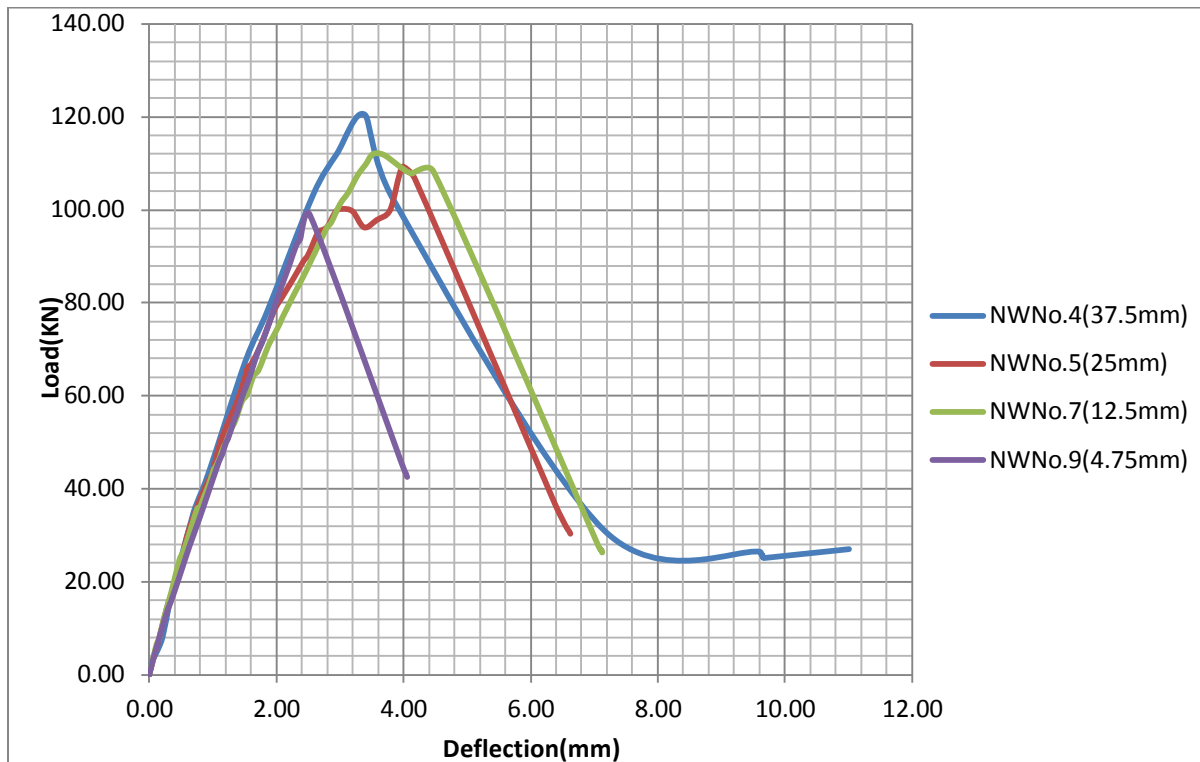


Figure 6:12: Load-Deflection diagram for different aggregate sizes with the similar concrete compressive strength

Figure 6-12 shows, the shear capacity of specimens with large aggregate size are greater than the shear capacity of specimens with small aggregate size. The extreme cases, NWNo.4 (with $a_{gmax}=37.5mm$) and NWNo.9 (with $a_{gmax}=4.75mm$) show that there is a clear effect of aggregate size on shear capacity of normal strength concrete beams. Not only is the shear capacity, the post peak behavior of the failure is influenced by aggregate size. It can be seen from Figure 6-12, failure of specimens with larger aggregate size are more ductile than specimens with smaller aggregate size.

Crack width is another indication of the effect of aggregate size on shear capacity of beams. Shear crack width in RC members are usually accompanied by slip along shear cracks which create shear

transfer by aggregate interlock. Crack width of specimens with larger aggregate size is used wider than that of specimens with smaller aggregate size (see figure 6-1 to figure 6-5). The wider the crack, full dilatancy is developed both in contact density model and simplified shift model. But for narrow cracks, dilatancy is provoked only in contact density model.

It was discussed in section 2.2.2.3, as the size (diameter) of the coarse aggregate increases, the roughness of the crack surfaces increases, allowing higher shear stresses to be transferred across the cracks. In high strength concrete beams and some light weight concrete beams, the cracks penetrate pieces of the aggregate rather than going around them, resulting in a smoother crack surface. This decrease in the shear transferred by aggregate interlock along the cracks reduces V_c . Roughness of the cracked surface of the specimens used in this experiment is shown in Figure 6-13

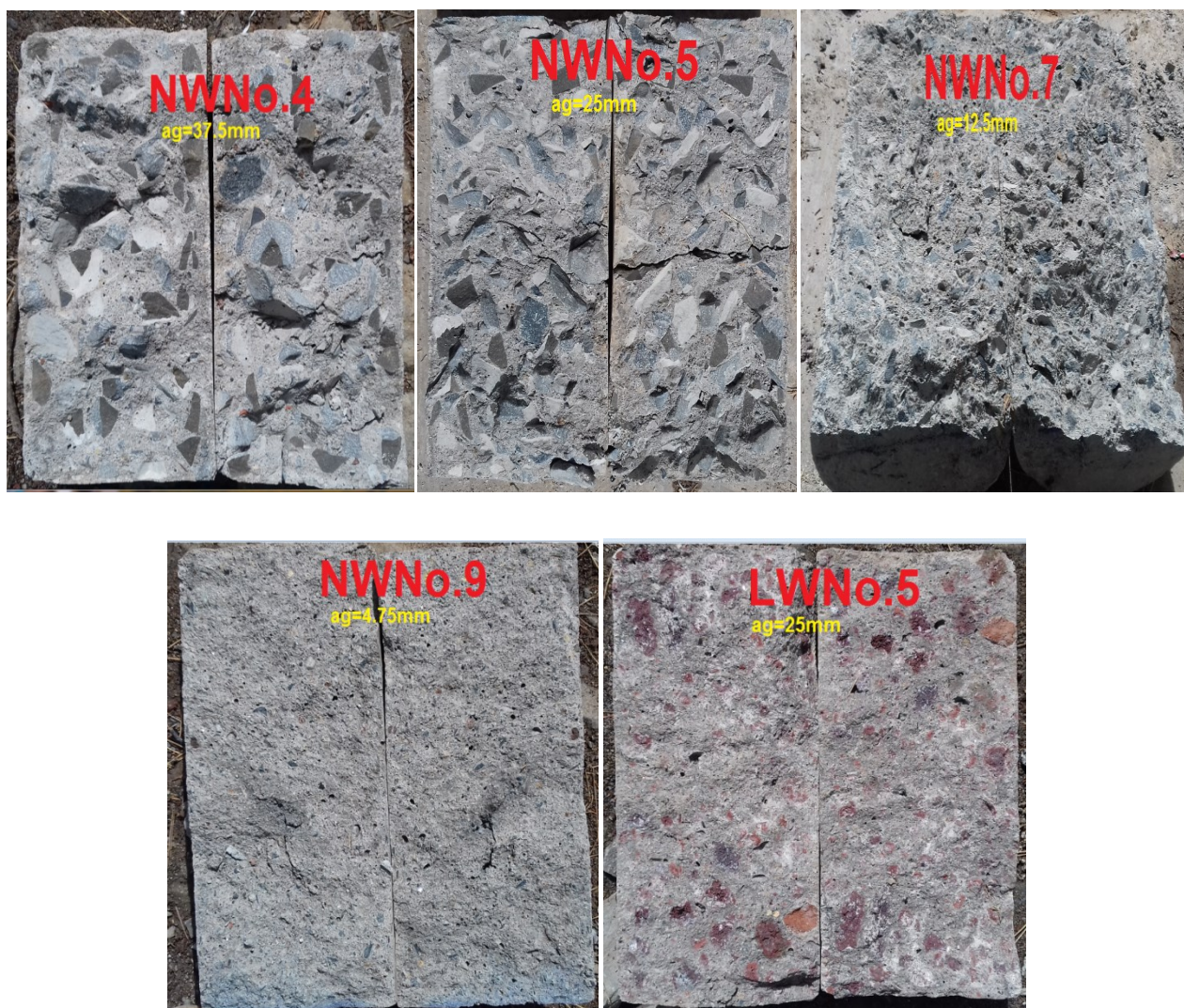


Figure 6:13 : Roughness of the cracked surface of specimens

6.1.3 Effect of aggregate type

The bond between the aggregate particles and the cement paste can be strong enough in HSC and LWAC to cause the aggregate to fracture at cracks (see Figure 6-13) which in turn reduces the shear stress which can be transferred across cracks by means of aggregate interlock.

The experimental result for the two specimens, NWNo.5 and LWNo.5 shown in Figure 6-14 proves the hypothesis.

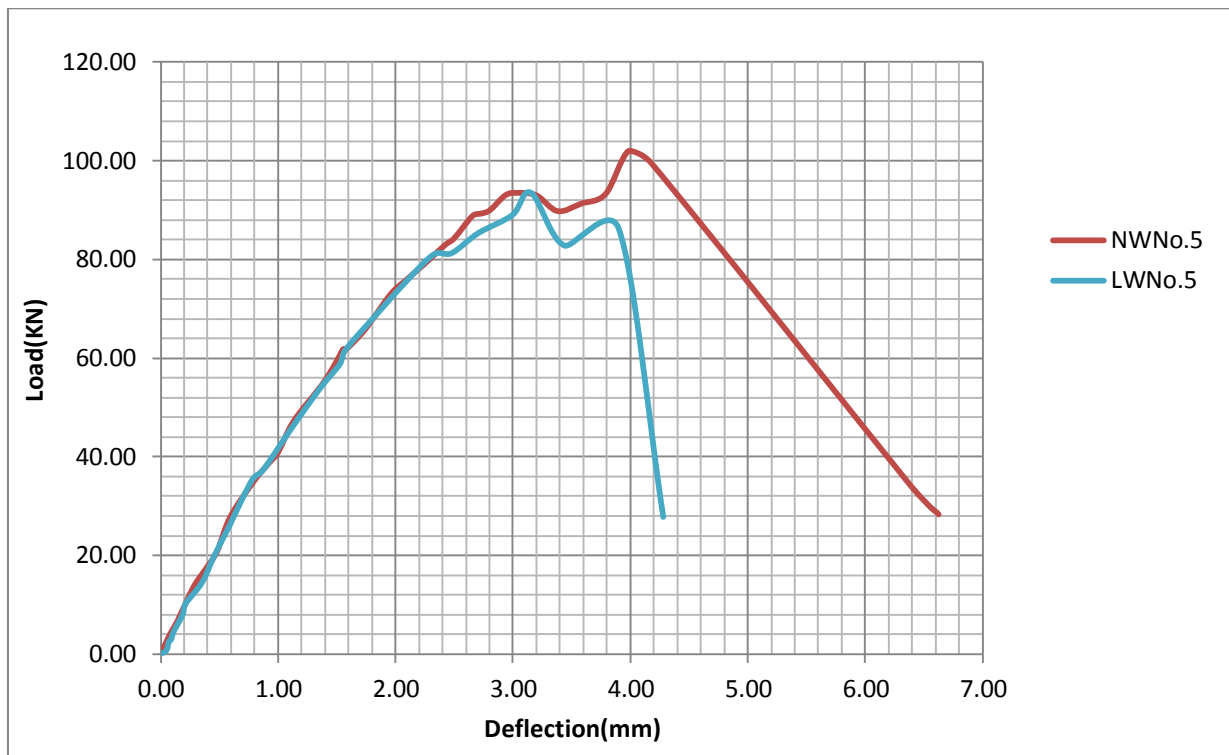


Figure 6:14: Load-Deflection diagram for specimen NWNo.5 and LWNo.5

Examining Figure 6-14, Specimen LWNo.5 exhibits brittle behavior of failure due to the propagation of the cracks directly through the aggregates (see Figure 6-13).

Relatively a ductile behavior was observed for specimen NWNo.5 which is associated with more rough fracture surfaces dominated by the distribution of aggregates.

Compressive and tensile strength of the two specimens shown in table 4-5 is approximately the same but the shear capacity of the two specimens is quite different. This implies, fracture behavior of aggregates play a great roll in shear transfer and compressive strength of concrete is not the only factor.

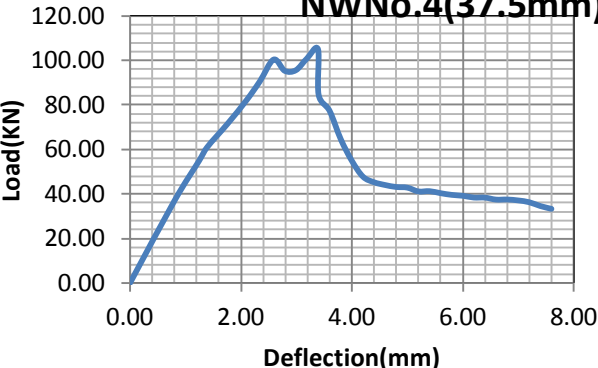
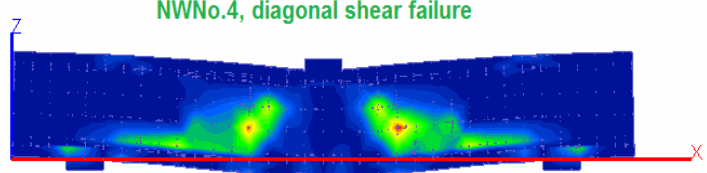
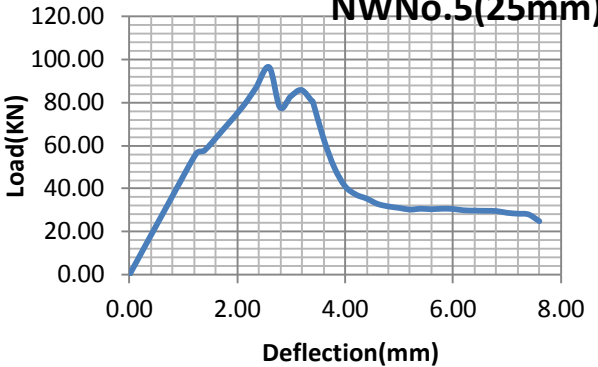
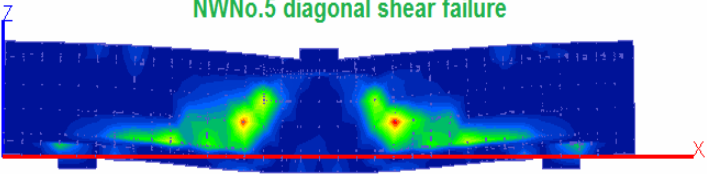
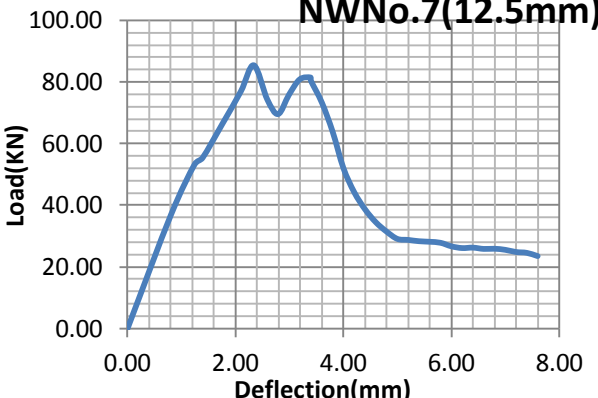
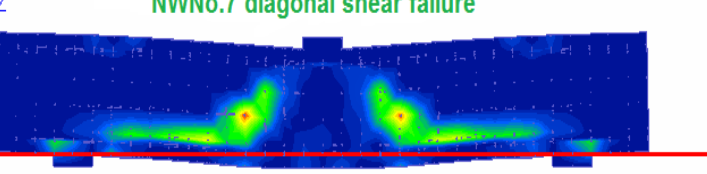
During the testing of specimen LWNo.5, water was leaking out after the specimen is cracked. Which is a good implies that scoria is good at internal curing.

6.2 Result from finite element analysis using DuCOM-COM3

6.2.1 Result

The load deflection diagram for the specimens is presented below. To avoid the effect of compressive strength on the shear behavior of the specimens, the specimens were modeled as having similar grade of concrete.

Table 6-1: Load-deflection and failure mode of finite element analysis

Load-Deflection	Failure mode
<p style="text-align: center;">NWNo.4(37.5mm)</p> 	<p style="text-align: center;">NWNo.4, diagonal shear failure</p> 
<p style="text-align: center;">NWNo.5(25mm)</p> 	<p style="text-align: center;">NWNo.5 diagonal shear failure</p> 
<p style="text-align: center;">NWNo.7(12.5mm)</p> 	<p style="text-align: center;">NWNo.7 diagonal shear failure</p> 

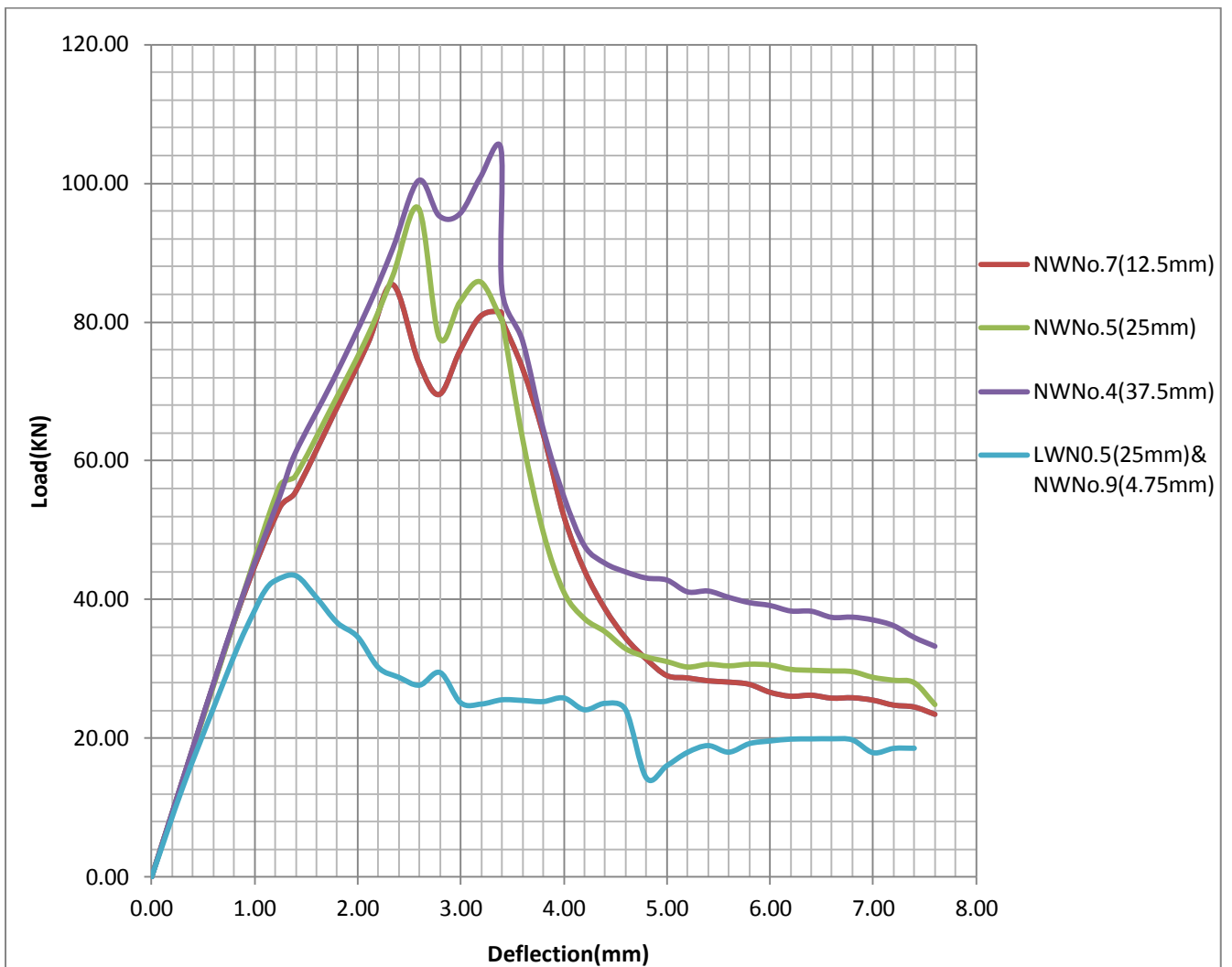
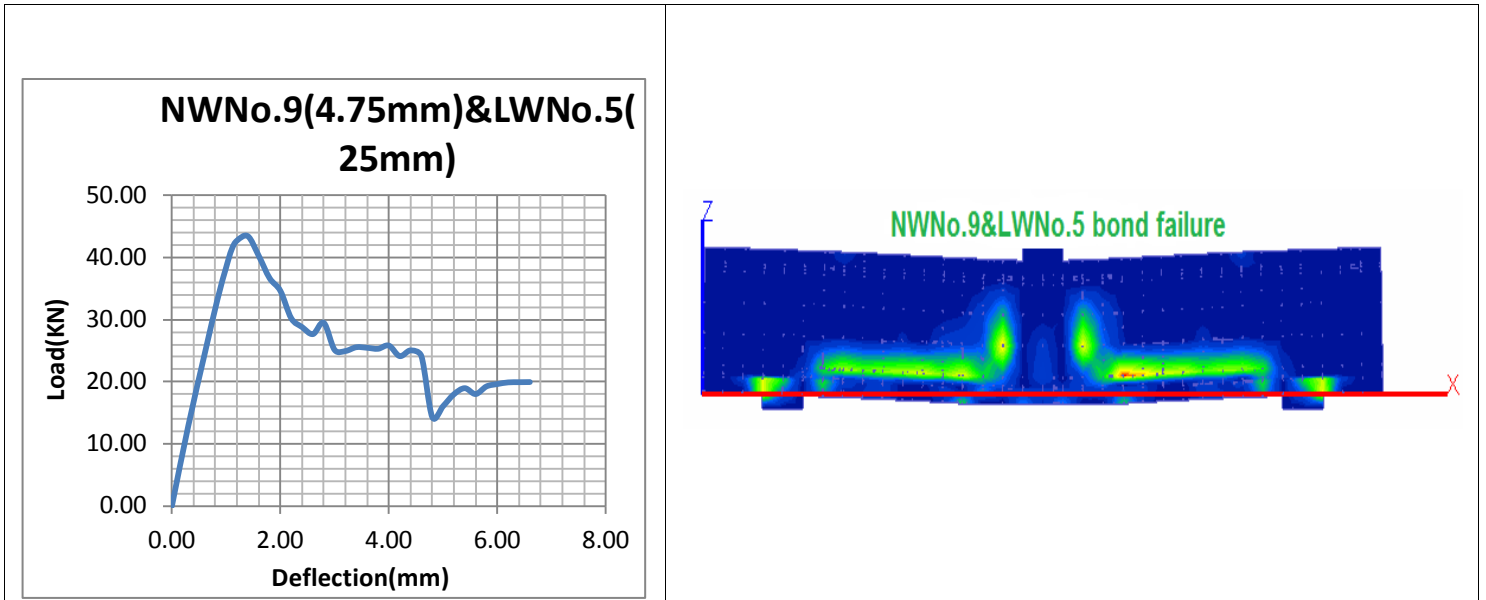


Figure 6:15: Summary of Load-deflection diagram from the finite element analysis

6.2.2 Effect of aggregate size and type

The effect of aggregate size and type is clearly shown in Figure 6-15. As can be seen from the load deflection diagram, the specimens whose aggregate size is 37.5mm and 25mm has about 10kN difference, 25mm and 12.5mm has about 6kN difference. Specimens LWNo.5 (scoria) and NWno.9 (mortar) has small and equal capacity. This is because; shear transfer factor is used in the analysis. Researchers recommended the shear transfer factor for mortar, high strength concrete and light weight concrete to be taken as the same.

6.3 Comparison between result from analytical simulation and experiment

The analytical simulation on DuCOM-COM3 involved 5 beams. The specimens used in the finite element modeling were identical to the specimens that were tested during the experimental program.

Comparison between load- deflection diagram for these five series of specimens and experimental results is shown in the figures below.

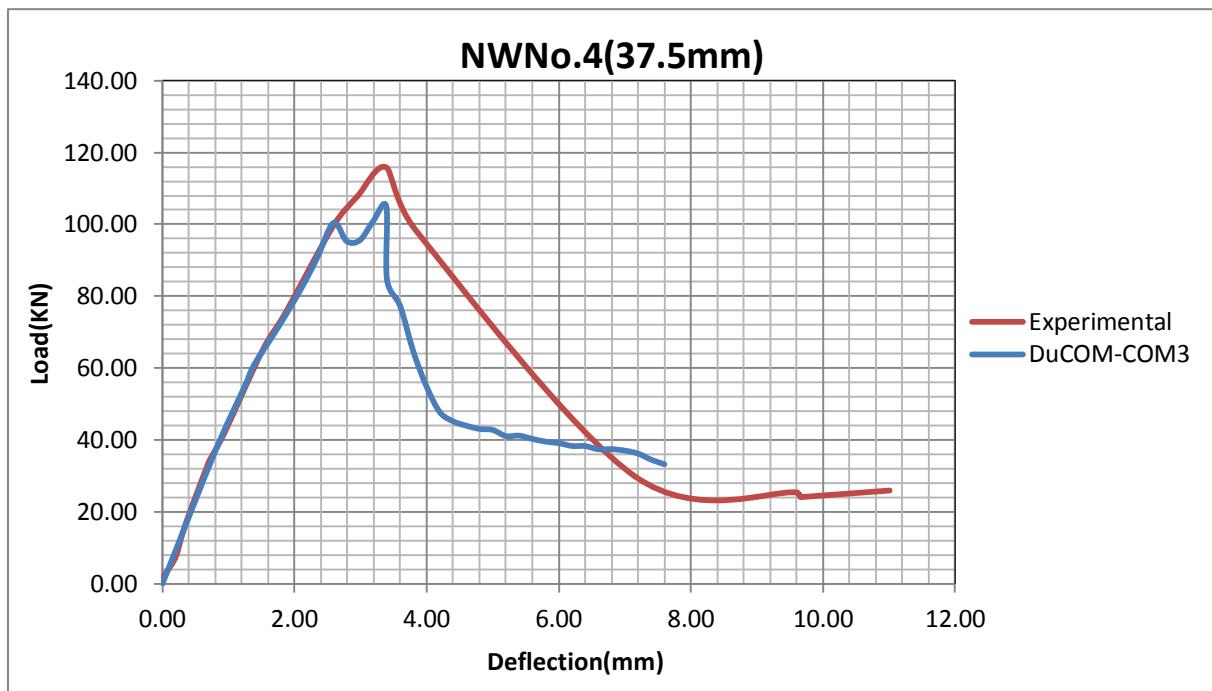


Figure 6:16: Load – Deflection diagram

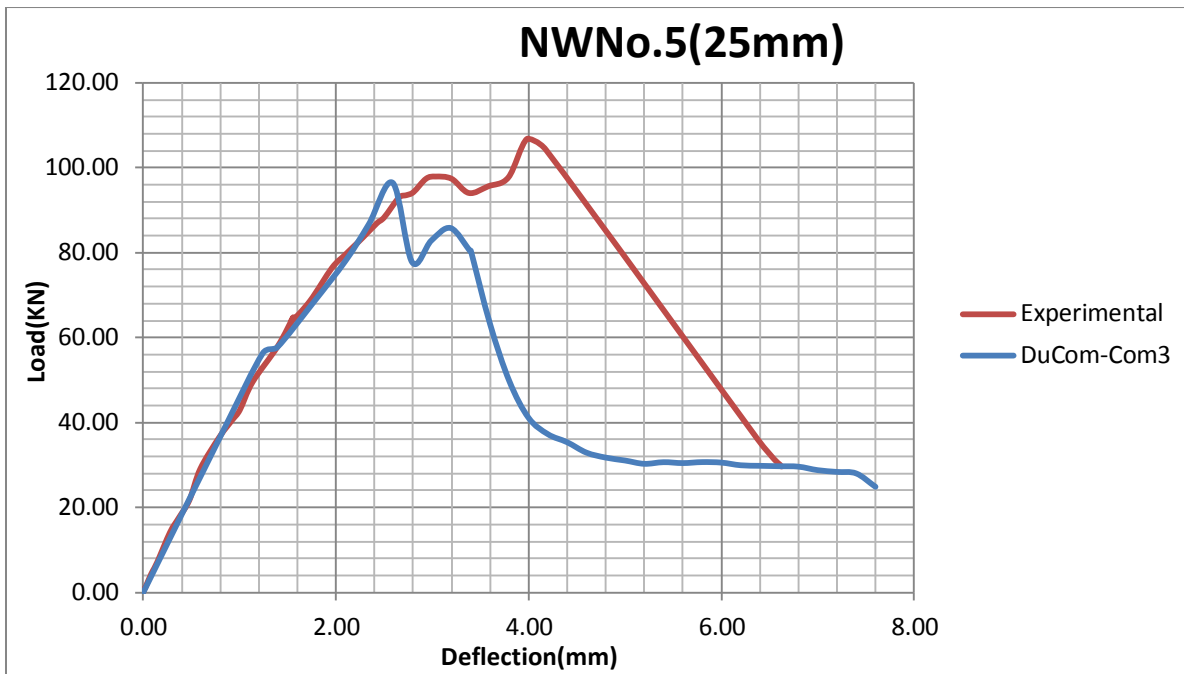


Figure 6:17: Load – Deflection Diagram

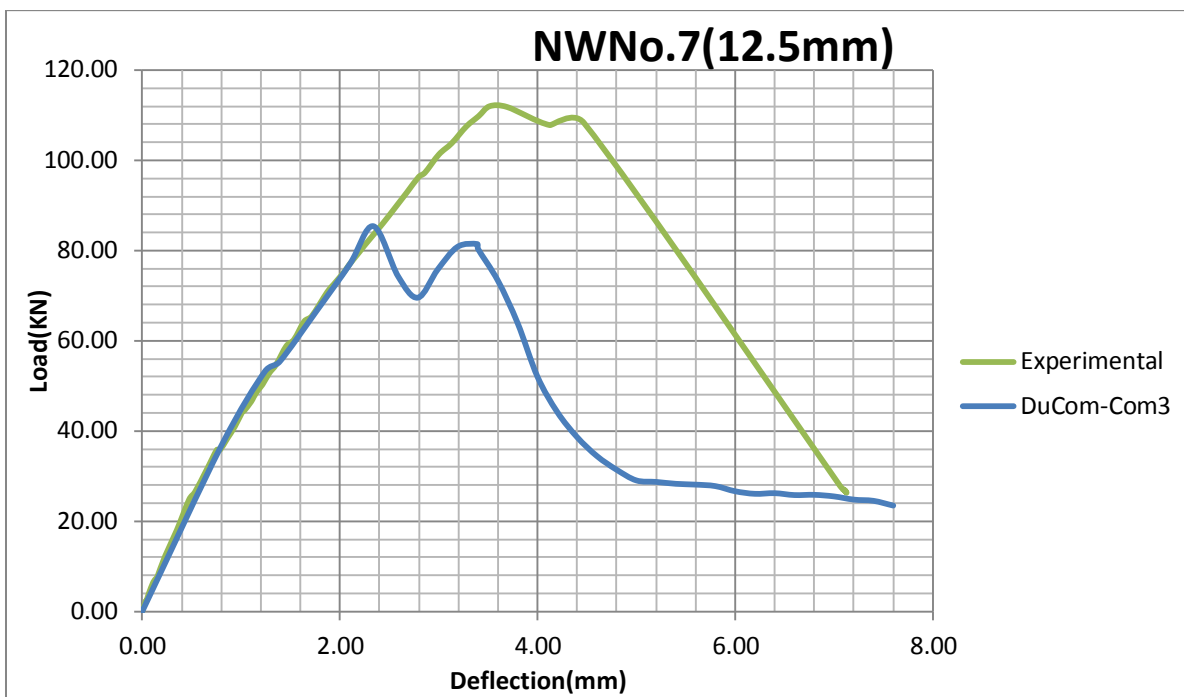


Figure 6:18: Load-Deflection diagram

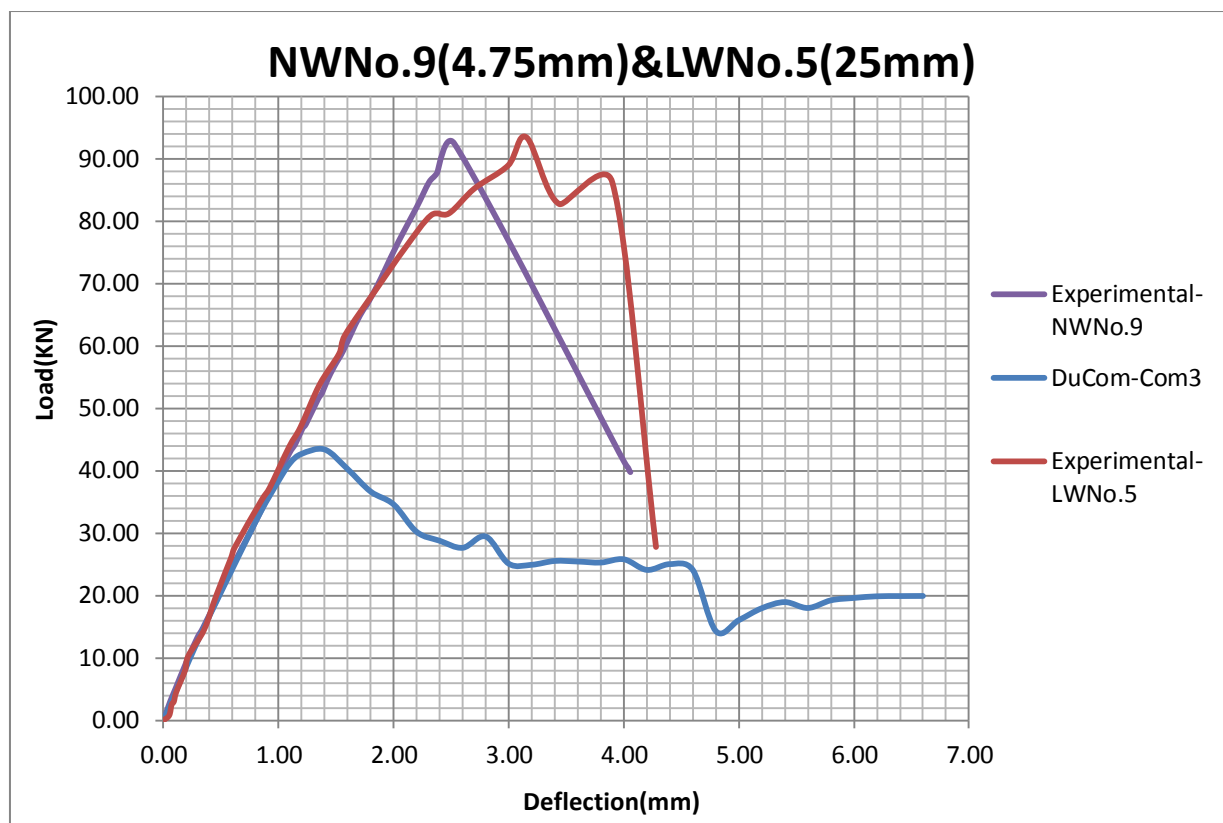


Figure 6:19: Load-Deflection diagram

From the above figures it can be observed that both the experiment and the analytical simulation exhibited a typical shear failure. However the ultimate capacity from the load-deflection diagram did not much for any of the series with the experimental result. This could be because the tensile strength of concrete that was used for the analytical simulation was the lower bound tensile strength and shear capacity of beams are highly influenced by the tensile capacity of the concrete. But further investigation is recommended to study the difference between these two results.

Unlike the analytical result experimental result of specimen NWNo.5 (25mm) is less than NWNo.7 (12.5mm). This may be due to the mix design of the concrete used in the experiment. The mix design was done according to ACI. As it can be seen from the detailed mix design procedure attached in appendix of this document, Aggregate size and paste volume are inversely proportional. The logic behind this is, for the same volume of concrete, when larger aggregate size is used, the surface area is less than to that of smaller aggregate sizes. For a small surface area the amount of paste needed is small. This approach has a side effect on concrete fracture energy. Using larger aggregate size with small paste increases the weak interfacial zones. This means, when a crack is propagating through the specimen, it will cross many interfacial zones. But for smaller aggregate sizes the crack will cross less amount of interfacial zone, this is because the amount of aggregate is small.

6.4 Comparison of Code equations with experimental results

Design equations used in different Codes of practice for predicting the shear capacity of reinforced concrete slender beams was discussed in chapter 3. The effect of aggregate size was not considered in those equations. Figure 6.20 shows the plot of the experimental (measured) ultimate shear forces (V_{exp}) and predicted ultimate shear force (V_{pre}), for all the 5 code equations discussed in chapter 3.

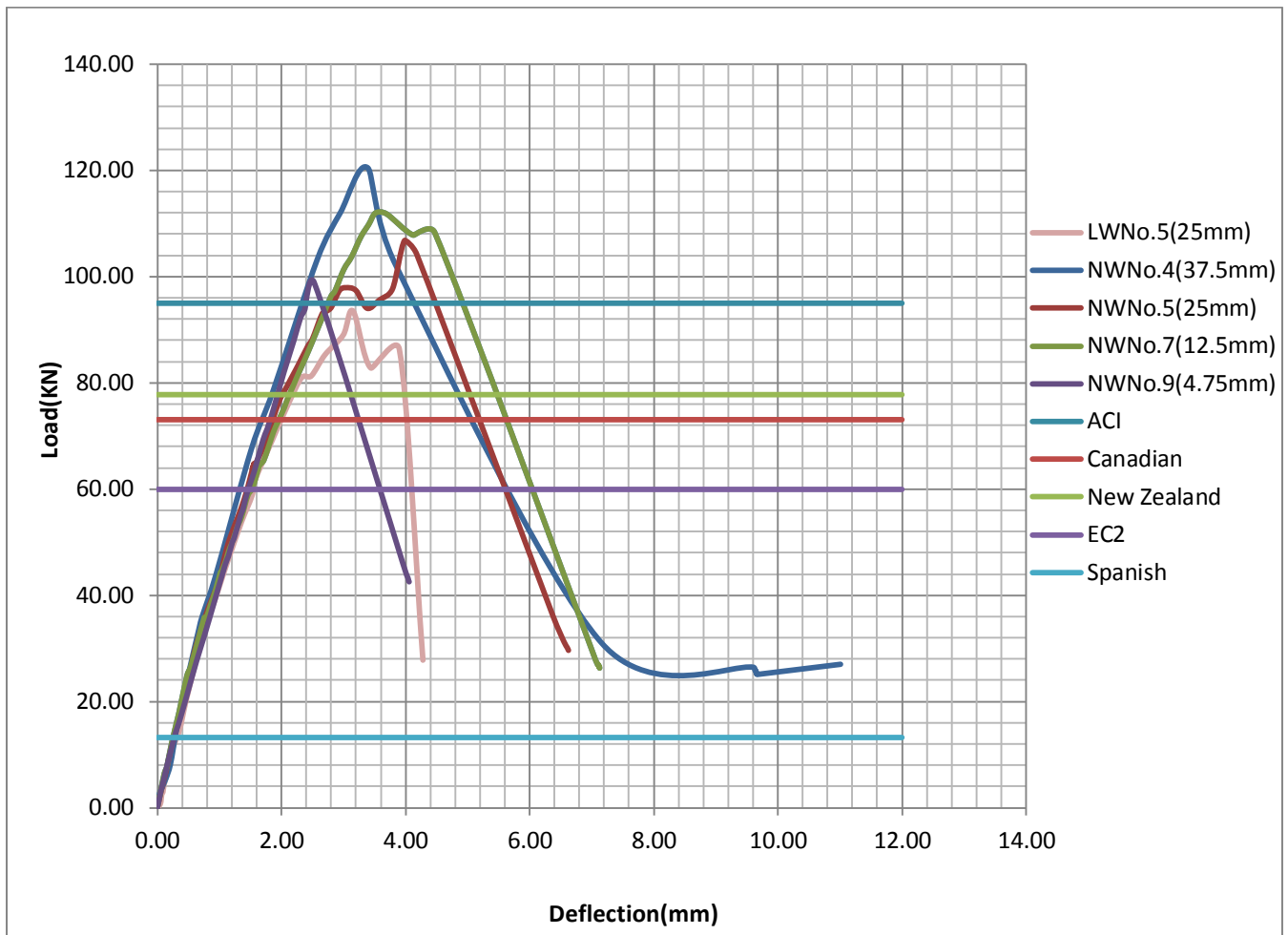


Figure 6:20: Comparison of prediction of Code equations with experimental results.

It can be seen from Figure 6.20 the (V_{exp}/V_{pre}) Spanish EHE-99 Code Eq. 16 is much greater than 1, which shows that this code significantly underestimate the shear capacity of reinforced concrete slender beams, as compared to ACI Code Eq. 12, Euro Code EC2 Eq. 15, New Zealand Code Eq. 14 and Canadian Code Eq. 13. Also it can be seen ACI overestimates the shear capacity of Specimens with maximum aggregate size less than 12.5mm, which leads to unsafe prediction.

Summary of results for the Margin of Safety (V_{exp}/V_{pre}) of empirical equations used in different Codes for predicting the shear capacity of normal strength reinforced concrete slender beams is shown in the table below.

Table 6-2: Margin of Safety (V_{exp}/V_{pre}) of empirical equations used in different Codes for predicting the shear capacity of normal strength reinforced concrete slender beams.

Code	Margin of Safety				
	NWNo.4	NWNo.5	NWNo.7	NWNo.9	LWNo.5
ACI	1.218914	1.113536	1.179071	1.018058	0.984314
Canadian	1.584571	1.447582	1.532777	1.323461	1.279595
New Zealand	1.488617	1.359923	1.439959	1.243318	1.202109
EC2	1.931676	1.764678	1.868535	1.613369	1.559893
Spanish	8.751673	7.995072	8.465608	7.309547	7.067271

Table 6-2 clearly shows the effect of aggregate size on the margin of safety of empirical equations used in different codes.

CHAPTER 7 CONCLUSION AND RECOMMENDATION

7.1 Conclusion

In this study effect of aggregate size and type has been studied by reviewing well-known Building Codes and their basic models, through experimental program on five shear-critical specimens, and through analytical simulation of 5 shear-critical beam specimens. After examining these analyses, the following points are put forward.

1. Building code provisions of shear capacity calculation doesn't consider aggregate size as a factor affecting the shear capacity of beams.
2. The effect of aggregate type on shear capacity is addressed in ACI and EC2.
3. The experimental program revealed that shear behavior of beams is affected by the type of aggregate.
4. Beams with larger aggregate size exhibited a ductile post peak failure while beams with smaller aggregate size exhibited brittle failure.
5. Larger aggregate sizes give comparably higher shear capacity.
6. The aggregate type used in this experiment didn't affect the compressive strength and tensile strength of the concrete.
7. Spanish EHE-99 Code significantly underestimates the shear capacity of reinforced concrete slender beams, which leads to uneconomical design and ACI code overestimates the shear capacity of Specimens with maximum aggregate size less than 12.5mm, which leads to unsafe prediction.

7.2 Recommendation

1. Using light weight aggregate (scoria) results a sounding result in compressive strength and good in internal curing. Hence, can be used as a replacement of normal weight aggregate with further studies related with flexure and initial stiffness.
2. The effect of aggregate shall be considered in prediction of shear capacity of slender beams in building codes.
3. Possible maximum aggregate size shall be used to maximize the shear capacity within the limitation of aggregate size given in the codes to avoid congestion.
4. Since shear behavior of beams is affected by different factors, this study should be further expanded to see the effect of aggregate size and type in relation to these factors, like with web reinforcement.
5. The effect of paste volume and aggregate volume (in relation to aggregate size) in a mix design of concrete according to ACI shall be investigated in relation to the fracture energy.

REFERENCES

1. Edward G. Sherwood, Evan C. Bentz, and Michael P. Collins “Effect of Aggregate Size on Beam-Shear Strength of Thick Slabs” ,ACI structural journal,Technical paper, Title no. 104-S19, March-April 2007.
2. Kenneth S. Harmon, PE , “Engineering properties of structural lightweight concrete”, Carolina Stalite Company – United States
3. Ethiopian Building Code Standard, “Structural Use of Concrete”, (EBCS 2-1995), Ministry of Works & Urban Development, Addis Ababa, Ethiopia, 1995.
4. American Concrete Institute Committee 318, “Building Code Requirements for Structural Concrete”, ACI 318-08, American Concrete Institute, Detroit, MI, 2008.
5. Eurocode 2 - Design of Concrete Structures - Part 1 (Eurocode EC 2) - prEN 1992-1-1 November 2002 [ENG].
6. Edward G. Sherwood, “One-Way Shear Behaviour of Large, Lightly-Reinforced Concrete Beams and Slabs” , A thesis submitted in conformity with the requirements for the degree of Doctor of Philosophy, Department of Civil Engineering, University of Toronto , 2008
7. Sagaseta and Vollum, “Influence of beam cross-section, loading arrangement and aggregate type on shear strength” , Magazine of Concrete Research, Volume 63 Issue 2
8. ASCE-ACI Task Committee 426 on Shear and Diagonal Tention of the Committee on Masonary and Reinforced Concrete of the Structural Divivision, “The Shear Strength of Reinforced Concrete Members” , Journal of the structural division, June.1973
9. Aurelio Muttoni and Miguel Fernandez Ruiz, “Shear Strength of Members Without Transverse Reinforcement as Function of Critical Shear Crack Width” , ACI structural journal,Technical paper, Title no. 105-S17
10. K. J. Weight and J. G. Macgregor, “Reinforced Concrete Mechanics & Design”, 6th ed.

New Jersey, US: Pearson Education, 2012.

11. Abebe Dinku, "The Need For Standardization of Aggregates For Concrete Production in Ethiopian Construction Industry", Civil Engineering Department, Addis Ababa University, Ethiopia.
12. ASCE-ACI Committee 445, "Recent Approaches to Shear Design of Structural Concrete," American Society of Civil Engineers, December 1998.
13. Shuaib H. Ahmed, Shamsoon Fareed, S.F.A.Rafeeqi, "Shear Strength of Normal and Light Weight Reinforced Concrete Slender Beams without Web Reinforcement", NED University of Engineering & Technology, Karachi-Pakistan, 2014
14. M. P. Collins, E. C. Bentz, E. G. Sherwood, and L. Xie, "An Adequate Theory for The Shear Strength of Reinforced Concrete Structures," 2007.
15. J. Vecchio Frank, "Analysis of shear-critical reinforced concrete beams," *ACI Structural Journal*, vol. 97, January - February 2000.

Appendix

Concrete Mixed Design Procedures

The process of determining required and specifiable characteristics of a concrete mixture is called mix-design. It leads to the development of a concrete specification. Mix design is the process of proportioning concrete mixtures. It consists of two interrelated steps, to produce as economically as possible and concrete of good performance. These are:

1. selection of the suitable ingredients (cement, aggregate, water and admixtures) &
2. determining their relative quantities (“proportioning”)

A properly proportioned concrete mix should possess the following qualities:-

- a. Acceptable workability of the freshly mixed concrete
- b. Durability, strength, and uniform appearance of the hardened concrete and
- c. Economy

Trail Mix- Design Using ACI Methods for Conventional Concrete (C25 with a maximum size of aggregate=37.5mm).

Materials properties:-

Concrete with compressive strength of 25 Mpa (C-25) is required to be produced

- from materials quality test we have the following result.
 - a) cement; type 1; specific gravity= 3.15
 - b) coarse aggregates:
 - ✓ bulk specific gravity=2.744
 - ✓ absorption capacity=1.33%
 - ✓ moisture content=1.78%
 - ✓ compacted unit weight=1657.24KN/m³
 - c) fine aggregate (sand)
 - ✓ bulk specific gravity=2.45
 - ✓ absorption capacity= 1.01%
 - ✓ moisture content=2.04%
 - ✓ fines modulus=3.00

➤ The mix design procedures are as follows:-

1. choice of slump

Table 1 Recommended slumps for various types of construction (ACI-2111_91)

Types of construction	Maximum Slump (mm)	Minimum Slump (mm)
Reinforced foundation walls and footings	75	25
Plain footings, caissons, and substructure walls	75	25
Beams and reinforced walls	100	25
Building columns	100	25
Pavements and slabs	75	25
Mass concrete	75	25

From table 1, assume that a type of construction is beams and reinforced wall.

This implies, maximum slump= 100mm and minimum slump= 25mm.

2. maximum size of aggregates
 - sand or fine aggregates =4.75mm
 - coarse aggregates =37.5mm
3. Estimation of mixing water and air content

Assume non air entrained concrete

Table 2 Approximate Mixing Water and Air Content Requirements for Different Slumps and Nominal Maximum Sizes of Aggregates(ACI-2111_91)

NON-AIR-ENTRAINED CONCRETE								
Slump (mm)	9.5 mm	12.5 mm	19 mm	25 mm	37.5 mm	50 mm	75 mm	150 mm
25 to 50	207	199	190	179	166	154	130	113
75 to 100	228	216	205	193	181	169	145	124
150 to 175	243	228	216	202	190	178	160	-
More than 175	-	-	-	-	-	-	-	-
Approximate amount of entrapped air in non-air-entrained concrete (%)								
Slump (mm)	9.5 mm	12.5 mm	19 mm	25 mm	37.5 mm	50 mm	75 mm	150 mm
All	3.0	2.5	2.0	1.5	1.0	0.5	0.3	0.2

From table 2 of ACI standards, for non-air entrained and slump of 75-100, the water in 1m³ of concrete is 181Kg.

4. Water to cement ratio selection table 3

Table 2 Relationship between water-cement or water-cementations materials ratio and compressive strength of concrete(ACI-2111_91)

Compressive strength at 28 days (MPa)	Water-cement ratio by weight (Non-air-entrained concrete)
40	0.42
35	0.47
30	0.54
25	0.61
20	0.69
15	0.79

From table 3, for C-25 and non-air entrained concrete water to cement ratio is 0.61.

5. Cement content calculation

For slump of 75-100

Water content=181Kg/m³

Water/cement=0.61

$$\begin{aligned}
 \text{cement content} &= \text{water content} / \left(\frac{w}{c}\right) \\
 &= \frac{181}{0.61} \\
 &= \underline{\underline{296.721 \text{ Kg/m}^3}}
 \end{aligned}$$

6. Estimation of course aggregates content (table 4)

Table 4 Volume of oven-dry-rodded coarse aggregate per unit volume of concrete for different fineness moduli of fine aggregate.(ACI-2111_91)

Nominal maximum size of aggregate (mm)	2.40	2.60	2.80	3.00
9.5	0.50	0.48	0.46	0.44
12.5	0.59	0.57	0.55	0.53
19	0.66	0.64	0.62	0.60
25	0.71	0.69	0.67	0.65
37.5	0.75	0.73	0.71	0.69

50	0.78	0.76	0.74	0.72
75	0.82	0.80	0.78	0.76
150	0.87	0.85	0.83	0.81

From table 4 of ACI, for maximum size of aggregate= 37.5mm and fines modules for sand = 3.00, the volume of coarse aggregate per unit volume of concrete is

$$= 0.69$$

$$\text{required dry mass of C.A} = 0.69 * 1657.24$$

$$= \underline{1143.4956 \text{ kg/m}^3}$$

7. Estimation of fine aggregates content

At the end of Step 6, all ingredients of the concrete have been estimated except the fine aggregate. Its quantity is determined by difference. Either of the two procedures may be employed:

- The weight method or
- The absolute volume method

If the weight of the concrete per unit volume is assumed or can be estimated from experience, the required weight of fine aggregate is simply the difference between the weight of fresh concrete and the total weight of the other ingredients. Therefore, In this paper the weight method preferred.

- **Content of fine aggregate (F.A) = unit weight of concrete – (C.A + cement + water)**

First estimate the unit weight of fresh concretes from table 5.

Table 5 First estimate of concrete weight (kg/m3)

Nominal maximum size of aggregate (mm)	Non-air-entrained concrete
9.5	2280
12.5	2310
19	2345
25	2380
37.5	2410
50	2445
75	2490
150	2530

From the table 5 the unit weight of fresh concrete corresponding to max. Aggregate size of 19mm and non- air entrained is **2410kg/m³**.

$$\text{Fine aggregate content} = [2410 - (1143.4956+296.7213+181)] = \underline{\underline{788.7831\text{kg/m}^3}}$$

8. Moisture adjustment

Absorbed water does not become part of the mixing water and it must be removed from the mixing water, if moisture content is greater than absorption capacity. But, if absorption capacity is greater than moisture content of aggregate, we need to add water up to its moisture capacity. Therefore, in this case since the moisture content of the aggregates are greater than their absorption capacity, water should be deducted from the mixing water.

$$\text{Removed water from C.A} = 1.78 - 1.33 = \mathbf{0.45\%}$$

$$\text{Removed water from F.A} = 2.04 - 1.01 = \mathbf{1.03\%}$$

$$\begin{aligned} \text{Total water required} &= 181 - [1143.4956 * \left(\frac{0.45}{100}\right) + 788.7831 * \left(\frac{1.03}{100}\right)] \\ &= \mathbf{167.7298\text{Kg/m}^3} \end{aligned}$$

❖ The estimated ingredients for a meter cube of concrete is therefore, summarized as follows.

Ingredients	Weight per m3(kg/m3)
Course aggregate	1143.4956
Fine aggregate	788.7831
Cement	296.721
Water	167.7298
Conc. Unit weight	2396.7295

9. Trial batch

12 Cylinders are needed of 6 for compressive strength 100mm diameter and 200mm height and 6 for tensile strength test 150mm diameter and 300mm height=0.0412m³

$$\text{Beam Concrete volume} = 1.7*0.2*0.25 = 0.085\text{m}^3$$

$$\text{Sub Total} = 0.0412 + 0.085 = 0.1262\text{m}^3$$

Considering 5% waste = 0.0063m³

$$V_{\text{total}} = 0.1262 + 0.0063 = \mathbf{0.133m^3}$$

❖ Ingredients for the trail batch

Ingredients	Weight per m ³ (kg/m ³)
Course aggregate	$1143.496 * 0.133 = 152.085$
Fine aggregate	$788.783 * 0.133 = 104.908$
Cement	$296.721 * 0.133 = 39.464$
Water	$167.7298 * 0.133 = 22.308$

Trail Mix- Design Using ACI Methods for Conventional Concrete (C25 with a maximum size of aggregate=25mm).

Materials properties:-

Concrete with compressive strength of 25 Mpa (C-25) is required to be produced

- from materials quality test we have the following result.

d) cement; type 1; specific gravity= 3.15

e) course aggregates:

- ✓ bulk specific gravity=2.744
- ✓ absorption capacity=1.33%
- ✓ moisture content=1.78%
- ✓ compacted unit weight=1657.24KN/m³

f) fine aggregate (sand)

- ✓ bulk specific gravity=2.45
- ✓ absorption capacity= 1.01%
- ✓ moisture content=2.04%
- ✓ fines modulus=3.00

➤ The mix design procedures are as follows:-

1. choice of slump

Table 1 Recommended slumps for various types of construction (ACI-2111_91)

Types of construction	Maximum Slump (mm)	Minimum Slump (mm)
Reinforced foundation walls and footings	75	25
Plain footings, caissons, and substructure walls	75	25
Beams and reinforced walls	100	25
Building columns	100	25
Pavements and slabs	75	25
Mass concrete	75	25

From table 1, assume that a type of construction is beams and reinforced wall.

This implies, maximum slump= 100mm and minimum slump= 25mm.

2. maximum size of aggregates
 - sand or fine aggregates =4.75mm
 - coarse aggregates =25mm
3. Estimation of mixing water and air content

Assume non air entrained concrete

Table 2 Approximate Mixing Water and Air Content Requirements for Different Slumps and Nominal Maximum Sizes of Aggregates(ACI-2111_91)

NON-AIR-ENTRAINED CONCRETE								
Slump (mm)	9.5 mm	12.5 mm	19 mm	25 mm	37.5 mm	50 mm	75 mm	150 mm
25 to 50	207	199	190	179	166	154	130	113
75 to 100	228	216	205	193	181	169	145	124
150 to 175	243	228	216	202	190	178	160	-
More than 175	-	-	-	-	-	-	-	-
Approximate amount of entrapped air in non-air-entrained concrete (%)								
Slump (mm)	9.5 mm	12.5 mm	19 mm	25 mm	37.5 mm	50 mm	75 mm	150 mm
All	3.0	2.5	2.0	1.5	1.0	0.5	0.3	0.2

From table 2 of ACI standards, for non-air entrained and slump of 75-100, the water in 1m³ of concrete is 193Kg.

4. Water to cement ratio selection table 3

Table 2 Relationship between water-cement or water-cementitious materials ratio and compressive strength of concrete(ACI-2111_91)

Compressive strength at 28 days (MPa)	Water-cement ratio by weight (Non-air-entrained concrete)
40	0.42
35	0.47
30	0.54
25	0.61
20	0.69
15	0.79

From table 3, for C-25 and non-air entrained concrete water to cement ratio is 0.61.

5. Cement content calculation

For slump of 75-100

Water content=193Kg/m³

Water/cement=0.61

$$\begin{aligned}
 \text{cement content} &= \text{water content} / \left(\frac{w}{c}\right) \\
 &= \frac{193}{0.61} \\
 &= \underline{\underline{316.3934 \text{ Kg/m}^3}}
 \end{aligned}$$

6. Estimation of coarse aggregates content (table 4)

Table 4 Volume of oven-dry-rodded coarse aggregate per unit volume of concrete for different fineness moduli of fine aggregate.(ACI-2111_91)

Nominal maximum size of aggregate (mm)	2.40	2.60	2.80	3.00
9.5	0.50	0.48	0.46	0.44
12.5	0.59	0.57	0.55	0.53
19	0.66	0.64	0.62	0.60
25	0.71	0.69	0.67	0.65
37.5	0.75	0.73	0.71	0.69
50	0.78	0.76	0.74	0.72
75	0.82	0.80	0.78	0.76
150	0.87	0.85	0.83	0.81

From table 4 of ACI, for maximum size of aggregate= 25mm and fines modulus for sand = 3.00, the volume of coarse aggregate per unit volume of concrete is

$$= 0.65$$

$$\text{required dry mass of C.A} = 0.65 * 1657.24$$

$$\underline{\underline{= 1077.206/m^3}}$$

7. Estimation of fine aggregates content

At the end of Step 6, all ingredients of the concrete have been estimated except the fine aggregate. Its quantity is determined by difference. Either of the two procedures may be employed:

- The weight method or
- The absolute volume method

If the weight of the concrete per unit volume is assumed or can be estimated from experience, the required weight of fine aggregate is simply the difference between the weight of fresh concrete and the total weight of the other ingredients. Therefore, In this paper the weight method preferred.

- **Content of fine aggregate (F.A) = unit weight of concrete – (C.A + cement + water)**

First estimate the unit weight of fresh concretes from table 5.

Table 5 First estimate of concrete weight (kg/m³)

Nominal maximum size of aggregate (mm)	Non-air-entrained concrete
9.5	2280
12.5	2310
19	2345
25	2380
37.5	2410
50	2445
75	2490
150	2530

From the table 5 the unit weight of fresh concrete corresponding to max. Aggregate size of 19mm and non- air entrained is **2380kg/m³**.

$$\text{Fine aggregate content} = [2380 - (1077.206+316.3934+193)] = \underline{\underline{793.400kg/m^3}}$$

8. Moisture adjustment

Absorbed water does not become part of the mixing water and it must be removed from the mixing water, if moisture content is greater than absorption capacity. But, if absorption capacity is greater than moisture content of aggregate, we need to add water up to its moisture capacity. Therefore, in this case since the moisture content of the aggregates are greater than their absorption capacity, water should be deducted from the mixing water.

$$\text{Removed water from C.A} = 1.78 - 1.33 = \mathbf{0.45\%}$$

$$\text{Removed water from F.A} = 2.04 - 1.01 = \mathbf{1.03\%}$$

$$\begin{aligned} \text{Total water required} &= 193 - \left[\frac{1077.206 * (0.45)}{100} + \frac{793.400 * (1.03)}{100} \right] \\ &= \mathbf{179.9806 \text{ Kg/m}^3} \end{aligned}$$

❖ The estimated ingredients for a meter cube of concrete is therefore, summarized as follows.

Ingredients	Weight per m ³ (kg/m ³)
Course aggregate	1077.206
Fine aggregate	793.400
Cement	316.3934
Water	179.9806
Conc. Unit weight	2366.98

9. Trial batch

I need 12 Cylinders of 6 for compressive strength 100mm diameter and 200mm height and 6 for tensile strength test 150mm diameter and 300mm height = 0.0412m³

$$\text{Beam Concrete volume} = 1.7 * 0.2 * 0.25 = 0.085 \text{ m}^3$$

$$\text{Sub Total} = 0.0412 + 0.085 = 0.1262 \text{ m}^3$$

$$\text{Considering 5\% waste} = 0.0063 \text{ m}^3$$

$$V_{\text{total}} = 0.1262 + 0.0063 = \mathbf{0.133 \text{ m}^3}$$

❖ Ingredients for the trail batch

Ingredients	Weight per m ³ (kg/m ³)
Course aggregate	1077.21*0.133=143.268
Fine aggregate	793.40*0.133= 105.5222
Cement	316.3934*0.133= 42.08
Water	179.9806*0.133= 23.94

Trail Mix- Design Using ACI Methods for Conventional Concrete (C25 with a maximum size of aggregate=12.5mm).

Materials properties:-

Concrete with compressive strength of 25 Mpa (C-25) is required to be produced

- from materials quality test we have the following result.

1. cement; type 1; specific gravity= 3.15
2. course aggregates:
 - ✓ bulk specific gravity=2.744
 - ✓ absorption capacity=1.33%
 - ✓ moisture content=1.78%
 - ✓ compacted unit weight=1657.24KN/m³
3. fine aggregate (sand)
 - ✓ bulk specific gravity=2.45
 - ✓ absorption capacity= 1.01%
 - ✓ moisture content=2.04%
 - ✓ fines modulus=3.00

➤ The mix design procedures are as follows:-

- ❖ choice of slump

Table 1 Recommended slumps for various types of construction (ACI-2111_91)

Types of construction	Maximum Slump (mm)	Minimum Slump (mm)
Reinforced foundation walls and footings	75	25
Plain footings, caissons, and substructure walls	75	25
Beams and reinforced walls	100	25

Building columns	100	25
Pavements and slabs	75	25
Mass concrete	75	25

From table 1, assume that a type of construction is beams and reinforced wall.

This implies, maximum slump= 100mm and minimum slump= 12.5mm.

- ❖ maximum size of aggregates
 - sand or fine aggregates =4.75mm
 - coarse aggregates =12.5mm
- ❖ Estimation of mixing water and air content

Assume non air entrained concrete

Table 2 Approximate Mixing Water and Air Content Requirements for Different Slumps and Nominal Maximum Sizes of Aggregates(ACI-2111_91)

NON-AIR-ENTRAINED CONCRETE								
Slump (mm)	9.5 mm	12.5 mm	19 mm	25 mm	37.5 mm	50 mm	75 mm	150 mm
25 to 50	207	199	190	179	166	154	130	113
75 to 100	228	216	205	193	181	169	145	124
150 to 175	243	228	216	202	190	178	160	-
More than 175	-	-	-	-	-	-	-	-
Approximate amount of entrapped air in non-air-entrained concrete (%)								
Slump (mm)	9.5 mm	12.5 mm	19 mm	25 mm	37.5 mm	50 mm	75 mm	150 mm
All	3.0	2.5	2.0	1.5	1.0	0.5	0.3	0.2

From table 2 of ACI standards, for non-air entrained and slump of 75-100, the water in 1m³ of concrete is 216Kg.

- ❖ Water to cement ratio selection table 3

Table 2 Relationship between water-cement or water-cementitious materials ratio and compressive strength of concrete(ACI-2111_91)

Compressive strength at 28 days (MPa)	Water-cement ratio by weight (Non-air-entrained concrete)
40	0.42
35	0.47

30	0.54
25	0.61
20	0.69
15	0.79

From table 3, for C-25 and non-air entrained concrete water to cement ratio is 0.61.

❖ Cement content calculation

For slump of 75-100

Water content=216Kg/m³

Water/cement=0.61

$$\begin{aligned}
 \text{cementcontent} &= \text{watercontent} / \left(\frac{w}{c}\right) \\
 &= \frac{216}{0.61} \\
 &= \underline{\underline{354.0984 \text{ Kg/m}^3}}
 \end{aligned}$$

❖ Estimation of coarse aggregates content (table 4)

Table 4 Volume of oven-dry-rodded coarse aggregate per unit volume of concrete for different fineness moduli of fine aggregate.(ACI-2111_91)

Nominal maximum size of aggregate (mm)	2.40	2.60	2.80	3.00
9.5	0.50	0.48	0.46	0.44
12.5	0.59	0.57	0.55	0.53
19	0.66	0.64	0.62	0.60
25	0.71	0.69	0.67	0.65
37.5	0.75	0.73	0.71	0.69
50	0.78	0.76	0.74	0.72
75	0.82	0.80	0.78	0.76
150	0.87	0.85	0.83	0.81

From table 4 of ACI, for maximum size of aggregate= 12.5mm and fines modules for sand = 3.00, the volume of coarse aggregate per unit volume of concrete is

$$= 0.53$$

$$\text{requerredrymassofC.A} = 0.53 * 1657.24$$

$$= \underline{\underline{878.3372/m^3}}$$

❖ Estimation of fine aggregates content

At the end of Step 6, all ingredients of the concrete have been estimated except the fine aggregate. Its quantity is determined by difference. Either of the two procedures may be employed:

- The weight method or
- The absolute volume method

If the weight of the concrete per unit volume is assumed or can be estimated from experience, the required weight of fine aggregate is simply the difference between the weight of fresh concrete and the total weight of the other ingredients. Therefore, In this paper the weight method preferred.

- **Content of fine aggregate (F.A) = unit weight of concrete – (C.A + cement + water)**

First estimate the unit weight of fresh concretes from table 5.

Table 5 First estimate of concrete weight (kg/m³)

Nominal maximum size of aggregate (mm)	Non-air-entrained concrete
9.5	2280
12.5	2310
19	2345
25	2380
37.5	2410
50	2445
75	2490
150	2530

From the table 5 the unit weight of fresh concrete corresponding to max. Aggregate size of 19mm and non- air entrained is **2310kg/m³**.

$$\text{Fine aggregate content} = [2310 - (878.3372+354.0984+216)] = \underline{\underline{861.5644\text{kg/m}^3}}$$

❖ Moisture adjustment

Absorbed water does not become part of the mixing water and it must be removed from the mixing water, if moisture content is greater than absorption capacity. But, if absorption capacity is greater than moisture content of aggregate, we need to add water up to its moisture capacity. Therefore, in

this case since the moisture content of the aggregates are greater than their absorption capacity, water should be deducted from the mixing water.

$$\text{Removed water from C.A} = 1.78 - 1.33 = \mathbf{0.45\%}$$

$$\text{Removed water from F.A} = 2.04 - 1.01 = \mathbf{1.03\%}$$

$$\begin{aligned} \text{Total water required} &= 216 - \left[878.3372 * \left(\frac{0.45}{100} \right) + 861.5644 * \left(\frac{1.03}{100} \right) \right] \\ &= \mathbf{203.173\text{Kg/m}^3} \end{aligned}$$

❖ The estimated ingredients for a meter cube of concrete is therefore, summarized as follows.

Ingredients	Weight per m ³ (kg/m ³)
Course aggregate	878.3372
Fine aggregate	861.5644
Cement	354.0984
Water	203.173
Conc. Unit weight	2297.173

❖ Trial batch

I need 12 Cylinders of 6 for compressive strength 100mm diameter and 200mm height and 6 for tensile strength test 150mm diameter and 300mm height = 0.0412m³

$$\text{Beam Concrete volume} = 1.7 * 0.2 * 0.25 = 0.085\text{m}^3$$

$$\text{Sub Total} = 0.0412 + 0.085 = 0.1262\text{m}^3$$

$$\text{Considering 5\% waste} = 0.0063\text{m}^3$$

$$V_{\text{total}} = 0.1262 + 0.0063 = \mathbf{0.133\text{m}^3}$$

❖ Ingredients for the trail batch

Ingredients	Weight per m ³ (kg/m ³)
Course aggregate	878.337*0.133=116.82
Fine aggregate	861.5644*0.133= 114.59

Cement	$354.0984 * 0.133 = 47.1$
Water	$203.173 * 0.133 = 27.022$

Trail Mix- Design Using ACI Methods for Conventional Concrete (C25 with a maximum size of aggregate=4.75mm).

Materials properties:-

Concrete with compressive strength of 25 Mpa (C-25) is required to be produced

- from materials quality test we have the following result.

4. cement; type 1; specific gravity= 3.15

5. coarse aggregates:

- ✓ bulk specific gravity=2.744
- ✓ absorption capacity=1.33%
- ✓ moisture content=1.78%
- ✓ compacted unit weight=1657.24KN/m³

6. fine aggregate (sand)

- ✓ bulk specific gravity=2.45
- ✓ absorption capacity= 1.01%
- ✓ moisture content=2.04%
- ✓ fines modulus=3.00

➤ The mix design procedures are as follows:-

1. choice of slump

Table 1 Recommended slumps for various types of construction (ACI-2111_91)

Types of construction	Maximum Slump (mm)	Minimum Slump (mm)
Reinforced foundation walls and footings	75	25
Plain footings, caissons, and substructure walls	75	25
Beams and reinforced walls	100	25
Building columns	100	25
Pavements and slabs	75	25
Mass concrete	75	25

From table 1, assume that a type of construction is beams and reinforced wall.

This implies, maximum slump= 100mm and minimum slump= 4.75mm.

2. maximum size of aggregates
 - sand or fine aggregates =4.75mm
 - coarse aggregates =4.75mm
3. Estimation of mixing water and air content

Assume non air entrained concrete

Table 2 Approximate Mixing Water and Air Content Requirements for Different Slumps and Nominal Maximum Sizes of Aggregates(ACI-2111_91)

NON-AIR-ENTRAINED CONCRETE								
Slump (mm)	9.5 mm	12.5 mm	19 mm	25 mm	37.5 mm	50 mm	75 mm	150 mm
25 to 50	207	199	190	179	166	154	130	113
75 to 100	228	216	205	193	181	169	145	124
150 to 175	243	228	216	202	190	178	160	-
More than 175	-	-	-	-	-	-	-	-
Approximate amount of entrapped air in non-air-entrained concrete (%)								
Slump (mm)	9.5 mm	12.5 mm	19 mm	25 mm	37.5 mm	50 mm	75 mm	150 mm
All	3.0	2.5	2.0	1.5	1.0	0.5	0.3	0.2

From table 2 of ACI standards, for non-air entrained and slump of 75-100, the water in 1m³ of concrete is 236.75Kg.

4. Water to cement ratio selection table 3

Table 2 Relationship between water-cement or water-cementitious materials ratio and compressive strength of concrete(ACI-2111_91)

Compressive strength at 28 days (MPa)	Water-cement ratio by weight (Non-air-entrained concrete)
40	0.42
35	0.47
30	0.54
25	0.61
20	0.69
15	0.79

From table 3, for C-25 and non-air entrained concrete water to cement ratio is 0.61.

5. Cement content calculation

For slump of 75-100

Water content=236.75Kg/m³

Water/cement=0.61

$$\begin{aligned} \text{cementcontent} &= \text{watercontent} / \left(\frac{w}{c}\right) \\ &= \frac{236.75}{0.61} \\ &= \underline{\underline{388.115 \text{ Kg/m}^3}} \end{aligned}$$

6. Estimation of course aggregates content (table 4)

Table 4 Volume of oven-dry-rodded coarse aggregate per unit volume of concrete for different fineness moduli of fine aggregate.(ACI-2111_91)

Nominal maximum size of aggregate (mm)	2.40	2.60	2.80	3.00
9.5	0.50	0.48	0.46	0.44
12.5	0.59	0.57	0.55	0.53
19	0.66	0.64	0.62	0.60
25	0.71	0.69	0.67	0.65
37.5	0.75	0.73	0.71	0.69
50	0.78	0.76	0.74	0.72
75	0.82	0.80	0.78	0.76
150	0.87	0.85	0.83	0.81

From table 4 of ACI, for maximum size of aggregate= 25mm and fines modules for sand = 3.00, the volume of course aggregate per unit volume of concrete is

$$= 0.234$$

$$\text{requereddrymassofC.A} = 0.234 * 1657.24$$

$$= \underline{\underline{387.79416/m^3}}$$

7. Estimation of fine aggregates content

At the end of Step 6, all ingredients of the concrete have been estimated except the fine aggregate. Its quantity is determined by difference. Either of the two procedures may be employed:

- The weight method or
- The absolute volume method

If the weight of the concrete per unit volume is assumed or can be estimated from experience, the required weight of fine aggregate is simply the difference between the weight of fresh concrete and the total weight of the other ingredients. Therefore, In this paper the weight method preferred.

➤ **Content of fine aggregate (F.A) = unit weight of concrete – (C.A + cement + water)**

First estimate the unit weight of fresh concretes from table 5.

Table 5 First estimate of concrete weight (kg/m³)

Nominal maximum size of aggregate (mm)	Non-air-entrained concrete
9.5	2280
12.5	2310
19	2345
25	2380
37.5	2410
50	2445
75	2490
150	2530

From the table 5 the unit weight of fresh concrete corresponding to max. Aggregate size of 19mm and non- air entrained is **2232.5kg/m³**.

Fine aggregate content = $[2232.5 - (387.794+388.115+236.75)] = \underline{\underline{1219.8412\text{kg/m}^3}}$

8. Moisture adjustment

Absorbed water does not become part of the mixing water and it must be removed from the mixing water, if moisture content is greater than absorption capacity. But, if absorption capacity is greater than moisture content of aggregate, we need to add water up to its moisture capacity. Therefore, in this case since the moisture content of the aggregates are greater than their absorption capacity, water should be deducted from the mixing water.

Removed water from C.A = $1.78 - 1.33 = \mathbf{0.45\%}$

Removed water from F.A = $2.04 - 1.01 = \mathbf{1.03\%}$

$$\text{Total water required} = 236.75 - \left[387.79416 * \left(\frac{0.45}{100} \right) + 1219.8412 * \left(\frac{1.03}{100} \right) \right]$$

$$= 222.440 \text{ Kg/m}^3$$

❖ The estimated ingredients for a meter cube of concrete is therefore, summarized as follows.

Ingredients	Weight per m ³ (kg/m ³)
Course aggregate	387.794
Fine aggregate	1219.8412
Cement	388.115
Water	222.440
Conc. Unit weight	2218.1902

9. Trial batch

I need 12 Cylinders of 6 for compressive strength 100mm diameter and 200mm height and 6 for tensile strength test 150mm diameter and 300mm height = 0.0412m³

Beam Concrete volume = 1.7*0.2*0.25 = 0.085m³

Sub Total=0.0412+0.085=0.1262m³

Considering 5% waste = 0.0063m³

V_{total} = 0.1262 + 0.0063 = **0.133m³**

❖ Ingredients for the trail batch

Ingredients	Weight per m ³ (kg/m ³)
Course aggregate	387.794* 0.133=51.577
Fine aggregate	1219.841* 0.133=162.24
Cement	388.115*0.133= 51.62
Water	222.440*0.133= 29.58